IEC PAS 63151

Edition 1.0 2018-01

PUBLICLY AVAILABLE SPECIFICATION

PRE-STANDARD

colour inside

Measurement procedure for the assessment of specific absorption rate of human exposure to radio frequency fields from hand-held and body-mounted wireless communication devices – Vector measurement-based systems (Frequency range of 30 MHz to 6 GHz)

IEC PAS 63151:2018-01(en)

IEC Central Office
3, rue de Varembé
CH-1211 Geneva 20
Switzerland

Tel.: +41 22 919 02 11
info@iec.ch
www.iec.ch

About the IEC
The International Electrotechnical Commission (IEC) is the leading global organization that prepares and publishes International Standards for all electrical, electronic and related technologies.

About IEC publications
The technical content of IEC publications is kept under constant review by the IEC. Please make sure that you have the latest edition, a corrigenda or an amendment might have been published.

IEC Catalogue - webstore.iec.ch/catalogue
The stand-alone application for consulting the entire bibliographical information on IEC International Standards, Technical Specifications, Technical Reports and other documents. Available for PC, Mac OS, Android Tablets and iPad.

IEC publications search - webstore.iec.ch/advsearchform
The advanced search enables to find IEC publications by a variety of criteria (reference number, text, technical committee,…). It also gives information on projects, replaced and withdrawn publications.

IEC Just Published - webstore.iec.ch/justpublished
Stay up to date on all new IEC publications. Just Published details all new publications released. Available online and also once a month by email.

Electropedia - www.electropedia.org
The world's leading online dictionary of electronic and electrical terms containing 21 000 terms and definitions in English and French, with equivalent terms in 16 additional languages. Also known as the International Electrotechnical Vocabulary (IEV) online.

IEC Glossary - std.iec.ch/glossary
67 000 electrotechnical terminology entries in English and French extracted from the Terms and Definitions clause of IEC publications issued since 2002. Some entries have been collected from earlier publications of IEC TC 37, 77, 86 and CISPR.

IEC Customer Service Centre - webstore.iec.ch/csc
If you wish to give us your feedback on this publication or need further assistance, please contact the Customer Service Centre: sales@iec.ch.

IEC PAS 63151

Edition 1.0 2018-01

PUBLICLY AVAILABLE SPECIFICATION

PRE-STANDARD

colour
inside

Measurement procedure for the assessment of specific absorption rate of human exposure to radio frequency fields from hand-held and body-mounted wireless communication devices – Vector measurement-based systems (Frequency range of 30 MHz to 6 GHz)

INTERNATIONAL
ELECTROTECHNICAL
COMMISSION

ICS 17.220.20, 17.240 ISBN 978-2-8322-5178-2

Warning! Make sure that you obtained this publication from an authorized distributor.

CONTENTS

INTERNATIONAL ELECTROTECHNICAL COMMISSION

____

MEASUREMENT PROCEDURE FOR THE ASSESSMENT OF SPECIFIC ABSORPTION RATE OF HUMAN EXPOSURE TO RADIO FREQUENCY FIELDS FROM HAND-HELD AND BODY-MOUNTED WIRELESS COMMUNICATION DEVICES –

Vector measurement-based systems (Frequency range of 30 MHz to 6 GHz)

FOREWORD

1) The International Electrotechnical Commission (IEC) is a worldwide organization for standardization comprising all national electrotechnical committees (IEC National Committees). The object of IEC is to promote international co-operation on all questions concerning standardization in the electrical and electronic fields. To this end and in addition to other activities, IEC publishes International Standards, Technical Specifications, Technical Reports, Publicly Available Specifications (PAS) and Guides (hereafter referred to as "IEC Publication(s)"). Their preparation is entrusted to technical committees; any IEC National Committee interested in the subject dealt with may participate in this preparatory work. International, governmental and non-governmental organizations liaising with the IEC also participate in this preparation. IEC collaborates closely with the International Organization for Standardization (ISO) in accordance with conditions determined by agreement between the two organizations.
2) The formal decisions or agreements of IEC on technical matters express, as nearly as possible, an international consensus of opinion on the relevant subjects since each technical committee has representation from all interested IEC National Committees.
3) IEC Publications have the form of recommendations for international use and are accepted by IEC National Committees in that sense. While all reasonable efforts are made to ensure that the technical content of IEC Publications is accurate, IEC cannot be held responsible for the way in which they are used or for any misinterpretation by any end user.
4) In order to promote international uniformity, IEC National Committees undertake to apply IEC Publications transparently to the maximum extent possible in their national and regional publications. Any divergence between any IEC Publication and the corresponding national or regional publication shall be clearly indicated in the latter.
5) IEC itself does not provide any attestation of conformity. Independent certification bodies provide conformity assessment services and, in some areas, access to IEC marks of conformity. IEC is not responsible for any services carried out by independent certification bodies.
6) All users should ensure that they have the latest edition of this publication.
7) No liability shall attach to IEC or its directors, employees, servants or agents including individual experts and members of its technical committees and IEC National Committees for any personal injury, property damage or other damage of any nature whatsoever, whether direct or indirect, or for costs (including legal fees) and expenses arising out of the publication, use of, or reliance upon, this IEC Publication or any other IEC Publications.
8) Attention is drawn to the Normative references cited in this publication. Use of the referenced publications is indispensable for the correct application of this publication.
9) Attention is drawn to the possibility that some of the elements of this IEC Publication may be the subject of patent rights. IEC shall not be held responsible for identifying any or all such patent rights.

A PAS is a technical specification not fulfilling the requirements for a standard, but made available to the public.

IEC PAS 63151 has been prepared by IEC technical committee 106: Methods for the assessment of electric, magnetic and electromagnetic fields associated with human exposure.

The text of this PAS is based on the following document:	This PAS was approved for publication by the P-members of the committee concerned as indicated in the following document
Draft PAS	**Report on voting**
106/410/DPAS	106/420/RVDPAS

Following publication of this PAS, which is a pre-standard publication, the technical committee or subcommittee concerned may transform it into an International Standard.

This PAS shall remain valid for an initial maximum period of 3 years starting from the publication date. The validity may be extended for a single period up to a maximum of 3 years, at the end of which it shall be published as another type of normative document, or shall be withdrawn.

This publication has been drafted in accordance with the ISO/IEC Directives, Part 2.

A bilingual version of this publication may be issued at a later date.

IMPORTANT – The 'colour inside' logo on the cover page of this publication indicates that it contains colours which are considered to be useful for the correct understanding of its contents. Users should therefore print this document using a colour printer.

INTRODUCTION

This Publicly Available Specification (PAS) specifies the requirements for vector measurement-based systems to measure the Specific Absorption Rate (SAR) of devices that are used in close proximity to the human body or head.

This PAS is published in order to make available the current state of the technology. It is planned to publish a standard as Part 3 of the IEC 62209 series. When IEC 62209-3 is published this PAS will be withdrawn.

This PAS acknowledges the need for fast and accurate systems to determine the human exposure to radio frequency fields from hand-held and body mounted wireless communication devices.

As SAR measurement systems are used for showing compliance with national and international exposure limits the test procedures have to be standardized. The standardization is necessary to achieve comparable results for the approval process.

Vector measurement-based systems and protocols can differ from traditional SAR measurement systems and protocols. These systems use more advanced field reconstruction methods, allowing the application of indirect measurement approaches in which the SAR is evaluated in three dimensions from a limited number of measurement points which may be located in a limited part of the volume of interest, or even outside this volume. Such new SAR assessment approaches result in significantly reduced SAR measurement times.

MEASUREMENT PROCEDURE FOR THE ASSESSMENT OF SPECIFIC ABSORPTION RATE OF HUMAN EXPOSURE TO RADIO FREQUENCY FIELDS FROM HAND-HELD AND BODY-MOUNTED WIRELESS COMMUNICATION DEVICES –

Vector measurement-based systems (Frequency range of 30 MHz to 6 GHz)

1 Scope

This Publicly Available Specification (PAS) specifies protocols and test procedures for the reproducible measurement of the peak spatial-average specific absorption rate (psSAR) induced inside a simplified model of the head or the body by radio-frequency (RF) transmitting devices, with a defined uncertainty. It provides requirements for systems using vector measurement-based systems. Such systems determine the psSAR by 3D field reconstruction within the volume of interest by specifying the requirements for the measurement system, calibration, uncertainty assessment and validation methods. The protocols and procedures apply for a significant majority of people including children during use of hand-held and body-worn wireless communication devices.

This PAS is applicable to any wireless communication device intended to be used at a position near the human head or body at distances up to and including 200 mm. This PAS can be employed to evaluate SAR compliance of different types of wireless communication devices used next to the ear, in front of the face, mounted on the body, combined with other RF-transmitting or non-transmitting devices or accessories (e.g. belt-clip), or embedded in garments. The overall applicable frequency range is from 30 MHz to 6 GHz.

The system validation procedures provided within this PAS cover frequencies from 600 MHz to 6 GHz.

NOTE Some specifications (e.g., validation antennas and other procedures or requirements) are not yet defined over the full frequency range within the scope of this document but will be included in a future revision.

The device categories covered include but are not limited to mobile telephones, cordless microphones, auxiliary broadcast devices and radio transmitters in personal computers, desktop, laptop devices, multi-band, multi-antenna, and push-to-talk devices.

2 Normative references

The following documents are referred to in the text in such a way that some or all of their content constitutes requirements of this document. For dated references, only the edition cited applies. For undated references, the latest edition of the referenced document (including any amendments) applies.

ISO/IEC Guide 98-3, *Uncertainty of measurement – Part 3: Guide to the expression of uncertainty in measurement (GUM:1995)*

ISO/IEC 17025, *General requirements for the competence of testing and calibration laboratories*

IEC 62209-1:2016, *Measurement procedure for the assessment of specific absorption rate of human exposure to radio frequency fields from hand-held and body-mounted wireless communication devices – Part 1: Devices used next to the ear (Frequency range of 300 MHz to 6 GHz)*

IEC 62209-2, *Human exposure to radio frequency fields from hand-held and body-mounted wireless communication devices – Human models, instrumentation, and procedures – Part 2: Procedure to determine the specific absorption rate (SAR) for wireless communication devices used in close proximity to the human body (frequency range of 30 MHz to 6 GHz)*

IEC 62479, *Assessment of the compliance of low-power electronic and electrical equipment with the basic restrictions related to human exposure to electromagnetic fields (10 MHz to 300 GHz)*

IEC TR 62630:2010, *Guidance for evaluating exposure from multiple electromagnetic sources*

IEC/IEEE 62704 (all parts), *Determining the peak spatial-average specific absorption rate (SAR) in the human body from wireless communications devices, 30 MHz to 6 GHz*

3 Terms and definitions

For the purposes of this document, the terms and definitions given in IEC 62209-1, IEC 62209-2 and the following apply.

ISO and IEC maintain terminological databases for use in standardization at the following addresses:

- IEC Electropedia: available at http://www.electropedia.org/
- ISO Online browsing platform: available at http://www.iso.org/obp

3.1
vector probe
probe which measures both the magnitude and phase of an electric or magnetic field

3.2
scalar probe
probe which measures only the amplitude of the electric or magnetic field

3.3
vector measurement-based system
system consisting of multiple sensors which together provide information about the amplitude distribution or the amplitude and phase distribution of the electric or magnetic fields over a specified volume

3.4
analysis bandwidth (of a signal analyser)
maximum frequency span of observation for a system capable of spectral analysis. The analysis bandwidth is generally characterized by a certain flatness (± tolerance) of the responses of the system in the defined range of frequencies

4 Symbols and abbreviated terms

For the purposes of this document, the symbols and abbreviated terms in IEC 62209-1 and IEC 62209-2 apply.

5 Overview of the measurement procedure

The objective of this clause is to give the user of this PAS a quick overview about the test procedures in this PAS. The user of the PAS shall refer to the respective clauses for more details when using the flowchart.

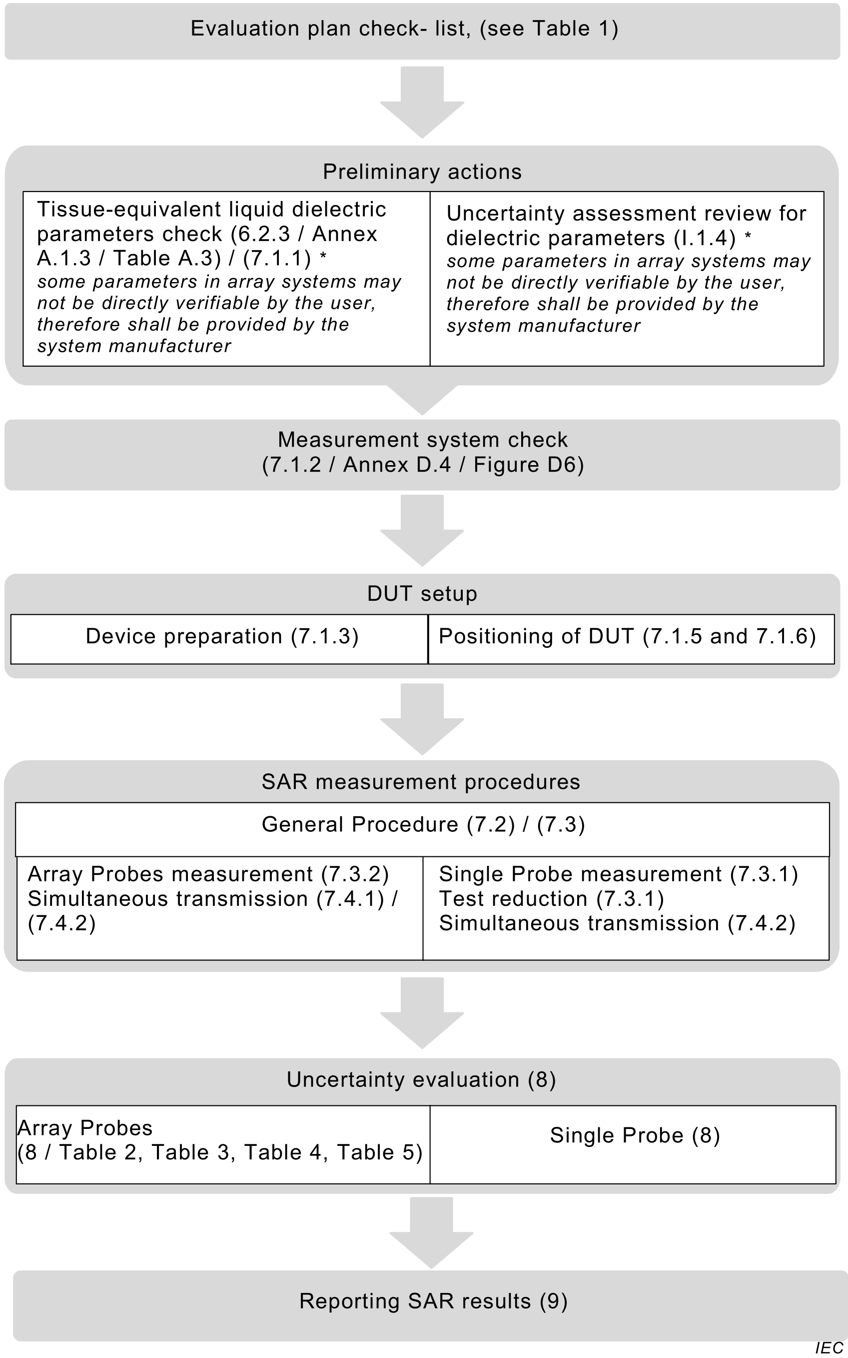

Figure 1 – Evaluation plan checklist

Table 1 – Evaluation plan checklist

Stage	Evaluation steps	Action
Evaluation plan check-list Planning of the measurement configurations	What type of device is being evaluated? Review of antenna contained and wireless technologies supported, singly or in combination. What are the test positions applicable? Working under laboratory conditions and following good laboratory practice and documentation, prepare to conduct the necessary evaluation.	Complete check-list based on evaluation plan (Table 1, Figure 1)
Preliminary actions and Measurement *system check*	A dielectric measurement of the tissue simulating medium shall be performed for systems with open phantoms, and the result shall be recorded. *System check* needs to be performed to verify the correct working of the system components (Annex D.3).	Shall be conducted before starting a project and repeated according to 7.1.2
DUT set-up Preparation of DUT	The protocol for SAR assessment defines all the permutations of operational conditions that should be tested. The essential steps include: Preparing the DUT by establishing a connection to a network simulator Configuring the DUT to operate on the appropriate test frequencies Positioning the DUT in relation to the phantom	Ensure the DUT is configured in the correct way and radiating appropriately when positioned against the phantom.
SAR measurements procedures General SAR procedure	This stage is the actual procedure of measurement of SAR. The procedure is iterative to ensure that the highest value of the peak spatial-average SAR of a DUT is captured. This is done by a systematic process looking at all device test positions, configurations and operating modes in all frequency bands accordingly (7.2). Systems can incorporate single probe (7.3.1) or array probes (7.3.2). Some accepted techniques that may be used to either reduce or accelerate the measurement process.	Determining highest SAR Ensure the rationale for test reduction is recorded and reported if used
Uncertainty evaluation	Guidelines and approximation formulas are provided (clause 8), enabling the estimation of each individual uncertainty component. The uncertainty budget shall cover the appropriate frequency range with regards to equipment used in the SAR system. For array systems, see (Table 2 to Table 5)	Determine uncertainty and complete the uncertainty table
Reporting SAR results	The final report describes the results of the evaluations, provides sufficient technical details to allow for repeatability of the evaluations performed and reports the results by comparison with the relevant limit (clause 9). The production of the test report will be the demonstration of compliance with this PAS.	Prepare the final report and consider the requirements listed in clause 9.

6 Measurement system specifications

6.1 General requirements

A vector measurement-based system consists of the phantom (a SAM phantom representing the human head and/or a flat phantom representing the human body) filled with tissue-equivalent medium, the electronic measurement instrumentation, one or multiple probes, a field reconstruction algorithm (Annex C) and DUT holder. The peak spatial-average SAR shall be assessed from the SAR distribution induced in the volume of the phantom from the electromagnetic fields produced by the DUT. The vector measurement-based system shall reconstruct the SAR in the volume of the phantom from the electric or magnetic fields measured by the probes. The vector measurement-based system may be a single probe system (scanning a single probe in the volume of the phantom) or an array system having multiple probes. The measurement system calibration shall be traceable to national standards and with quantified and documented measurement uncertainties. In addition, the systems shall meet the validation requirements specified in Annex D.

The information contained in the captured field shall be sufficient to determine the peak spatial-average SAR with an uncertainty meeting the requirements of this PAS. The manufacturer of the measurement system shall document the field reconstruction algorithms. The phantoms are filled with the required homogeneous tissue-equivalent medium. In the case of movable probes inside the phantom, the tissue-equivalent medium shall be a low-viscosity fluid to allow free movement of the probes within it. For a fixed probe-array no such constraint applies.

The tests shall be performed in a laboratory conforming to the following environmental conditions:

– The ambient temperature shall be within the range of 18 °C to 25 °C.
– In open systems where tissue-simulating material is in direct contact with air, tissue-equivalent medium dielectric properties shall be verified regularly following the procedures described in IEC 62209-1 and IEC 62209-2.
– In hermetic systems, the manufacturer shall provide either
    a) a procedure for the accurate measurement of dielectric properties, or
    b) documentation of the dielectric parameters and corresponding medium temperature and ambient temperature that were measured for the specific phantom when it was manufactured or during system recalibration.
– In hermetic systems, the manufacturer shall provide a demonstration of the stability of the dielectric properties of the tissue-simulating material over a period of time which is equal to or greater than the calibration interval of the SAR measurement system.
– Prior to tissue-equivalent medium dielectric properties measurement and SAR measurements, the DUT, test equipment, tissue simulating medium and phantom shall have been kept in the laboratory for their temperatures to have stabilized (i.e., they shall not have been recently moved from another area with a different ambient temperature, such as a refrigerator or storage area).
– Between the measurement of the dielectric parameters and the SAR measurement, the temperature of the tissue simulating medium shall not vary by more than 2 °C or by more than 5 %, in both ε and σ according to the temperature sensitivity measurement of the tissue simulating medium, whichever temperature range is less (both ε and σ shall stay within the tolerance of the targets), unless active temperature compensation is employed by the SAR measurement system. If active temperature compensation is used, the manufacturer of the measurement system shall provide documentation of the temperature measurement and compensation algorithms and the uncertainty of the temperature compensation. See Annex I.1.14.5 to determine the temperature sensitivity uncertainty of the tissue simulating medium.
– The effect of reflections from cables, test equipment, or other reflectors shall be determined using the SAR *system check* procedure with and without reflectors present or where necessary with the judicious placement of absorbing materials and/or the use of ferrite beads on cables.
– SAR measurements of DUT shall only be performed when the effects of reflections, secondary RF transmitters, etc., result in a peak spatial-average SAR (for 1 g or 10 g mass, whichever is applicable to the test) of less than 0,012 W/kg by measuring the peak spatial-average SAR at (approximately) 0,4 W/kg (used to establish the above 3 % limit) using the SAR *system check* procedure. When the effect of cables and reflectors is more than 0,012 W/kg, ferrite beads, RF absorbers and other mitigation techniques shall be applied to reduce the induced error. If the preceding limit cannot be achieved, a value higher than 3 % (0,012 W/kg) has to be considered in the uncertainty budget in the "RF ambient conditions – reflections" row, provided it can be demonstrated that the SAR contribution due to reflections determined by the *system check* procedure is less than 10 % of the SAR measured for the DUT. The requirement on reflections shall be verified at least every year or whenever the *system check* shows unexpected results.
– During testing the DUT shall not be connected to any wireless network except a base station simulator in the lab.

NOTE The terms *system validation* and *system check* are italicised because they refer to specific test protocols described for the purposes of this PAS.

System validation according to the protocol defined in Annex D shall be done at least once per year by the system manufacturer, including when a new system is put into operation and whenever modifications have been made to the system, such as a new software version with e.g., updated field reconstruction algorithms, different type or version of readout electronics or different types of probes. The full system validation defined in Annex D shall be performed the first time for a new measurement system. It may be unnecessary to perform a complete system validation each subsequent time. A reduced set of measurements may be performed if it can be demonstrated and documented by the system manufacturer that the set is sufficient to warrant acceptance according to the criteria (e.g., if the frequency dependent sensitivity of the sensors is constant due to reasons of sensor design, then the number of frequencies may be reduced). The antennas used for *system validation* shall be designed and validated to meet the requirements specified in this PAS (see Annex F).

NOTE System validation is normally performed by the system manufacturer, even though it is defined such that it can also be performed independently by any third party.

The measurement system shall be validated as a complete system (i.e., consisting of all parts, including the full sensor array, the dielectric medium, phantom shell, electronics, etc.). The measurement probe or probe array shall be calibrated in conditions equivalent to the final operating conditions meeting the requirements of this PAS. Probe or probe-array calibration shall be documented by the system manufacturer.

Where this PAS explicitly specifies performance characteristics for the measurement system or a part of the measurement system, the manufacturer of the system or of the part, or the system integrator shall document conformity with the provisions of this PAS.

6.2 Phantom specifications

6.2.1 Head Phantom specifications – shell

The SAM phantom shall be used as the head phantom. The rationale for the SAM phantom and the geometrical properties of the SAM phantom are provided in Annex A. The head SAR procedures in this PAS are applicable to the SAM phantom requirements in IEC 62209-1. For some system configurations, this may not be restricted to a sagittally-bisected horizontal SAM phantom. The phantom container may be open (i.e., the tissue-equivalent material is in direct contact with air) or hermetic.

6.2.2 Body Phantom specifications – shell

The flat phantom shall comply with requirements specified in Annex A. The phantom container may be open (i.e., the tissue-equivalent material is in direct contact with air) or hermetic.

6.2.3 Tissue-equivalent medium material properties

The phantom shall be filled with tissue-equivalent medium with the required dielectric properties. The dielectric parameters shall be evaluated and compared with the values given in Table A.3 using linear interpolation. This measurement can be performed using the equipment and procedures described in IEC 62209-1:2016, Annex J. The measured dielectric properties, not the values of Table A.3, shall be used in the SAR calculations.

To minimize reflections from the tissue-equivalent medium surface that is distal from the measurement (phantom) surface, the depth of the medium should be at least 15 cm from the flat body phantom inner surface or from the SAM inner surface above the ear reference point. In such case, the uncertainty due to such reflections does not need to be added to the budget. A medium depth of less than 15 cm may be used if it is demonstrated (e.g., using numerical simulations) that the effect on peak spatial-average SAR is less than 1 % under worst-case conditions. If it is more than 1, detailed evaluation of the maximum uncertainty shall be documented and added to the uncertainty budget. For the case of systems with hermetic phantoms, the depth of tissue-equivalent medium for the individual phantom shall be reported by the manufacturer.

6.3 Hand and Device holder considerations

The requirements of IEC 62209-1 and IEC 62209-2 apply.

6.4 Measurement system requirements

6.4.1 General

The vector measurement-based system may be a scanning system (moving a single probe in the volume of the phantom) or an array system with multiple probes. The requirements for scanning systems are provided in subclause 6.4.2, and the requirements for array systems are provided in subclause 6.4.3.

6.4.2 Single probe measurement system specifications

The single probe measurement system shall comply with the following:

– The probe and scanning system and reconstruction algorithm shall allow the determination of the spatial SAR distribution in the required regions of the phantom with known uncertainty for a near-field antenna placed outside the phantom. The requirements on the uncertainty are provided in 8.2.

– The manufacturer of the measurement system shall provide documentation to the user defining the measurement region and frequency range where the requirements of this PAS are met.

– The spatial resolution of the measurement grid and the reconstruction algorithm shall allow the fields to be reconstructed anywhere within the defined measurement region and to the boundary between the tissue-equivalent medium and the phantom shell.

– The accuracy of the probe tip positioning at a measurement point shall be documented and the related uncertainty shall be evaluated according to Annex I.1.10.

– All relevant uncertainty contributions as defined in clause 8 shall be assessed and documented.

– The dynamic range of the measurement system shall be such that the measurement uncertainty budget is valid for 1 g average SAR values from 0,1 W/kg to 10 W/kg for all modulations. The peak spatial-average SAR cube can be located anywhere in the region of the phantom in which the uncertainty is defined by the system manufacturer.

– Probe calibration shall be performed in conditions equivalent to its final operating condition meeting the requirements of this PAS. Calibration of the probe separately from the system is allowed, provided that the electrical interface characteristics between the probe and readout electronics are specified and implemented during measurements. The probe shall be calibrated together with the identical type of equipment (amplifier, filtering, data acquisition, etc.). The probe shall be calibrated at the appropriate operating frequency and temperature range, according to the methodology described in IEC 62209-1.

6.4.3 Array measurement system specifications

The array measurement system shall comply with the following:

– The probe array shall allow the measurement of the electric or magnetic field that is used as an input to the reconstruction algorithms that enable the determination of the spatial SAR distribution in the required regions of the phantom with known uncertainty for a near-field antenna placed outside the phantom. The requirements on the uncertainty are provided in 8.2.

– The manufacturer of the measurement system shall mark the extent of the measurement region on the flat phantom and document this region as well as the frequency range where the requirements of this PAS are met. At the head phantoms, the marking is not required as the DUT position and orientations are specified in the test procedure. Markings shall be such that phantom shell requirements of this PAS are still respected.

– For the head phantom, the SAR evaluation region of the system after field reconstruction shall include all points within the projection of the outline of the wireless device.

– The deviation of the locations of the probes in the array from their specified locations shall be documented and the related uncertainty shall be evaluated according to Annex I.1.2. These positions shall not vary by more than ±0,1 mm as a function of temperature and pressure. If the displacement is larger, the probe displacement shall be documented and the uncertainty shall be assessed by the system manufacturer.

– The spatial resolution of the measurement grid and the reconstruction algorithm shall allow the reconstruction of the fields anywhere within the defined measurement region and to the boundary between the tissue-equivalent medium and the phantom shell. The manufacturer shall document the types and spatial distribution of probes in the array. In particular, it shall be specified for each probe in the array:

  1) its location within the phantom;

  2) whether it is sensitive to incident magnetic or electric field;

  3) which polarizations of the incident field it is designed to receive;

  4) if they measure magnitude of the field only or magnitude and phase.

– All relevant uncertainty contributions as defined in clause 8 shall be assessed and documented.

– The dynamic range of the measurement system shall be such that the measurement uncertainty budget is valid for 1 g average SAR values from 0,1 W/kg to 10 W/kg for all modulations. 1 g and 10 g SAR cubes can be located anywhere in the region of the phantom in which the uncertainty is guaranteed by the manufacturer.

– Probe-array shall be calibrated at the considered operating frequency range and temperature range in conditions equivalent to its final operating condition meeting the requirements of this PAS. The probe-array sub-system shall be calibrated in the final phantom assembly, with the same or electrically equivalent read-out electronics used for the system and identical type of equipment (amplifiers, filtering, data acquisition etc.), at the appropriate operating frequencies and temperature range, with one of the methods described in the Annex B.

6.5 Device holder specification

The requirements for the device holder in IEC 62209-1 and IEC 62209-2 apply respectively for measurements at the head and flat phantoms. The DUT is preferably mounted on a piece of low relative permittivity (< 1,2) and low loss foam before being mounted into the device holder to avoid any direct contact between the device holder and the DUT. If this is not possible, the device holder shall provide the minimum amount of contact to the DUT to give a secure hold and maintain the required position during the measurement.

When the highest reported SAR is greater than 75 % of the compliance limit and the DUT has been measured in contact with the device holder, the highest SAR test condition among all frequency bands and positions shall be tested again for each single transmitter, without using the holder. In this case, the DUT position shall be realized by using low-loss foam material and non-conductive adhesive (e.g., tape or elastic bands). The peak spatial-average SAR both with and without holder conditions shall be reported. If the difference between these values is greater than the expanded ($k = 2$) uncertainty for measurement repeatability, then all SAR test conditions that are within the expanded ($k = 2$) uncertainty (see Clause 8) of the compliance limit shall be measured without the holder.

The effect of the hand on the exposure of the head phantom is not considered in this PAS. Refer to IEC 62209-1 for a rationale.

With array systems using closed flat phantom, a holder may not be needed in certain test positions. The DUT may for example be disposed over the flat phantom, in direct contact with the phantom or using a low-loss and low-permittivity high density foam spacer providing a separation distance.

6.6 Reconstruction algorithm and peak spatial-averaging specifications

Unlike SAR measurement systems defined in IEC 62209-1 and IEC 62209-2, a vector measurement-based system does not determine the peak spatial-average SAR directly from measurement points on a 3D grid covering the peak spatial averaging volume. Therefore, the purpose of the reconstruction algorithm is to determine the distribution of the SAR in the volume of interest such that the peak spatial-average SAR can be evaluated with known uncertainty using the electric and/or magnetic fields measured by the vector measurement-based system.

The following requirements on reconstruction and peak spatial-average SAR shall be met:

– The reconstruction algorithm shall determine the SAR distribution in the phantom from the measured electric and/or magnetic field from the sensors. The SAR distribution shall be determined within a volume containing all peak spatial-average SAR volumes (primary and secondary).
– The averaging volume shall be in the shape of a cube, except that the front face of the volume shall conform to the phantom shell and the back face shall be equally distorted. The four side walls of the cube shall be parallel to the line normal to the phantom at the centre of the front face of the averaging volume (Figure 2).
– The software of the measurement equipment shall provide error messages to the user if the peak spatial-average SAR is outside the spatial region for which the uncertainty requirements of this PAS are met.

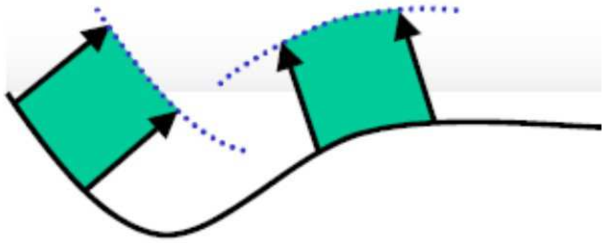

Figure 2 – Illustration of the shape and orientation relative to a curved phantom surface of the distorted cubic volume for computing peak spatial-average SAR

7 Protocol for SAR assessment

7.1 Measurement preparation

All measurements should be carried out with good laboratory practice, e.g., in accordance with ISO/IEC 17025, or any other local and national requirements for device certification. This PAS does not contain detailed information needed to configure devices for specific wireless technologies, such as transmission mode or data rate settings for satisfying national requirements to ensure that the maximum SAR is obtained.

7.1.1 Preparation of tissue-equivalent medium

Tissue equivalent medium shall yield relative permittivity and conductivity values within ±10 % of the target values at the frequencies at which the SAR is measured. Annex I.1.14 shall be used to correct the measured SAR for the deviations in permittivity and conductivity. If the correction ΔSAR has a negative sign, the measured SAR results shall not be corrected.

For systems using open phantom, the dielectric properties of the tissue-equivalent medium shall be measured within 24 h before the SAR measurements and every two days of continuous use. The dielectric properties of the tissue-equivalent medium may be measured less frequently (but not less than once per week) if the laboratory can document compliance with dielectric properties of the tissue-equivalent medium material as specified in IEC 62209-1 and in IEC 62209-2.

If the tissue simulating medium is in a hermetically sealed phantom the test laboratory may not be able to directly measure the dielectric properties of the tissue-equivalent medium. In this case, the manufacturer of the measurement system shall document compliance with dielectric properties of the tissue-equivalent medium during production, as specified in IEC 62209-1 and in IEC 62209-2, as well as the recommended procedure and measurement interval only if the latter is longer than the validity period of the system calibration. The compliance certificate shall be valid for the intervals between the measurements of dielectric properties of the tissue-equivalent medium.

7.1.2 System check

A *system check* according to the procedures of Annex D shall be completed within 24 hours before performing SAR measurements for the DUT. The purpose of the *system check* is to verify that the system operates within its specifications. The *system check* is a test of repeatability with a calibrated antenna to ensure that the system works correctly during the compliance test. The *system check* shall be performed in order to detect possible drift over short time periods and other uncertainties in the system, such as:

– unacceptable changes in the parameters of the tissue simulating medium, e.g. due to water evaporation or temperature changes;
– component failures;
– component drift;
– operator errors in the set-up or the software parameters;
– adverse conditions in the system, e.g., RF interference.

NOTE 1 The terms *system validation* and *system check* are italicised because they refer to specific test protocols described for the purposes of this PAS.

The *system check* procedure shall be performed on the same SAR measurement system, using the same SAR probe(s) and tissue-equivalent medium as the SAR evaluation of the DUT for each frequency band tested.

7.1.3 Preparation of the device under test

The requirements for the preparation of the DUT as specified in IEC 62209-1 and IEC 62209-2 apply.

7.1.4 Operating modes

For DUT operating modes, the requirements of IEC 62209-1 and IEC 62209-2 apply.

7.1.5 Position of the DUT in relation to the phantom

For the positioning of the DUT, the requirements of IEC 62209-1 and IEC 62209-2 apply.

7.1.6 Positions of the DUT in relation to the flat phantom for large DUT

If the DUT is equal to or larger than the measurement area supported by the phantom, the scan shall be divided into smaller regions. The DUT shall be shifted such that multiple scans can be combined to encompass at least the projection of the DUT over the flat phantom. When the DUT is shifted over the measurement area, the coupling between the DUT and phantom may be affected and differ from that with a larger phantom. Therefore, this procedure may not apply if there is a significant change in the shape of the SAR distribution between scans; otherwise, this effect shall be taken into account in the uncertainty evaluation.

To limit the measurement errors due to coupling variations, the scanned areas of the DUT from two successive tests shall overlap by at least one third in the shift direction as shown in Figure 3. The formula below provides the minimum number of tests to perform for a DUT equal to or larger than the measurement area, when successive SAR evaluations with one third overlapping section are combined:

$$NB_{\text{tests}} = NB_{\text{sublength}} \times NB_{\text{subwidth}} \tag{1}$$

$$NB_{\text{tests}} = \text{roundup}\left(((\left(\frac{L'}{L}\right)) \times (1 + \frac{1}{3})) \times \text{roundup}((\frac{W'}{W})\right) \times (1 + \frac{1}{3})) \tag{2}$$

Where:

L'	is the length of the DUT
W'	is the width of the DUT
L	is the length of the measurement area recommended by the manufacturer
W	is the width of the measurement area recommended by the manufacturer
NB_{tests}	is the number of tests performed on DUT sub-divisions for a complete SAR evaluation of the DUT
$NB_{\text{sublength}}$	is the number of sub-divisions of the DUT length
NB_{subwidth}	is the number of sub-divisions of the DUT width

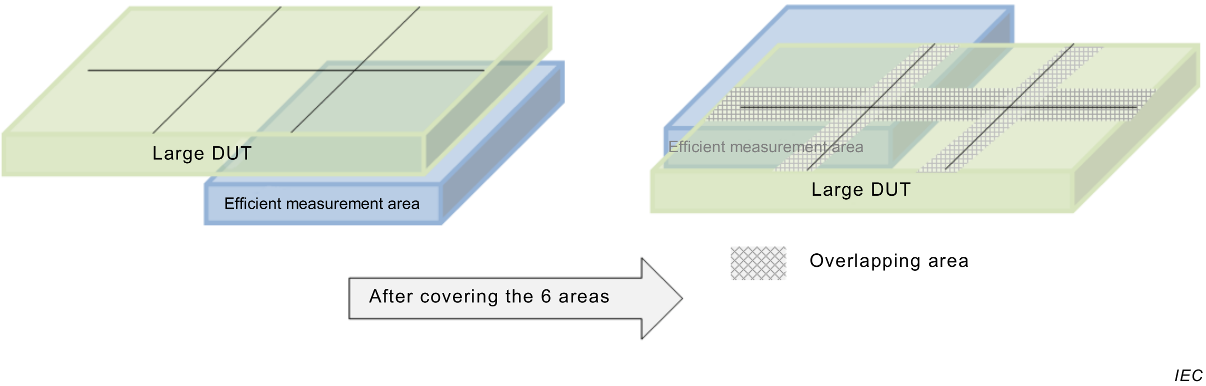

Figure 3 – Measurements performed by shifting a large device over the efficient measurement area of the system including overlapping areas – in this case: 6 tests performed

7.1.7 Test frequencies for DUT

A DUT shall be compliant with applicable exposure standards at all transmitting frequencies. However, testing at every channel is impractical and unnecessary. The purpose of this subclause is to define a practical subset of channels where SAR measurements are to be performed. This subset of channels is chosen so as to give a characterization of a DUT with any applicable exposure standards.

NOTE In some cases of Wi-Fi technology and other wide band systems such as WiMAX, the maximum output power of a channel may vary across the frequency band. The required test channels may not include the channel with the highest RF transmit power. For example, for Wi-Fi based technologies, the channels operating at the band edge may produce lower power in order to comply with specific out-of-band limits, therefore it may be necessary to perform the testing on the channel adjacent to the band edge channel. For other devices, the maximum output power of different channels may be optimized differently. Therefore, before performing testing using the specific channels required by this standard, the maximum output power of the channels need to be verified to determine the chosen channels are indeed producing the highest rated output of the device. The process used to establish the channels for testing purposes shall be documented in the test report.

For each operating mode of a wireless technology used by the DUT, tests shall be performed at the channel closest to the centre of each transmit frequency band. If the width of the transmit frequency band ($\Delta f = f_{\text{high}} - f_{\text{low}}$) exceeds 1 % of its centre frequency f_{c}, then the channels at the lowest and highest frequencies of the transmit band shall also be tested. Furthermore, if the width of the transmit band exceeds 10 % of its centre frequency, the following formula shall be used to determine the number of channels, N_{c}, to be tested:

$$N_{\text{c}} = 2 \times \text{roundup}\left[[10 \times \frac{(f_{\text{high}} - f_{\text{low}})}{f_{\text{c}}}] \right] + 1 \tag{3}$$

Where:

f_{c} is the centre frequency channel of the transmission band in Hz

f_{high} is the highest frequency channel of the transmission band in Hz

f_{low} is the lowest frequency channel of the transmission band in Hz

N_{c} is the number of channels

NOTE 1 The function $\text{roundup}(x)$ rounds its argument x to the next highest integer. Thus, the number of channels, N_{c}, will always be an odd number. The channels tested shall be equally spaced apart in frequency (as much as possible) and shall include the channels at the lowest and highest frequencies. Probe calibrations shall be valid for all test frequencies and liquid dielectric parameters at those frequencies. Substantially large transmission bands may require multiple probe calibration points and different tissue-equivalent liquids to cover the entire frequency band.

NOTE 2 Regulatory agencies may have different requirements on the number of channels to be tested per transmission band, according to frequency allocations and other wireless technology requirements.

NOTE 3 If the test frequency yielding the highest output power does not correspond to the middle channel, the test requirements may vary among different national regulatory authorities.

7.2 Tests to be performed

In order to determine the highest value of the peak spatial-average SAR of a device, all device positions, configurations and operational modes shall be tested for each frequency band according to step 1 to step 3 below.

Step 1:

The tests shall be performed at the channel that is closest to the centre of the transmit frequency band (f_{c}) for:

a) all device positions on the body phantom (if testing of DUT against body phantom is required);
b) all cheek and tilt positions on the left and right head phantoms (if testing of DUT against head phantom is required);
c) all configurations for each device position in a), e.g., with device slide or cover open and closed or antenna extended and retracted;
d) all operational modes, e.g., different resource block allocations in LTE or modulations, for each device position in Step 1 a) and configuration in Step 1 b) in each frequency band;
e) all antennas used.

Step 2:

For the test condition providing the highest peak spatial-average SAR determined in step 1, perform the tests at all other test frequencies as required by 7.1.7 (e.g., lowest and highest channels). In addition, for each device position, configuration and operating mode where the peak spatial-average SAR value determined in step 1a), step 1b) and step 1c) is greater than or equal to half of the applicable SAR limit, testing of other channels of 7.1.7 is required as well, otherwise it is not required.

Step 3:

Examine all data to determine the highest value of the peak spatial-average SAR found in step 1 to step 2 for each operation mode in each frequency band.

7.3 General measurement procedure

This clause documents the procedure to be performed for each of the test conditions described in 7.2. For single probe systems, the measurement procedure of 7.3.1 shall be applied. For array systems, the measurement procedure of 7.3.2 shall be applied.

7.3.1 Measurement procedure for single probe systems

If a single probe measurement system is used, the general measurement procedure of IEC 62209-1 or IEC 62209-2 (as appropriate) shall be applied, except that the zoom scan described in the procedure may not be required due to the use of the field reconstruction algorithm. Additionally, reference and drift measurements IEC 62209-1 or IEC 62209-2 may be replaced by the following procedure:

- If the DUT power drifts by more than 2 % during the SAR measurement period, the SAR shall be measured at a fixed reference point immediately before and after the SAR evaluation. The reference point shall be within 10 mm of the inner surface of the phantom where the measured local field exceeds the lower detection limit of the measurement system. The SAR drift of the DUT is estimated as the difference between the two measured single-point SAR values.
- If the SAR drift exceeds 5 % then the provisions of Annex I.4.3 shall apply

7.3.2 Measurement procedure for array systems

If an array system is used, the following procedure and requirements shall be applied:

a) Measure the electric or magnetic field over the measurement region.

b) Apply the reconstruction algorithm to reconstruct the SAR distribution in the applicable volume of the phantom.

c) Apply the averaging algorithm to determine the peak spatial-average SAR.

Commercial devices typically have output power drifts within ±5 %. Some devices could have significant fluctuations in output power that are not classifiable as undesirable power drift but rather are a characteristic of the normal operating behaviour of the device. In these cases, methods such as power scaling shall be applied with the aim of ensuring that an accurate and conservative SAR is obtained.

7.4 SAR measurements for simultaneous transmission

DUTs with multiple antennas or multiple transmitters (with single or multiple antennas) transmitting simultaneously require special test considerations. The methods to combine the fields in order to determine the combined SAR distribution differ depending on whether the corresponding RF transmitters emit waveforms that are correlated or uncorrelated in time (IEC TR 62630).

7.4.1 SAR measurements for non-correlated signals

When two or more signals are non-correlated (e.g., transmission at different frequencies, modulations, or data streams), the combined SAR at each location, r, in the phantom is calculated from simple summation of the SAR values of the individual transmitters:

$$SAR_{\mathrm{T}}(r) = \sum_{k=1}^{N} SAR_{\mathrm{k}}(r) \qquad (4)$$

Prior to averaging and search of the peak spatial-average SAR, each SAR distribution shall be assessed separately. After field reconstruction and determination of the individual SAR distributions, $SAR_k(r)$, the summation given in the above equation is performed. The averaging and search of the peak-spatial average SAR are then conducted.

The above procedure applies regardless of whether the N non-correlated signals are turned on separately or transmitting simultaneously. SAR measurement while signals are transmitting simultaneously is possible only if the measurement system is capable of distinguishing the signals so that they can be processed separately.

For measurement equipment, capable of distinguishing between various signals and frequency contributions, direct SAR assessment for simultaneous transmission, including carrier aggregation technologies (with contiguous or non-contiguous transmitting channels), can be performed providing that all the transmission frequencies fall within a valid range of both the probe calibration and the tissue equivalent medium. In such a case, the following procedure applies:

a) The DUT is set to transmit simultaneously at frequencies f_1, f_2, f_N... in the considered supported transmission mode.
b) The DUT is positioned to the phantom according to 7.1.5.
c) Measurement system is set to measure SAR at frequency f_1, so that frequency contributions falling within the $f_1 \pm B_a/2$ range are assessed. B_a is the analysis bandwidth of the probe or probe-array readout electronics. The procedure described here supposes B_a is larger than the signal bandwidth B_s.
d) If $f_i \pm B_{si}/2$, for any transmitter i between 2 and N, is contained in the $f_1 \pm B_a/2$ range, then the SAR is measured directly as in the case of single-frequency transmission mode. This is equally applied to the case where more than two signal bands fall within B_a.
e) If there is no overlap between $f_i \pm B_{si}/2$, for any index transmitter index i, and $f_1 \pm B_a/2$ range, then measure SAR for the f_1 transmission mode.
f) If there is overlap between $f_i \pm B_{si}/2$ and $f_1 \pm B_a/2$ range, then (i) reduce the analysis bandwidth to match a bandwidth as small as possible but no lower than B_{s1} and avoid overlap, then apply step g); (ii) enlarge and/or move the analysis bandwidth so that the span from the minimum frequency to the maximum frequency of the two signals falls within the analysis bandwidth, then apply step d).

   NOTE Depending on measurement system technology, the analysis bandwidth can be in the radiofrequency range or DC centred using downconverting techniques.

g) Set the measurement system to measure SAR at frequency f_2, so that frequency contributions falling within the $f_2 \pm B_a/2$ range are assessed. Apply step d), step e) and step f) for transmitter 2 as appropriate.
h) Repeat step d), step e), step f) and step g) for all other transmission modes.
i) Use one of the four alternatives defined in clause 6.4.3.2 of IEC 62209-1:2016 to obtain the combined SAR.

7.4.2 SAR measurements for correlated signals

DUTs with multiple antennas transmitting correlated signals simultaneously represent a particular case of devices such as MIMO transmitters with digital beam-forming capabilities and require special test considerations. Signals of such DUTs can be classified based on the change of relative phases of signal in a normal communication. In general, there are two types of signals that can be found in most of recent generation multi-antenna transmitters. The first, referred to as type 1, is signals with relative phases unchanged during a relatively long duration compared with symbol duration. This type of signals can be found in phased array antenna systems where the relative phases of signals fed to the antennas are controlled to form the radiation pattern of the array antenna toward a certain direction. In different operating environments, the relative phases may change to obtain different desired radiation patterns. Yet, as soon as transmitting direction is determined and the pattern is formed, the relative phases will be fixed during certain duration, and will only change when the radiation pattern is configured to another form. In fact, the duration that relative phases are kept unchanged is relatively long, compared with the duration of a symbol in normal communication. The second type, referred to as type 2, on the other hand, is signals with relative phases changed quickly in a relatively short duration. Such signals can be found in the systems utilizing MIMO techniques. Relative phases of signals will be changed from symbols to symbols due to the function of space-time block code (STBC) in the MIMO schemes. The relative phases of signals are changed from symbol to symbol according to the STBC coding, and no specified direction is formed during a normal communication.

As explained in IEC TR 62630, the correlated signals can only be transmitted at the same carrier frequency and SAR depends on the relative phase(s) between the signals.

For type 1 correlated signals, the peak spatial-average SAR is evaluated by one of the methods described in IEC TR 62630. Prior to averaging and search of the peak spatial-average SAR, each field distribution shall be assessed separately. After field reconstruction of each signal contribution, the combined SAR distribution is determined at each point either by summation of the E-field magnitudes, summation of the E-field components or summation of the complex E-field vectors (IEC TR 62630). The averaging and search of the peak-spatial average SAR are then conducted. Summation of the E-field magnitudes or E-field components provides a conservative overestimation compared to the summation of the E-field vectors. If both amplitude and phase of the electric field are known, it is possible to accurately evaluate peak spatial-average SAR under simultaneous transmission condition by combining the vector fields of each individual transmitter, transmitting separately at the highest time-averaged output power with single SAR measurements, in such case, clause 6.5.1 of IEC TR 62630:2010 applies to characterize the combined fields from correlated signals.

For type 1 correlated signals, the phase combination providing the highest peak spatial-average SAR shall be determined from among the set of phase combinations that the device is capable of. If summation of the complex E-field vectors is used, post-processing may be used to vary the phases prior to summation (i.e., for two signals, add a constant phase shift to the induced E-fields from the second signal, then add the SAR distributions from the first and second signals). Otherwise, other techniques can be used, such as measurement of all phase combinations or estimation from fewer phase combinations.

For type 2 correlated signals, the SAR shall be measured with all signals transmitting simultaneously. The signal integration time shall be sufficient to ensure that enough symbols are transmitted.

8 Uncertainty estimation

8.1 General

The uncertainty budget is applicable to either head or body SAR measurements. The estimate of the measurement repeatability, as verified by the *system check* measurement, is obtained by omitting the Type B contributions from the uncertainty budget. The uncertainty budget calculated in Table 2 to Table 5 is an example for the 1 g or 10 g SAR measurement of a DUT or a validation antenna.

Each input quantity is described together with an example of how the associated standard uncertainty is evaluated. These are general examples that may not be applicable to all measuring systems, and additional quantities may be required in a specific case as determined by the system manufacturer.

Further information for system manufacturers and calibration laboratories to assess the measurement system uncertainty is given in ISO/IEC Guide 98-3.

8.2 Requirements on the uncertainty evaluation

The expanded uncertainty is the result of an uncertainty evaluation, specific details of which are recorded in an uncertainty budget. Separate uncertainty budgets shall be evaluated for SAR measurements according to the following:

- The expanded uncertainty in the measured value of mass-averaged SAR (1 g or 10 g) shall be assessed in accordance with the guidance and explanation given in ISO/IEC Guide 98-3 and requirements specified in this PAS.
- The frequency range for which the uncertainty analysis is valid shall be specified.
- The reported uncertainty shall represent the maximum expanded uncertainty within this range.
- The expanded uncertainty in the *system check* and *system validation* measurements shall also be evaluated. The uncertainty shall be quoted at the 95 % confidence level, and the expanded uncertainty shall not exceed 30 % of the peak spatial-average SAR value in the range of 0,4 W/kg to 10 W/kg for SAR averaged over 1 g.
- If the expanded uncertainty for DUT testing is greater than 30 % and it is not related to errors due to incorrect test setup of the test equipment or device, reported data needs to take into account the percentage difference between the actual uncertainty and the 30 % target value (ISO/IEC Guide 98–3). The formula for reducing the applicable SAR limit by the excess uncertainty shall be as described in IEC 62479.

8.3 Description of uncertainty models

The combined standard uncertainty of the 1 g or 10 g SAR consists of uncertainty contributions from the following influences.

1) **Measuring system uncertainties to be specified by the manufacturer,** MM (Annex I.1 and top section of Table 2): The standard uncertainty for calibration of the vector measurement-based system is determined by the system calibration laboratory or manufacturer.
2) **Uncertainties in post-processing and corrections,** MN (Annex I.2 and bottom section of Table 2): applied to the measurand (i.e. SAR scaling, etc.).
3) **Measuring system uncertainties which are dependent on the device under test (DUT)** (Annex I.3 and Table 3): These uncertainties include those relating to device position (I.4.2), device holder (I.4.1), integration time (I.3.4), signal modulation (I.3.3), coupling between the antenna and the sensor array (I.3.2). The corresponding uncertainty may include a Type A uncertainty analysis based on a set of sources which shall be documented and demonstrated to be sufficient for ensuring a conservative assessment of the related uncertainty contribution. The analytical approach described in Annex H.5 may also be used.
4) **Environmental factors** (Annex I.4 and Table 3): The uncertainties caused by the laboratory environment in which the measuring system will be used. These uncertainties include those relating to temperature, ambient signals and reflections.
5) **DUT-related uncertainties** (Annex I.4 and Table 3): including drift in RF output, device holder effects, positional errors and modulation (if different from those in 2).

The types of devices under test for which the combined uncertainty estimate is valid shall be stated. For all other devices, additional tests may be required to establish the measurement uncertainty. The uncertainty analysis shall be performed at a set of frequencies which is sufficient to ensure that the uncertainty between the frequencies of characterization is not higher than at the frequencies of evaluation.

The measuring system uncertainties shall be assessed separately for head or body measurements and for 1 g or 10 g averaged SAR as required. All error terms are given as fractions or percentages. The measurement uncertainty shall be a realistic estimate of the uncertainty in the measured SAR of the device under test, and this will be multiplied by a coverage factor to provide a 95 % confidence level.

According to ISO/IEC Guide 98-3 the uncertainty is defined as the root-sum-squared of the uncertainty contributions. The following uncertainty components are defined that are described in Annex I:

Measuring system uncertainties to be specified by the manufacturer:

$$MS = \sqrt{MM^2 + MN^2} \quad (5)$$

where MM and MN are the errors in the measurement system and errors in the corrections and post-processing, respectively:

$$MM = \sqrt{CF^2 + ISO^2 + MSC^2 + AS^2 + LIN^2 + SL^2 + BE^2 + RE^2 + RT^2 + PP^2 + SE^2 + AB^2 + PS^2 + MAT^2 + HOM^2} \quad (6)$$

$$MN = \sqrt{REC^2 + POL^2 + SAV^2 + SARS^2 + SC^2} \quad (7)$$

SAR measurement of a DUT:

$$\Delta SAR = \sqrt{MS^2 + PAC^2 + MOD^2 + IT^2 + DN^2 + DP^2 + DH^2 + SD^2 + AC^2 + MSI^2} \quad (8)$$

For *system validation* measurement:

$$\Delta SAR = \sqrt{MS^2 + PAC^2 + MOD^2 + IT^2 + DN^2 + DP^2 + DH^2 + AC^2 + MSI^2 + DEX^2 + OVS^2} \quad (9)$$

For *system check* measurement:

$$\Delta SAR = \sqrt{MS^2 + PAC^2 + MOD^2 + IT^2 + DN^2 + DP^2 + DH^2 + AC^2 + MSI^2 + DEX^2 + OVS^2} \quad (10)$$

Table 2 to Table 5 show the templates for the uncertainty budgets of the above equations.

Table 2 – Uncertainty budget template for the evaluation of the measurement system uncertainty of the 1 g or 10 g psSAR to be carried out by the system manufacturer (N = normal, R = rectangular)

Symbol /notes	Quantity x_i (source of uncertainty)	Reference	Prob. Dist.*	Uncertainty	Divisor *q	$u(x_i)$	c_i	$u_i(y)$	v_i
Uncertainty in the measurement system to be specified by the manufacturer (*MM*)									
CF	Calibration	I.1.1							n
ISO	Vector probe or vector probe-array isotropy	I.1.2							n
MSC	Mutual sensor coupling	I.1.3							n
AS	Scattering within the array	I.1.4							n
LIN	System linearity	I.1.5							n
SL	Sensitivity limit	I.1.6							n
BE	Boundary Effect	I.1.7							n
RE	Readout Electronics	I.1.8							n
RT	Response Time	I.1.9							n
PP	Probe Positioning	I.1.10							n
SE	Sampling error	I.1.11							n
AB	Array Boundaries	I.1.12							n
PS	Phantom shell	I.1.13							n
MAT	Tissue-equivalent material parameters	I.1.14							n
HOM	Phantom Homogeneity	I.1.15							n
Uncertainty in corrections and post processing to be specified by the manufacturer (*MN*)									
REC	Reconstruction	I.2.2							n
POL	Impact of noise on interpolation and extrapolation	I.2.3							n
SAV	SAR averaging	I.2.4							n
SARS	SAR scaling	I.2.5							n
SC	SAR correction for deviations in permittivity and conductivity	I.2.6							n
MS	Uncertainty (k=1) and effective degrees of freedom						U=		v_{eff}=

* Probability distributions and divisors are chosen to best represent available knowledge of the quantities concerned.

n = number of repeated measurements used in the Type A evaluation.

Some uncertainty components may be evaluated in combination with other uncertainty components.

Table 3 – Uncertainty budget template for evaluating the uncertainty in the measured value of 1 g SAR or 10 g SAR from a DUT (N = normal, R = rectangular)

Symbol /notes	Quantity x_i (source of uncertainty)	Reference	Prob. Dist.*	Uncertainty	Divisor *q	$u(x_i)$	c_i	$u_i(y)$	v_i
Measuring system uncertainties to be specified by the manufacturer									
MS	Measuring system uncertainties to be specified by the manufacturer	Table 2							*n*
Measuring system uncertainties which are dependent on the DUT									
PAC	Probe or probe-array coupling with DUT	I.3.2							*n*
MOD	Modulation response	I.3.3							*n*
IT	Integration time	I.3.4							*n*
DN	Drift and noise	I.3.5							*n*
DUT-related uncertainties related uncertainties and environmental factors									
DP	Device positioning	I.4.2							*n*
DH	Device holder	I.4.1							*n*
SD	Measured SAR drift	I.4.3							*n*
AC	RF ambient conditions	I.4.4							*n*
MSI	Measurement system immunity/secondary reception	I.4.5							*n*
U	Expanded uncertainty and effective degrees of freedom						U=		v_{eff} =

* Probability distributions and divisors are chosen to best represent available knowledge of the quantities concerned.

n = number of repeated measurements used in the Type A evaluation.

Some uncertainty components may be evaluated in combination with other uncertainty components.

Table 4 – Uncertainty budget template for evaluating the uncertainty in the measured value of 1 g SAR or 10 g SAR from a validation antenna (N = normal, R = rectangular)

Symbol /notes	Quantity x_i (source of uncertainty)	Reference	Prob. Dist.*	Uncertainty	Divisor *q	$u(x_i)$	c_i	$u_i(y)$	v_i
Measuring system uncertainties to be specified by the manufacturer									
MS	Measuring system uncertainties to be specified by the manufacturer	Table 2							n
Measuring system uncertainties which are dependent on the DUT									
PAC	Probe or probe-array coupling with DUT	I.3.2							n
MOD	Modulation response	I.3.3							n
IT	Integration time	I.3.4							n
DN	Drift and noise	I.3.5							n
Validation antenna related uncertainties and environmental factors									
DP	Device positioning	I.4.2							n
DH	Device holder	I.4.1							n
AC	RF ambient conditions	I.4.4							n
MSI	Measurement system immunity/secondary reception	I.4.5							n
DEX	Deviation of experimental antennas	I.4.6							n
OVS	Other uncertainty contributions when using validation antennas	I.4.7							n
U	Expanded uncertainty and effective degrees of freedom						U=		v_{eff} =

* Probability distributions and divisors are chosen to best represent available knowledge of the quantities concerned.

n = number of repeated measurements used in the Type A evaluation.

Some uncertainty components may be evaluated in combination with other uncertainty components.

Table 5 – Uncertainty budget template for evaluating the uncertainty in the measured value of 1 g SAR or 10 g SAR from the *system check* (N = normal, R = rectangular)

Symbol /notes	Quantity x_i (source of uncertainty)	Reference	Prob. Dist.*	Uncertainty	Divisor *q	$u(x_i)$	c_i	$u_i(y)$	v_i
Measuring system uncertainties to be specified by the manufacturer									
MS	Measuring system uncertainties to be specified by the manufacturer	Table 2					1		∞
Measuring system uncertainties which are dependent on the DUT									
PAC	Probe or probe-array coupling with DUT	I.3.2					1		∞
MOD	Modulation response	I.3.3					0		∞
IT	Integration time	I.3.4					0		∞
DN	Drift and noise	I.3.5					1		∞
DUT-related uncertainties or system check antenna related uncertainties and environmental factors									
AC	RF ambient conditions	I.4.4					1		∞
MSI	Measurement system immunity/secondary reception	I.4.5					1		∞
DEX	Deviation of experimental antennas	I.4.6					1		∞
OVS	Other uncertainty contributions when using system check antennas	I.4.7					1		∞
U	Expanded uncertainty and effective degrees of freedom						U=		v_{eff} =
* Probability distributions and divisors are chosen to best represent available knowledge of the quantities concerned.									
n = number of repeated measurements used in the Type A evaluation.									
Some uncertainty components may be evaluated in combination with other uncertainty components.									

9 Measurement report

The requirements of IEC 62209-1 and IEC 62209-2 apply, as well as the reporting requirements specified in other clauses of this PAS.

Annex A
(normative)

Phantom specifications

A.1 SAM phantom specifications

The justification for the SAM phantom is provided in IEC 62209-1.

A.1.1 SAM phantom geometry

The dimensions of the SAM phantom have been derived from selected 90th percentile male head data reported by Gordon et al. [61], and are listed in Table A.1 and shown in Figure A.1. Table A.2 shows other pertinent dimensions for comparison. At the ear reference point (ERP), a thickness of 6 mm including the 2 mm shell is selected to model the external ear (pinna). This thin ear spacer also simulates users with small ears, and gives a conservative SAR representation. A system of reference points and reference lines is used to correlate the device positioning with the phantom (Figure A.2 and Figure A.3). The point “M” is the mouth reference point, “LE” is the left ear reference point (ERP), and “RE” is the right ERP. The ERPs are 15 mm posterior to the entrance to ear canal (EEC) along the B-M Line (back-mouth) (Figure A.2).

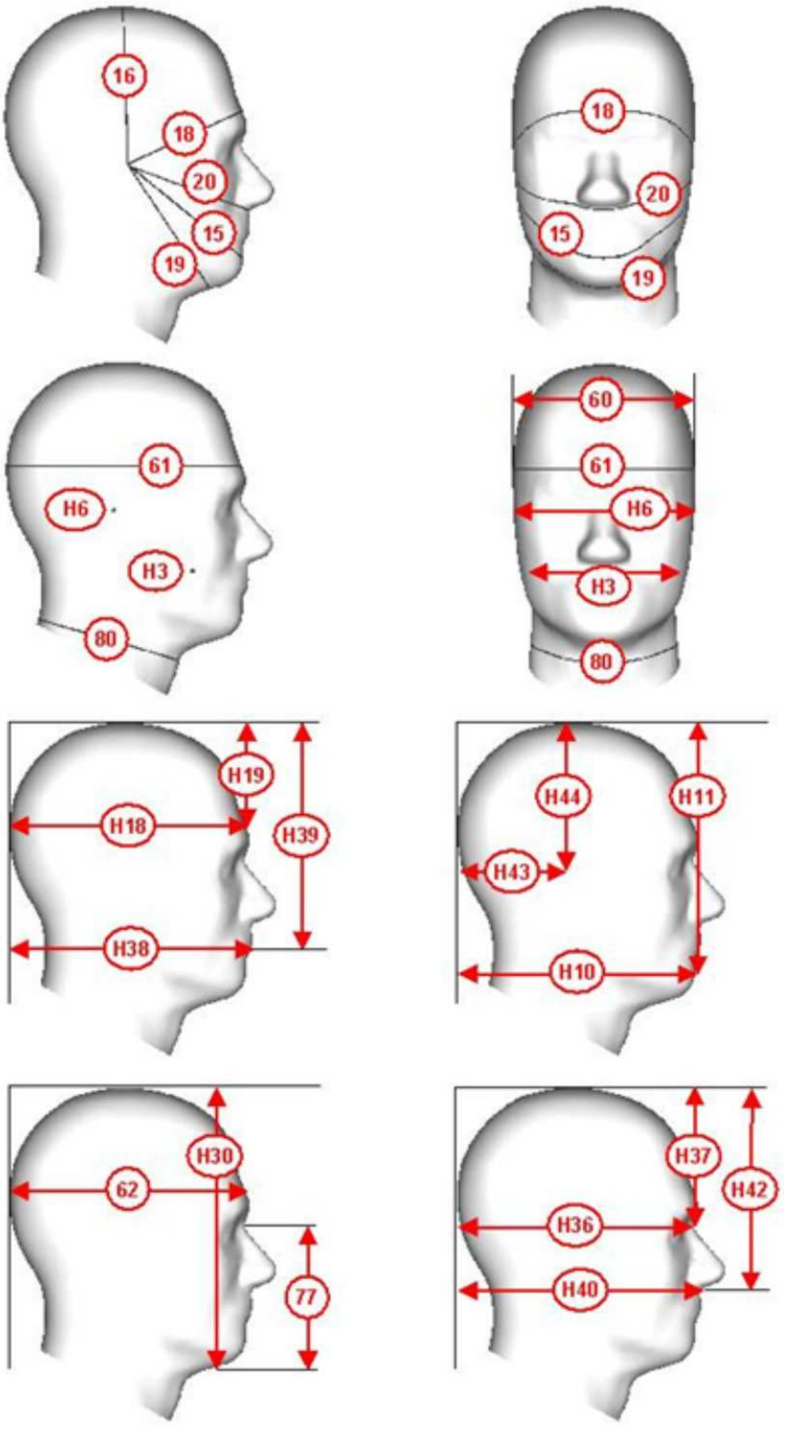

NOTE The dimensions in Table A.1 are used to define the SAM phantom. The dimensions in Table A.2 are measured on the SAM phantom and compared with the ARMY data

Figure A.1 – Illustration of dimensions in Table A.1 and Table A.2

Table A.1 – Dimensions used in deriving SAM phantom from the ARMY 90th percentile male head data (Gordon et al.[61])

Ref.	Anatomy	Gordon report [mm]			SAM [mm]	Deviation [%]
		Mean value	Std deviation	90th Percentile		
H15	Bitragion Chin Arc	325,8	13,4	343,1	329,3	-4,0
H16	Bitragion Coronal Arc	353,3	12,9	369,7	367,3	-0,6
H18	Bitragion Frontal Arc	304,3	10,6	318,2	314,1	-1,3
H19	Bitragion Submandibular Arc	304,2	14,5	323,2	333,5	3,2
H20	Bitragion Subnasale Arc	292	11,1	306,3	305,3	-0,3
H60	Head Breadth	151,7	5,4	158,6	158,4	-0,1
H61	Head Circumference	567,7	15,4	587,3	594,8	1,3
H62	Head Length	197,1	7,1	206	206,0	0,0
H77	Menton-Sellion Length	121,9	6,5	130,4	125,0	-4,1
H80	Neck Circumference	379,6	19,7	405,3	395,4	-2,5

Table A.2 – Additional SAM dimensions compared with selected dimensions from the ARMY 90th-percentile male head data (Gordon et al. [61]) – Specialist head measurement section

Ref.	Anatomy	Gordon report [mm]			SAM [mm]	Deviation [%]
		Mean value	Std deviation	90th Percentile		
H3	Bigonial Breadth	118,9	7,9	129,2	130,0	0,6
H6	Bitragion Breadth	144,8	6	152,3	152,7	0,2
H10	Chin-Back of Head	194,2	10,3	207,3	206,5	-0,4
H11	Chin-Top of Head	216,8	8,9	228,3	220,4	-3,5
H18	Glabella-Back of Head	199,7	7,2	208,5	209,2	0,3
H19	Glabella-Top of Head	96,2	7,3	105,6	104,4	-1,1
H30	Menton-Top of Head	232,0	8,8	243,3	246,7	1,4
H36	Sellion-Back of Head	197	7,1	205,9	205,3	-0,3
H37	Sellion-Top of Head	112	6,9	120,9	121,7	0,7
H38	Stomion-Back of Head	199,4	9,6	211,9	211,4	-0,2
H39	Stomion-Top of Head	186,3	7,8	196,3	196,3	0,0
H40	Subnasale-Back of Head	203,5	8,3	213,6	213,0	-0,3
H42	Subnasale-Top of Head	161,9	7,7	171,8	177,6	3,4
H43	Tragion-Back of Head	98,9	8,5	106,4	106,4	0,0
H44	Tragion-Top of Head	131	5,7	138,2	138,2	0,0

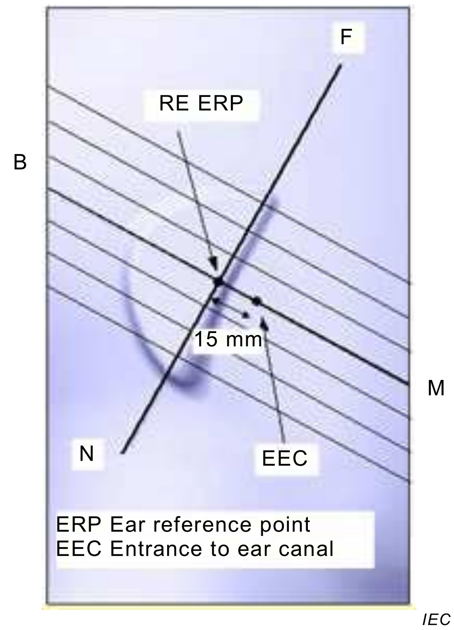

Key

B Direction of B-M line back endpoint

F Direction of N-F line front endpoint

N Direction of N-F line neck endpoint

M Mouth reference point

RE Right ear reference point (ERP)

Figure A.2 – Close up side view of phantom showing the ear region

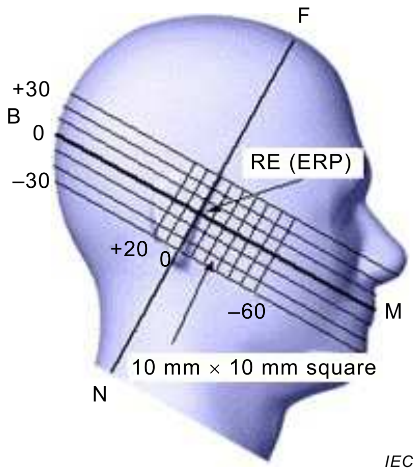

Key

B Line B-M back endpoint

M Line B-M front endpoint

N Line N-F neck endpoint

F Line N-F front endpoint

RE Right ear reference point (ERP)

Figure A.3 – Side view of the phantom showing relevant markings, dimensions are in mm

NOTE The full-head model is shown for illustration purposes only. The procedures in this PAS are derived primarily for the phantom set-up shown in Figure A.3.

The plane passing through the two ear reference points and M is defined as the reference plane. The line N-F (neck-front), also called the reference pivoting line, is along the front truncated edge of the ear. Both N-F and B-M lines shall be marked on the external phantom shell to facilitate handset positioning. Posterior to the N-F line, the thickness of the phantom shell with the shape of an ear is a flat surface 6 mm thick at the ERPs. Anterior to the N-F line, the ear is truncated as illustrated in Figure A.2. The ear truncation is introduced to preclude unstable handset positioning at the cheek.

The projection of the reference line B-M and reference line N-F shall be marked on the phantom. Additional lines may be chosen for convenience, but the additional lines are optional. The optional markings in Figure A.3 may be etched into the external surface of the phantom without affecting the compliance with phantom shell thickness and dielectric parameter requirements.

A.1.2 SAM Phantom shell

The phantom shell with integral solid ear spacer, as specified in the SAM CAD model, shall be constructed from chemical-resistant, non-hygroscopic, low-permittivity and low-loss material, with relative permittivity between 2 and 5; however, less than 2 is acceptable for frequencies up to 3 GHz. The loss tangent of the phantom shell shall be less than or equal to 0,05. It has been shown that at higher frequencies, particularly above 3 GHz, the permittivity of the phantom shell, has an increasing impact on SAR measurement uncertainty (ISO/IEC Guide 98-3). According to ISO/IEC Guide 98-3, the SAR is affected by the shell even though the shell is thin and has dielectric properties much lower than the tissue-equivalent medium. Specifically, they showed that the variation in the SAR depends not only on the frequency, but also on the relative permittivity of the shell and the distance between the antenna and the material. It was recommended that the effects of the shell shall be taken into account in the higher frequency range. Therefore, uncertainty evaluation shall be conducted above 3 GHz according to Annex I.1.13. The shape of the phantom shell shall have a tolerance of less than ±0,2 mm with respect to the SAM CAD file. In any area within the projection of the handset, the shell thickness shall be 2 mm ± 0,2 mm. The phantom shell shall be made of materials resistive to compounds used for making tissue-equivalent media (e.g., those listed in Annex I of IEC 62209-1:2016), to avoid damage and preserve the ±0,2 mm tolerances. For non-critical areas, i.e., the central strip containing the nose, as shown in Figure A.5, the thickness tolerance is allowed to be within ±1 mm.

The CAD file cross section for the reference plane is given in Figure A.4.

NOTE The CAD model is for use in the basic manufacture of the SAM phantom standard test fixture by groups having the necessary expertise and resources. Four *.IGES files of inner and outer surfaces for the left and right halves extracted from the CAD model of the SAM phantom are available on the support document folder of http://www.iec.ch/tc106. The four file names are:

1) sam_lft_in_6_11.igs
2) sam_lft_out_6_11.igs
3) sam_rt_in_6_11.igs
4) sam_rt_out_6_11.igs

Dimensions in millimetres

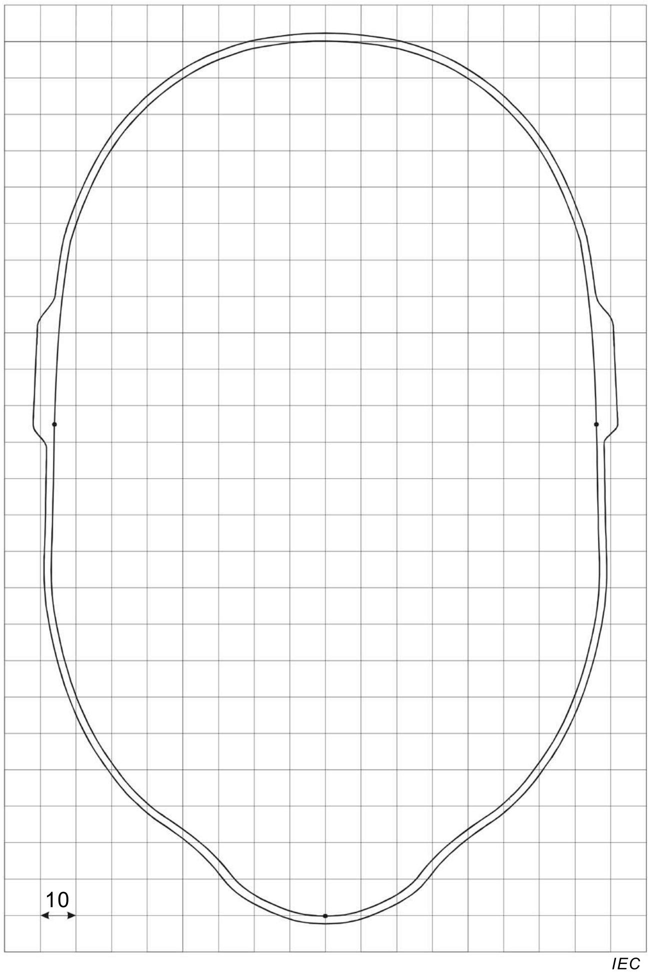

Figure A.4 – Cross-sectional view of SAM at the reference plane

A.1.3 Tissue Equivalent Medium

The phantom shall be filled with a homogeneous tissue-equivalent medium. The dielectric parameters of the tissue-equivalent medium are provided in A.4.

If the vector measurement-based system is a single probe measurement system, the phantom shall be an open container and the tissue-equivalent medium shall be a liquid, so as to allow the scanning system to move the probe. The sagittally-bisected phantom is recommended for devices having the peak spatial-average SAR near the ear (see Figure A.5). Other phantom orientations may be used if the peak spatial-average SAR is in another region of the head. Different phantom orientations may also be necessary for enabling probe access to certain regions of the SAM phantom for SAR measurement. For single probe systems, the orientation of the phantom should be chosen to minimize the measurement uncertainties (e.g., from probe isotropy and boundary effects). If the vector measurement-based system is an array system with fixed sensor locations, the phantom can be a closed container and the tissue-equivalent medium can be either solid or liquid. The orientation of the SAM phantom is irrelevant if a closed container is used.

To minimize reflections within the phantom, the depth of the homogeneous medium should be chosen such that the effect of reflections on peak spatial-average SAR is less than 1 %. If the effect of reflections on peak spatial-average SAR is more than 1 % but less than 3 %, the maximum uncertainty shall be added to the uncertainty budget.

For hermetic phantoms, the presence of air voids beneath the measurement surface will result in large measurement. Great care must be taken when designing and filling the phantoms to avoid this situation occurring.

Dimensions in millimetres

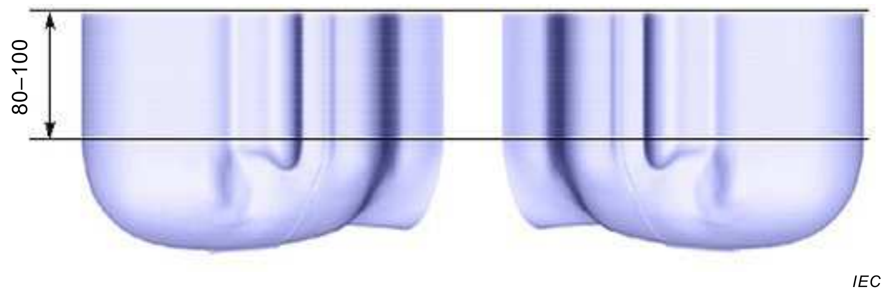

Figure A.5 – Sagittally bisected phantom with extended perimeter, used for single probe systems

Figure A.5 illustrates a sagittally bisected phantom with extended perimeter, used for single probe systems (shown placed on its side as used for device SAR tests). Other phantom orientations may be used if the peak spatial-average SAR is in another region of the head or to enable probe access to certain regions of the SAM phantom for SAR measurement. The orientation of the SAM phantom is irrelevant if a sealed phantom is used.

A.2 Flat phantom specifications

The shell of the flat phantom shall be constructed in the form of a container with a flat side that is in contact with the DUT.

Any flat phantoms used shall be large enough to allow SAR to be measured accurately using the *system validation* and *system check* antennas for 1 g and 10 g peak spatial-average SAR with less than 1 % influence from the phantom shape and dimensions.

For open containers, the flat phantom shall have the following shape and dimensions:

a) Unless specified in Step b), the shape of the phantom shall be an ellipse with a length of 600 mm ± 5 mm and a width of 400 mm ± 5 mm (Figure A.6).

b) For frequencies above 300 MHz, phantoms with other shapes and smaller dimensions are allowed as follows:

   – between 300 MHz and 800 MHz, the phantom flat phantom side that makes contact with the DUT may have any shape that encompasses an ellipse with a length of 0,6 λ_0 and a width of 0,4 λ_0, where λ_0 is the wavelength in air.

   – between 800 MHz and 6 GHz, the phantom side that makes contact with the DUT may have any shape that encompasses an ellipse with a length of 225 mm and a width of 150 mm.

Dimensions in millimetres

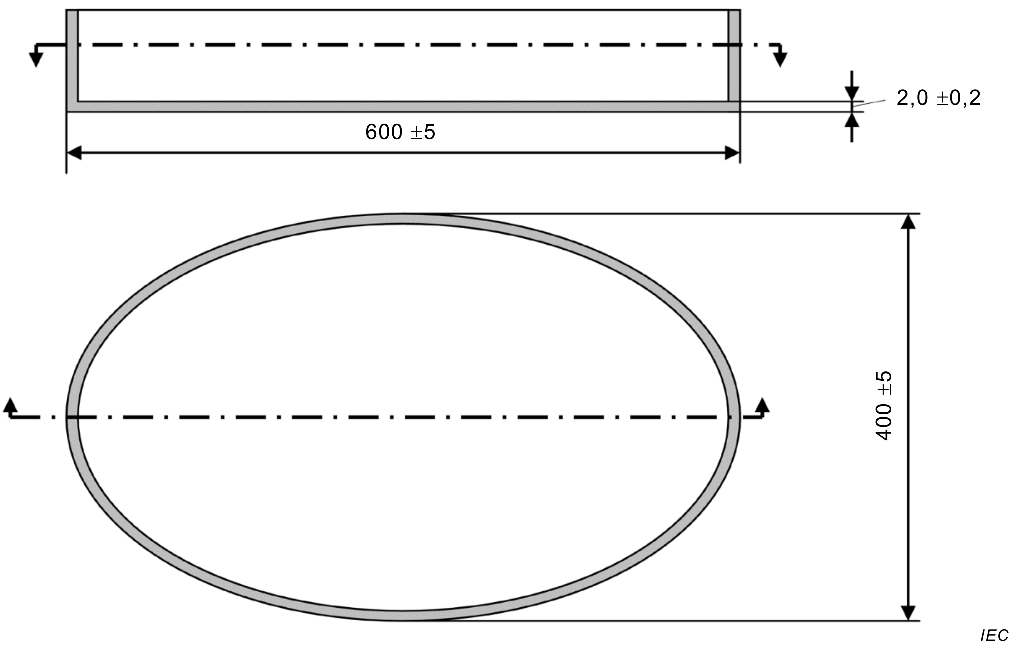

Figure A.6 – Dimensions of the elliptical phantom

The phantom shall be filled with tissue-simulant medium meeting the requirements of this PAS. To minimize reflections within the phantom, the depth of the homogeneous medium should be at least 15 cm. Medium depth of less than 15 cm can be used if it is demonstrated (e.g., using numerical simulations) that the effect of reflections on peak spatial-average SAR is less than 1 %. If the effect of reflections on peak spatial-average SAR is more than 1 %, detailed evaluation of the maximum uncertainty shall be documented and added to the uncertainty budget. The phantom shell shall be made of low-loss and low-permittivity material, having a loss tangent ≤ 0,05 and a relative permittivity of

$1 \leq \varepsilon_r' \leq 5$ for $f \leq 3$ GHz

$2 \leq \varepsilon_r' \leq 5$ for $f > 3$ GHz

The thickness of the flat face of the flat phantom shall be 2,0 mm with a tolerance of ± 0,2 mm.

Effects on SAR due to deviations of phantom shell parameters and thickness shall be included in the uncertainty estimation.

The phantom shell material shall be resistant to damage or reaction with tissue-equivalent medium chemicals used in it.

A.3 Specific phantoms

Other specific phantoms are applicable as described in the draft unified standard of IEC 62209-1 and IEC 62209-2. The Uniphantom is one of the instances of those phantoms; and its shape is different from that described earlier. The same requirements regarding the shell material, mechanical tolerance and tissue-equivalent media apply according to the requirements for single probe or array systems.

A.4 Tissue-equivalent medium

Table A.3 shows the target relative permittivity and conductivity of the tissue-equivalent medium. The justification for the parameters is provided in IEC 62209-1. For dielectric properties of the tissue-equivalent medium at other frequencies within the frequency range, a linear interpolation method shall be used. Examples of recipes for liquids having parameters as defined in Table A.3 are given in Annex I of IEC 62209-1:2016. This measurement can be performed using the equipment and procedures described in Annex J of IEC 62209-1:2016.

Table A.3 – Dielectric properties of the tissue-equivalent medium

Frequency (MHz)	**Relative permittivity** ε_r	**Conductivity** σ (S/m)
30	55,0	0,75
150	52,3	0,76
300	45,3	0,87
450	43,5	0,87
750	*41,9*	*0,89*
835	41,5	0,90
900	41,5	0,97
1 450	40,5	1,20
1 500	*40,4*	*1,23*
1 640	*40,2*	*1,31*
1 750	*40,1*	*1,37*
1 800	40,0	1,40
1 900	40,0	1,40
2 000	40,0	1,40
2 100	*39,8*	*1,49*
2 300	*39,5*	*1,67*
2 450	39,2	1,80
2 600	*39,0*	*1,96*
3 000	38,5	2,40
3 500	*37,9*	*2,91*
4 000	*37,4*	*3,43*
4 500	*36,8*	*3,94*
5 000	*36,2*	*4,45*
5 200	*36,0*	*4,66*
5 400	*35,8*	*4,86*
5 600	*35,5*	*5,07*
5 800	*35,3*	*5,27*
6 000	*35,1*	*5,48*

NOTE For convenience, permittivity and conductivity values at those frequencies which are not part of the original data provided by Drossos et al. or the extension to 5 800 MHz are provided (i.e., the values shown in italics). These values were linearly interpolated between the values in this table that are immediately above and below these values, except the values at 6 000 MHz that were linearly extrapolated from the values at 3 000 MHz and 5 800 MHz.

Annex B
(normative)

Calibration and characterization of dosimetric probes

B.1 Introduction

SAR is proportional to $|E|^2$. The SAR in a human phantom can therefore be determined either by directly measuring the magnitude of the electric field in the volume of the phantom as defined in IEC 62209-1 and IEC 62209-2 or by measuring the electric or magnetic field at sufficient points (e.g., using a single robot-controlled probe or a fixed array of sensors) and reconstructing the SAR at other locations in the phantom. There are several methods to achieve these goals; and each method has advantages and disadvantages. The scope of this PAS covers all methods that are based on reconstruction of the SAR on a limited number of measurement points. The precision and traceability of the calibration is essential to the accuracy of the SAR measurement method.

In general, the absolute sensitivity (amplitude) and the relative phase of each sensor has to be calibrated.

Calibration laboratories should be accredited by national metrological institutes to ISO/IEC 17025. This provides a means to ensure traceability, measurement capability and technical competence. Calibration equipment use primary and secondary standards. Primary standards have a valid calibration by an accredited calibration laboratory that establishes traceability to the SI system of measurement. Secondary standards do not have a traceable calibration but their performance and stability is verified (e.g., using in-house checks) using primary standards. Only primary standards shall be used where the accuracy of the equipment is relevant to the calibration accuracy (e.g., power meters, calibration antennas). An example of a secondary standard is an amplifier whose output is monitored by a power meter.

B.2 Types of calibration

B.2.1 Amplitude calibration with analytical fields

The most accurate method of calibrating a probe is to expose it to a field that is analytically known. Examples of such fields are fields in waveguide, the field magnitude inside tissue-equivalent liquids is known when the power is measured that goes inside the liquid. Techniques and design guidelines for waveguide calibration are described in IEC 62209-1:2016, Annex B. This method can be applied to single probes.

When performing an uncertainty analysis of the probe calibration in a waveguide, at least the parameters included in Table B.1 shall be considered.

Table B.1 – Uncertainty analysis of single-probe calibration in waveguide

	a		*b*	*c*	$u_i = (a/b) \times (c)$	
Uncertainty component	**Uncertainty** ± %	**Probability distribution**	**Divisor**	c_i	**Standard uncertainty** ± %	v_i
Incident or forward power				1		∞
Reflected power				1		∞
Liquid conductivity measurement				1		∞
Liquid permittivity measurement				1		∞
Liquid conductivity deviation				1		∞
Liquid permittivity deviation				1		∞
Frequency deviation				1		∞
Field homogeneity				1		∞
Field-probe positioning				1		∞
Field-probe linearity				1		∞
Modulation				1		∞
Noise				1		∞
Combined standard uncertainty		RSS				
NOTE Column headings *a, b, c* are for reference.						

B.2.2 Amplitude and phase calibration by transfer calibration

Transfer calibration uses one or more antennas (referred to as transfer calibration source) to excite an induced field (referred to as a reference field) that is not known analytically. The field generated by the transfer calibration antenna is instead determined by measurement for a given antenna input power, using a probe that has been calibrated in an analytical field. An example of a transfer calibration is the use of one or several transfer calibration antennas to calibrate a probe-array in a phantom, where the target SAR or reference field at the locations of the probes in the array inside the phantom have been evaluated by measurement using a single reference dosimetric probe for which amplitude calibration has been performed in a waveguide as described in A.2.1. Calibration of the field phase may require either the use of a phaseless approach to retrieve the phase of the reference fields (see Annex C) or a reference probe of different nature that would have been calibrated in phase using analytical fields. Each chosen approach may involve variations in the list of uncertainty contributions which shall be taken into account.

For ensuring an accurate transfer calibration, it is recommended to minimize the deviations between conditions used during the probe or probe-array calibration and conditions used for measurement of the reference fields with the reference probe. For example, the phantom geometry, dielectric parameters, temperature and sensor locations shall be as close as possible.

For calibration of array systems, lower overall uncertainty may be achieved if the sensors are calibrated *in-situ* within the array. This is because removing the sensor from the array for calibration will introduce additional measurement uncertainties due to mutual coupling of the sensors in the array, the mechanical support structure and boundary errors.

Transfer calibration introduces additional uncertainties compared to calibration in analytical fields. The predominant uncertainty contribution is typically the determination of the antenna target value. Other uncertainty contributions include the sensor search, sensor coupling and phantom shape. When performing an uncertainty analysis of a transfer calibration of an array system, at least the parameters included in Table B.2 shall be considered.

Table B.2 – Uncertainty analysis of transfer calibration of array systems

	a		*b*	*c*	$u_i = (a/b) \times (c)$	
Uncertainty component	**Uncertainty** ± %	**Probability distribution**	**Divisor**	c_i	**Standard uncertainty** ± %	v_i
Calibration instrumentation						
Incident or forward power or transmission coefficient measurement accuracy						∞
Reflected power or reflection coefficient measurement						∞
Noise						
Phantom						
Liquid conductivity measurement						∞
Liquid permittivity measurement						∞
Liquid conductivity deviation						∞
Liquid permittivity deviation						∞
Phantom shell shape and dielectric properties						
Application of reference fields						
Transfer calibration antenna target value or reference field measurement						∞
Transfer calibration antenna position						∞
Probe or probe-array						
Sensor mutual coupling						∞
Position and orientation of the probe or probe-array within the calibration setup						
Modulation						∞
Linearity						
Noise						∞
Combined standard uncertainty		RSS				

NOTE 1 Column headings *a, b, c* are for reference.

NOTE 2 Some of the lines may be doubled to take into account the impact of magnitude and phase on the measurement uncertainty.

B.2.3 Amplitude and phase calibration using numerical reference

This procedure is similar as above (B.2.2) but uses reference values for amplitude and phase of a transfer calibration antenna that had been determined by validated simulations instead by measurements. The field is instead determined by means of numerical modelling techniques complying with requirements from IEC/IEEE 62704-1 or IEC 62704-4. An example of such calibration would involve the use of one or several antennas to calibrate a probe-array in a phantom, where the target SAR or reference field at the locations of the probes in the array inside the phantom have been evaluated by numerical simulations with a Finite Difference

Time-Domain (FDTD) or a Finite Element Method (FEM) code. Such methods enable the assessment of both amplitude and phase of all components of the electromagnetic fields. IEC/IEEE 62704-1 and IEC 62704-4 provide details on evaluating the uncertainty of numerically simulated fields and SAR data in phantoms. In particular, the deviation between the physical antenna-phantom setup and the numerical model have to be carefully taken into account in the uncertainty budget.

The differences between numerical model and physical antenna with respect to the relevant reference values need to assess using the calibration method as described in Annex G (Calibration of Reference Antennas). The appropriate uncertainty value covering the maximum differences needs to be assessed.

For ensuring an accurate calibration using numerical reference, it is recommended to minimize the deviations between conditions used during the physical probe or probe-array calibration and conditions used for the numerical calculations of the reference fields. For example, the phantom geometry, dielectric parameters and sensor locations shall be as close as possible.

For calibration of array systems, lower overall uncertainty may be achieved if the sensors are calibrated *in-situ* within the array. This is because removing the sensor from the array for calibration will introduce additional measurement uncertainties due to mutual coupling of the sensors in the array, the mechanical support structure and boundary errors. Therefore calibration of the whole array against a numerical reference may be preferable to calibration of individual sensors against an analytic field.

Calibration using numerical reference introduces additional uncertainties compared to calibration in analytical fields. The predominant uncertainty contributions are typically the determination of the transfer calibration antenna target value or reference field, and the deviation between the physical antenna-phantom setup and its numerical model. Other uncertainty contributions include the sensor search, sensor coupling and phantom shape. When performing an uncertainty analysis of the calibration of an array system using numerical reference, at least the parameters included in Table B.3 shall be considered.

Table B.3 – Uncertainty analysis of transfer calibration of array systems

	a		*b*	*c*	$u_i = (a/b) \times (c)$	
Uncertainty component	**Uncertainty** ± %	**Probability distribution**	**Divisor**	c_i	**Standard uncertainty** ± %	v_i
Calibration instrumentation						
Incident or forward power or transmission coefficient measurement accuracy						∞
Reflected power or reflection coefficient measurement						∞
Noise						
Phantom						
Liquid conductivity measurement						∞
Liquid permittivity measurement						∞
Liquid conductivity deviation						∞
Liquid permittivity deviation						∞
Phantom shell shape and dielectric properties						
Application of reference fields						
Reference antenna target value or reference field – numerical modelling uncertainties supposing perfect source model						∞
Deviation between physical antenna and numerical reference antenna						
Reference antenna position						∞
Probe or probe-array						
Sensor mutual coupling						∞
Position of the probe or probe-array within the calibration setup						
Modulation						∞
Linearity						
Noise						∞
Combined standard uncertainty		RSS				

NOTE 1 Column headings *a, b, c* are for reference.

NOTE 2 Some of the lines may be doubled to take into account the impact of magnitude and phase on the measurement uncertainty.

Annex C
(informative)

Field Reconstruction Techniques

C.1 Introduction

Vector measurement-based systems and protocols use field reconstruction methods, allowing the application of indirect measurement approaches in which the SAR is evaluated in three dimensions from a limited number of measurement points that may be located in a limited part of the volume of interest, or even outside this volume.

The following sections provide information about methods used to reconstruct the SAR in the relevant volume of the phantom from measurements on a 2D surface or another sub-region. The objectives and background of field reconstruction techniques are covered in C.2 and C.3, respectively. C.4 describes examples of expansion techniques.

The requirements for field reconstruction techniques are covered in Clause 6.6.

C.2 Objective of Field Reconstruction Techniques

The objective of vector measurement-based systems in the context of this PAS is to determine the peak spatial SAR averaged over a cubical volume of 1 g or 10 g mass. For that purpose, the knowledge of the SAR distribution in exposed regions of the phantom is required. These regions typically include locations of the phantom that are in close proximity to the device antennas, as there may be evanescent modes that decay rapidly in the phantom. As only a limited number of points can be measured, the 3D SAR distribution in the relevant regions must be reconstructed from these measurements. Robot-based scanning systems measure a dense grid of points before interpolating and extrapolating over a short distance to obtain the 3D SAR distribution. Vector measurement-based systems do not yield such dense measurement grids. Hence, advanced reconstruction methods are required to obtain the 3D SAR distribution with sufficient reliability and accuracy.

C.3 Background

Field reconstruction techniques that are suitable for vector measurement-based SAR systems can be derived from the well-established theory of electromagnetic near-field measurements, especially planar 2D scanning based techniques. The principle relies on the measurement of the sampled distributions of the E-field and/or H-field over a 2D grid located in a source-free region, as depicted Figure C.1. In a general sense, the electric-field reconstruction, at an observation point of coordinates $\mathbf{r}(r,\theta,\phi)$, from the measured field over the scan surface S Sat $\mathbf{r}'(r',\theta',\phi')$ can be represented by the integral transform

$$E(r) = \int_S dr' D(r,r')E(r') \tag{C.1}$$

where

$E(r)$ is the 3D electric vector field

$E(r')$ is the 2D field over the scan surface S

$D(r,r')$ is the integral kernel

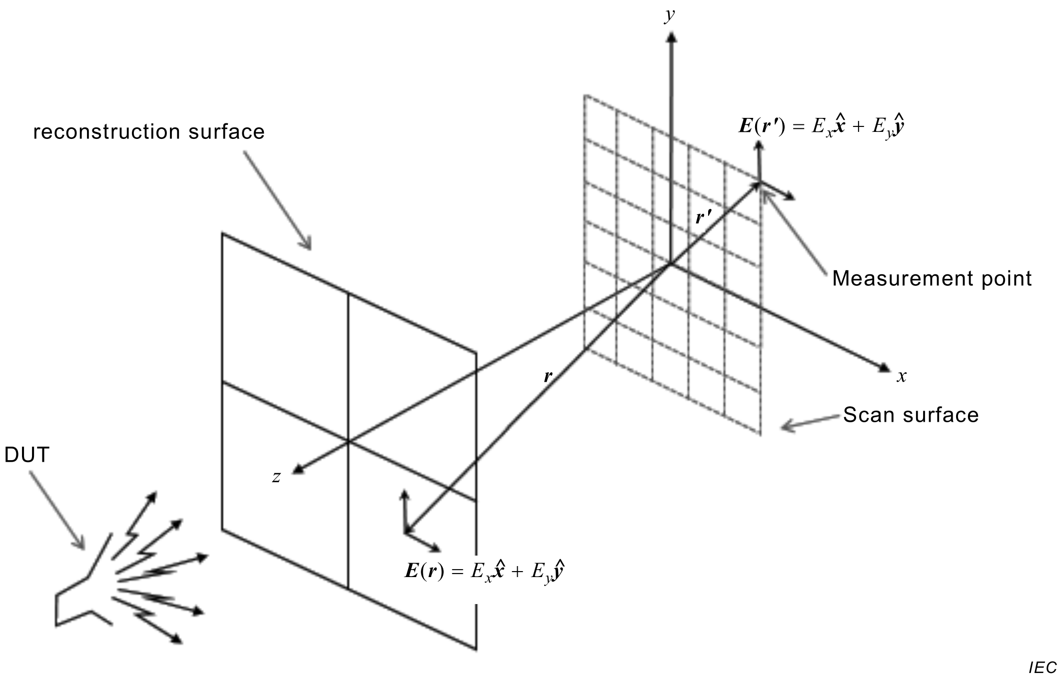

Figure C.1 – Coordinate system for 2D planar measurement-system

Numerous field expansion techniques allow the retrieval of the 3D electromagnetic field in the phantom volume from the sampled 2D fields. For instance, the electromagnetic field can be expanded in terms of Green's functions, plane-waves, or in general, in terms of orthogonal or non-orthogonal basis-functions. Notice that different formulations exist that require the representation of at least two orthogonal field components on the 2D scan area. For example, (i) tangential E-field or dual H fields, (ii) normal component and its normal derivative, or (iii) a mixture of E and H components. In practice, ideal electromagnetic field probes, such as the Hertzian dipole, do not exist. Hence, the calibration of the probes of the vector measurement-based SAR system is indeed key for the achievement of reasonable measurement uncertainty.

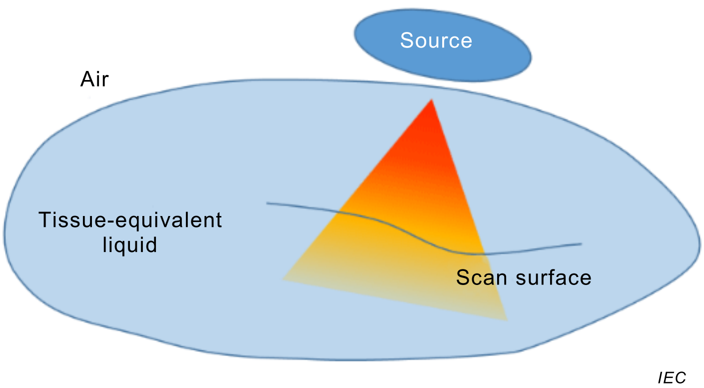

Figure C.2 – Generic configuration of SAR measurement system

Some particular assumptions might hold for the application of the 2D near-field measurement techniques to multiple-probe SAR systems, in which the probes are immersed within the tissue-equivalent medium enclosed in mannequins. The high dielectric contrast between the air (the source region) and the simulating liquid (the measurement region) gives rise to a spatially confined radiation, which is mainly in the direction orthogonal to the surface of the air-medium interface. Also, the large dissipation of the tissue-equivalent medium leads to negligible internal resonances and scattered fields by the boundaries. These hypotheses allow the tissue-equivalent liquid region to be considered as an open homogeneous medium, where the field reconstruction is only valid within the inner region as depicted in Figure C.2.

Reconstruction is feasible as the SAR distribution is constrained by Maxwell's equations (which in source-free homogeneous medium reduces to the Helmholtz equation [75]). It is well known, that this physical constraint allows the reconstruction of the full field from, e.g., complete knowledge of the field on an enclosing surface (Huygens' principle of expansion into spherical waves [47]), or complete knowledge of the field on an infinite plane (plane wave expansion [75]).

It should be pointed out that precise phase information of the electric field components is not necessary to compute the psSAR from the electric fields. Precise knowledge of the phase is only required where measured field components need to be propagated over an electrically large distance to the location of the averaging volume.

C.4 Reconstruction Techniques

C.4.1 Expansion Techniques

Fast array SAR measurement systems perform discrete sampling of a sub-region/surface within the phantom. If the sampling is sufficiently dense and the field strength outside the measurable exposure area is sufficiently low, reconstruction can be performed accurately by expansion techniques. Most commonly applied expansion methods require the knowledge of at least two field components as well as their relative phases. Phase information can either be obtained directly through phase measurements or reconstructed from intensity measurements.

As an example, the main steps of the PWS (plane wave spectrum) expansion principle based on 2D planar measurement systems, depicted in Figure C.3, can be described as follows: Considering the electric field $\boldsymbol{E}(\boldsymbol{R},z)|_{z=0}$ over the scan plane, its PWS $\hat{\boldsymbol{E}}(\boldsymbol{K},z)\big|_{z=0}$ is obtained as:

$$\hat{\boldsymbol{E}}(\boldsymbol{K},0) = \int_{\Sigma_0} \mathrm{dR}\, \boldsymbol{E}(\boldsymbol{R},0) e^{j\mathbf{K}.\mathbf{R}} \tag{C.2}$$

Where $\boldsymbol{R} = x.\hat{\boldsymbol{x}} + y.\hat{\boldsymbol{y}}$ spans the field over the scan-area Σ_0, and $\boldsymbol{K} = k_x.\hat{\boldsymbol{x}} + k_y.\hat{\boldsymbol{y}}$ is the spectral variable. The PWS over planes at distances z from the scan-surface can be computed introducing the propagator

$$P(\boldsymbol{K},z) = e^{-j\sqrt{(k^2-|\boldsymbol{K}|^2)}.z} \tag{C.3}$$

With the propagation contant $k = \omega\mu_0(\omega\varepsilon_0\varepsilon' - j\sigma)$;

$$\hat{\boldsymbol{E}}(\boldsymbol{K},z)\big|_{z\geq 0} = P(\boldsymbol{K},z) \int_{\Sigma_0} \mathrm{dR}\, \boldsymbol{E}(\boldsymbol{R},0) e^{j\mathbf{K}.\mathbf{R}} \tag{C.4}$$

The field distribution at the reconstruction distance z is then obtained through the inverse transform using the relation:

$$\boldsymbol{E}(\boldsymbol{r}) = \int_{K} \mathrm{dK}\, \hat{\boldsymbol{E}}(\boldsymbol{K},z)\, e^{-j\mathbf{K}.\mathbf{R}} \tag{C.5}$$

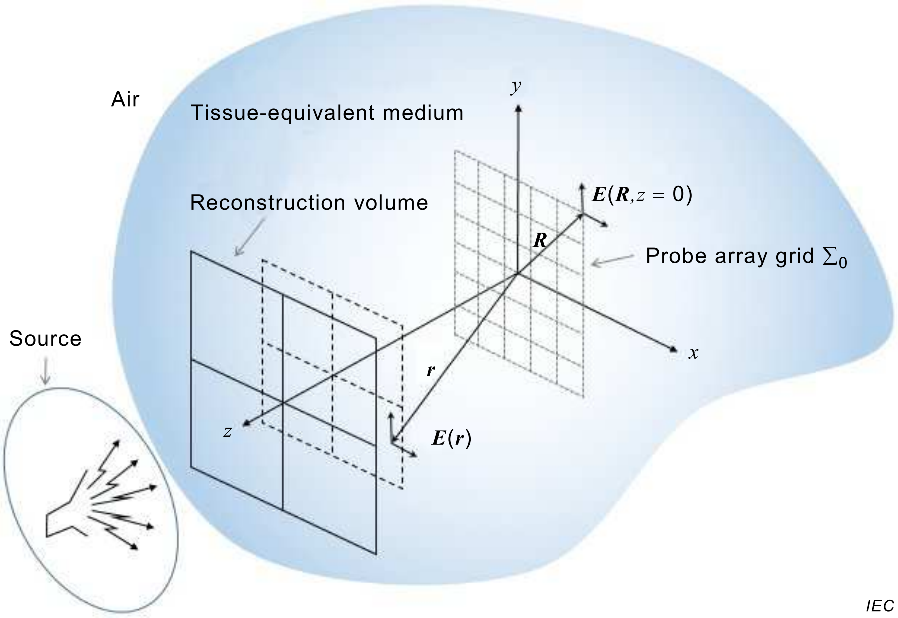

Figure C.3 – Schematic representation of 2D planar measurement-based SAR system and its coordinate system

In practice, the scan-area Σ_0 is sampled at the probe locations, and the spectral variable is discretised. The integral operations inherent to the field expansion in equation (C.2) and equation (C.5) become simple DFT (discrete Fourier transform) operations

C.4.2 Source Reconstruction Techniques

Source reconstruction methods, another well studied category of approaches, are derived from the equivalence theorem [2], which states that it is possible to find magnetic and/or electric current distributions on a surface that produce the same field within a region as the original source [6, 136]. Such equivalent current distributions can be constructed using, e.g., the measured amplitudes of the electric field components and used to obtain the overall field. Source reconstruction techniques do not necessarily require phase information [3] provided that the relevant domain that contains the source and the target fields are confined in a sufficiently small region with respect to the wavelength.

C.4.3 Source Base Function Decomposition

Conceptually between source reconstruction and expansion techniques are approaches that perform constructive synthesis of the SAR distribution from base functions derived from small generic, e.g., dipole or multipole, sources and match them to a measured field distribution.

C.4.4 Phase Reconstruction

If measurements only provide amplitude information, phase distributions can be recovered by approaches such as the Gerchberg-Saxton algorithm [53], which requires intensity measurements on two planes, gradient search methods [41], or solving of the Eikonal equation [121]. The resulting systems of equations are generally underdetermined and nonlinear. They also require the application of additional application-specific knowledge.

C.4.5 Other Approaches

Reconstruction approaches are not limited to the above-mentioned principal and currently most established methods. For some combinations of measurement and reconstruction approaches the reconstruction problem is in itself underdetermined and requires additional application-specific knowledge (e.g., spatial limits of the source, distance between source and phantom, etc.) and/or constrained optimization to obtain unique solutions.

C.5 Source reconstruction and SAR estimation from fields measured outside the phantom

The general formulation of the source reconstruction techniques enables the determination of a distribution of equivalent electric and magnetic currents on a closed surface surrounding the original source. This distribution radiates the same fields outside the reconstruction region [153] to [155]. In the case of a source device outside a phantom, the equivalent current distribution of the source can therefore be determined from the radiated fields measured outside the phantom by a single probe or multi-probe measurement system using standard antenna measurements techniques as shown in Figure C.4 [156]. This concept can be used to determine the fields induced in a body/head phantom and hence determine the SAR distribution from measured fields outside the phantom [157], [158].

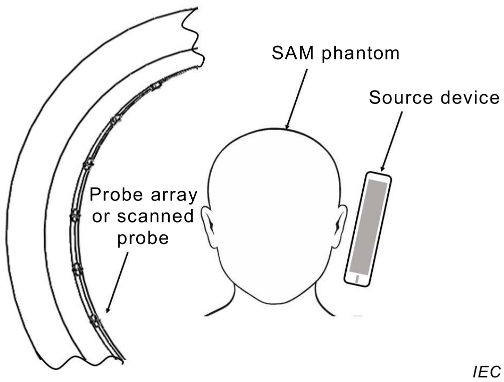

Figure C.4 – Source Reconstruction outside the phantom

Annex D
(normative)

SAR measurement system verification and validation

D.1 Introduction

The goal of this Annex is to define the *system check* and *system validation* procedures that enable users and third parties to verify system performance by applying consistent protocols:

a) *System check*: procedure that uses specific antennas to verify that the performance of the measurement system is repeatable and has not degenerated since the last calibration. The *system check* is performed within the manufacturer-defined specifications of frequency range and position on the phantom;

b) *System validation*: procedure that uses specific antennas to validate that a measurement system operates within the stated measurement uncertainty. In other words, it verifies that the accuracy is acceptable for use according to this PAS.

NOTE *System validation* is normally performed by the system manufacturer, even though it is defined such that it can also be performed independently by any third party. Validation of software updates can be done for each hardware version and does not necessarily have to be done on each specific system.

D.1.1 Objectives and purpose of *system check*

System check provides a fast and reliable method to verify that the SAR system is operational with no system component failure, including probe defects in an array system, drifts or deviation from target performance requirements. A *system check* also verifies the measurement repeatability of the SAR measurement system against calibrated *system check* antenna(s) before compliance testing.

a) In the case of an open system where the tissue-equivalent medium is exposed to air (e.g., robot-based scanning system), *system check* shall be performed prior to compliance tests or within 24 hours before the SAR evaluation and on the same SAR measurement system that is used for the SAR evaluation of the handset. SAR measurements are validated with the flat phantom only, using the same probe, system electronics and tissue-equivalent medium that are used for *system check* and measurements of the DUT.

b) For all other cases (e.g., sealed systems with fixed arrays), *system check* shall be performed before the first measurement and within seven days of any measurement of the DUT. It shall be performed on all phantoms used for the measurements, according to the measurement locations defined in this PAS to ensure that there are no potential component failures (e.g., broken sensors), performance degradation (e.g., changes in dielectric parameters) or system configuration errors (e.g., air bubbles).

The *system check* is a complete 1 g or 10 g peak spatial-average SAR measurement using a *system check* antenna (see D.3.1), according to the requirements of this PAS. The same measurement system (sensors, tissue-equivalent medium, and electronics), software version, calibration, and measurement parameters (e.g., resolution, reconstruction parameters, measurement time) shall be used for the *system check* as those used for the compliance tests.

The system check shall be performed using the same liquid as in the compliance test and at a chosen fixed frequency that is within ±10 % or ±100 MHz of the compliance test mid-band frequency, whichever is greater.

D.1.2 Objectives of *system validation*

The objective of system validation is to verify that the SAR measurement system (within its boundaries of the specifications and corresponding uncertainty as determined in clause 8) will not give erroneous measurement results for the measurement of the DUT. This is achieved by testing a sufficiently large set of well-characterised antennas having target values with minimal uncertainty that encompasses the range of field distributions and signal types encountered with currently available mobile communications devices.

The SAR measurement system is acceptable if the validation measurement results comply with the criterion defined in D.4. This criterion makes use of the measurement uncertainty that is determined in accordance with in subclause 8.2.

The general requirements for the validation tests are as follows. They shall cover the full range of frequencies, SAR levels, signal modulations and measurement locations supported by the phantom and within the requirements of this PAS. A relevant subset of the validation tests may be performed for a system that supports or is used for only specific phantom(s) or measurement requirements. The complete set of SAR distributions and results shall be reported according to measurement configurations defined in clause D.4 shall be evaluated using the reference antennas defined in Annex F and the target values defined in Table D.2 and Table D.3. Annex F defines a minimum set of antennas to be used for validation. Additional antennas may be added to Annex F (e.g., using an amended standard) if further analysis shows that this set of antennas is not comprehensive enough for validating vector measurement-based systems.

A system may be specified for being usable for a smaller range of frequencies or for a smaller measurement region supported by the phantom as specified hereafter. In these cases, the corresponding subset of the tests shall be performed, i.e., all the tests that fall in this subset of the specified range of use.

System validation is typically performed and documented by the system manufacturer for every system delivered, on an annual basis and whenever any changes of the hardware or software which may affect the SAR assessment are made. The full set of validation test must be performed at least once every year. For routine validation, it may be reduced if it can be demonstrated that it is sufficient to warranty that the full set would meet the acceptance criteria (e.g., if the frequency dependent sensitivity of the sensors is constant due to reasons of sensor design, then the number of frequencies may be reduced). The rationale and proof of reduction shall be documented and made available.

The concepts for validating single probe systems and array systems are different. For single probe systems, the performance of the measurement system components can be assessed separately, but this is not the case for array systems.

In general, the same *system validation* procedure applies to both single probe systems and probe-array systems using head and flat phantoms. The validation procedure for single probe systems is simpler and requires less test positions.

D.2 SAR measurement setup and procedure for *system check* and *system validation*

D.2.1 General

The reference antennas for *system validation* (Annex F) can also be used for *system check*. The peak spatial-average SAR measured for the required test conditions shall be normalized to target forward power at the RF input of the reference antenna according to procedures in this clause and compared to the target SAR values.

The following clause describes the required power measurement setup for *system check* and *system validation*. Assessment of RF forward power measurement uncertainty according to D.2.4 is also described.

D.2.2 Power measurement setups

Both *system check* and *system validation* procedures require accurately measured and stable forward power at the RF input of the reference antennas.

A recommended test setup for using off-the-shelf instrumentation with a reference antenna is shown in Figure D.1. The system includes a signal generator, an amplifier, 10 dB to 20 dB attenuators, a directional coupler, power meter(s), two power sensors, a 50-Ω-load, a precision short, cables, connectors and adapters. An alternative setup using a single directional coupler instead of a bidirectional coupler to establish reflected power from an S_{11} measurement at the input of the reference antenna may be used. When other equipment is used, the measurement setup shall be documented by applying similar procedures.

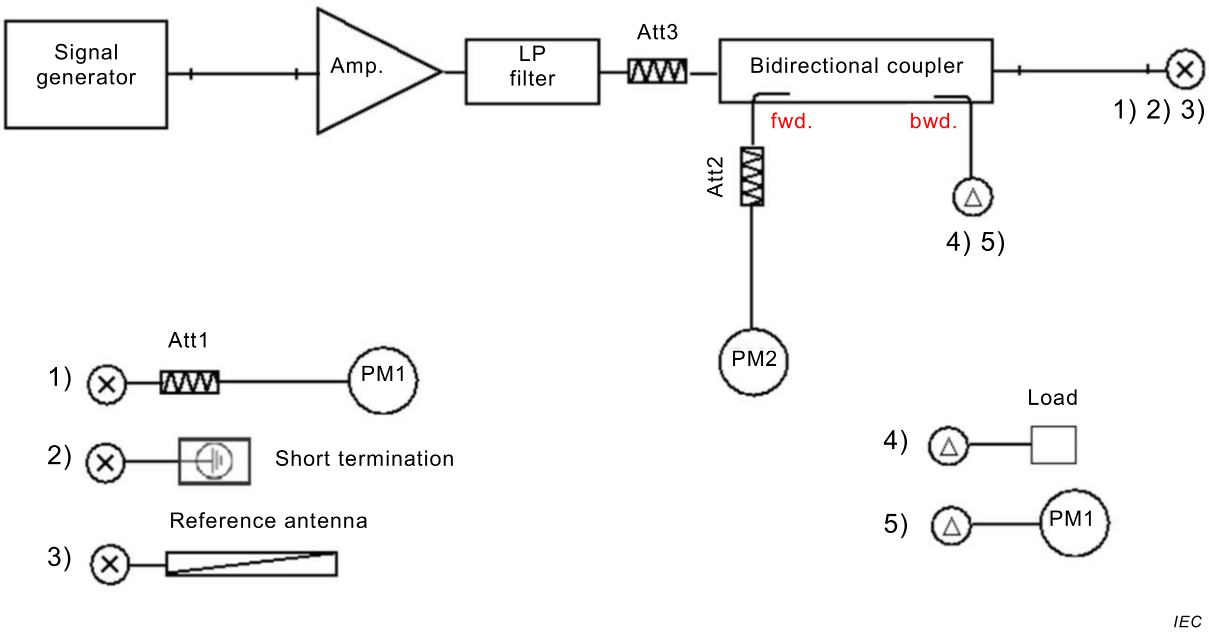

Figure D.1 – A Recommended power measurement setup for system check and system validation

The requirements of the components used in the setup shown in Figure D.1 are described in the following.

a) The signal generator and amplifier shall be stable (after warm-up). The forward power to the reference antenna shall be at least 10 mW to avoid the influence of measurement noise.

NOTE If the signal generator can deliver 15 dBm or more, an amplifier is not necessary for the lower power SAR evaluations. Some high-power amplifiers should not be operated at a level far below their maximum output power level (e.g., a 100 W power amplifier operated at 250 mW output can be quite noisy).

b) A low pass filter may be placed after the amplifier to reduce the effects of harmonics and noise from the amplifier.

NOTE For most amplifiers, this filter is typically not necessary if power stability is maintained for normal operation during the measurement.

c) An attenuator should be placed after the amplifier, before the directional coupler, to improve source matching and overall measurement accuracy (see manual of the specific power meter) (caution).

NOTE 1 This also allows the amplifier to operate at its optimal condition for improving system stability.

NOTE 2 The Att3 is not necessary when the return loss of Low pass filter is better than 20 dB at the input and output ports.

d) A directional coupler with a coupling coefficient ≥ 20 dB is recommended for monitoring the forward power and adjusting the signal generator output to maintain constant forward power. The coupler shall have a return loss ≥ 25 dB at the input and output ports. A high-quality coupler with respect to directivity and output matching is necessary to avoid additional errors.

e) The power meter PM2 should have a low drift and a resolution of ≤ 0,01 dBm, but otherwise its accuracy has no impact on the power setting.

f) The influence of the cable between the coupler and the reference antenna shall be evaluated as part of the uncertainty assessment.

g) The power meter PM1 and attenuator Att1 shall be of high quality and calibrated. The attenuator (≥10 dB) is used to improve the accuracy of the power sensor (some higher power heads come with a built-in calibrated attenuator). Attenuations can be off by up to 0,2 dB from the specified value; therefore, the exact attenuation at each test frequency shall be verified and used in the calculations.

h) To avoid linearity and range switching errors in power meter PM2 for *system check* performed at various power levels, the range of PM2 during actual measurement with the reference antenna shall be kept the same as that used during power setup with power meter PM1 connected directly to the cable.

i) The reference antenna shall be connected directly to the cable at location "X" in Figure D.1. If the power meter and reference antenna require different connector systems, a calibration grade, high-quality adapter shall be used. Preferably, the adapter is calibrated with attenuator Att1 at the input (location "X").

j) To avoid unacceptable power drifts during *system check*, the equipment should be allowed to warm-up for the duration recommended by the manufacturer(s) before any measurement.

D.2.3 Procedure to normalize the measured SAR

The test procedure is described in the following steps:

a) Connect the equipment as shown in Figure D.2, with the power meter PM1 and attenuator Att1 connected to the end of the cable. A 50 Ω termination shall be connected at the reverse coupled port of the directional coupler.

b) Adjust the power output from the signal generator until the forward power P_f at PM1 is at the desired power level.

c) Measure the forward coupled power P_{fc} at PM2.

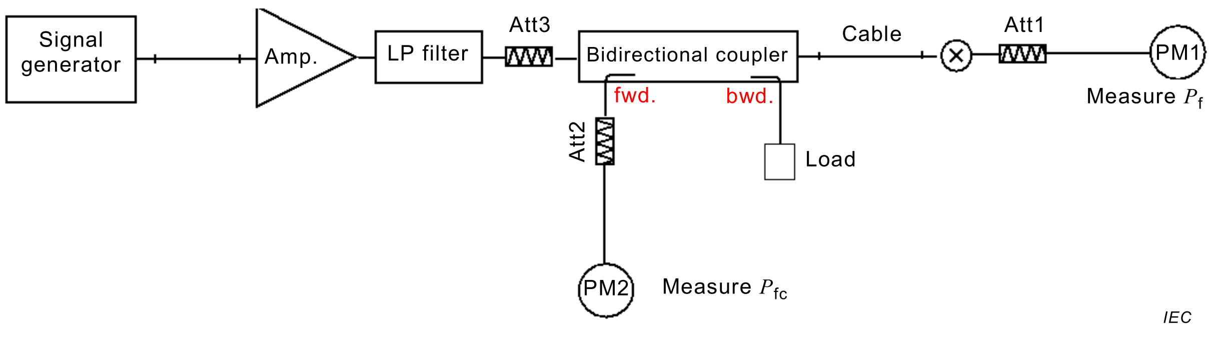

Figure D.2 – Equipment setup for measurement of forward power P_{fc}

d) Connect the equipment as shown in Figure D.3. The power meter PM1 and its attenuator are disconnected from the end of the cable and a short is placed instead. A power meter is connected to the reverse coupled port of the directional coupler, replacing the 50 Ω termination.

e) Adjust the power from the signal generator such that the forward coupled power at PM2 is equal to P_{fc} in step c).

f) Read the shorted reverse coupled power P_{rcs} at power meter PM1.

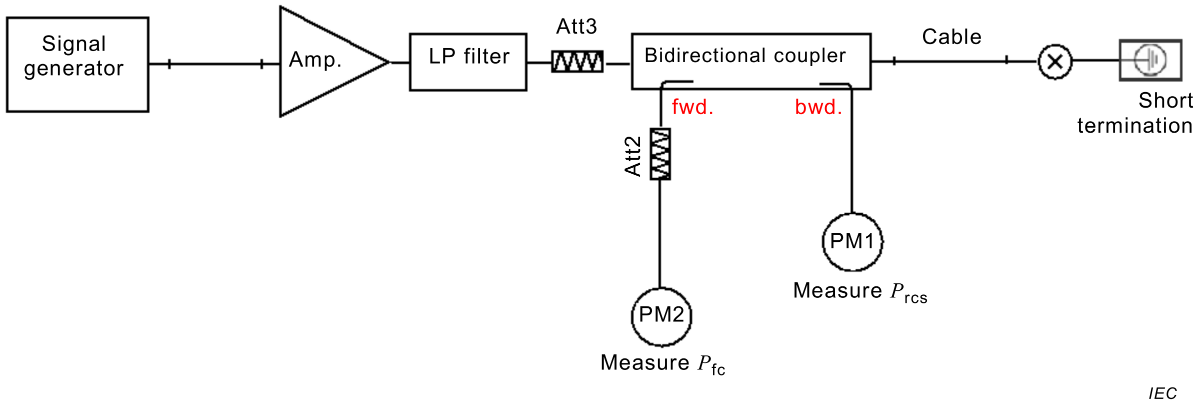

Figure D.3 – Equipment setup for measuring the shorted reverse coupled power P_{rcs}

g) Connect the equipment as shown in Figure D.4 with the reference antenna connected to the end of the cable, replacing the short termination.

h) Position the reference antenna at a test location on the phantom, at a test location shown in Figure D.5 and D.6

i) Adjust the power from the signal generator such that the forward coupled power at PM2 is equal to P_{fc}.

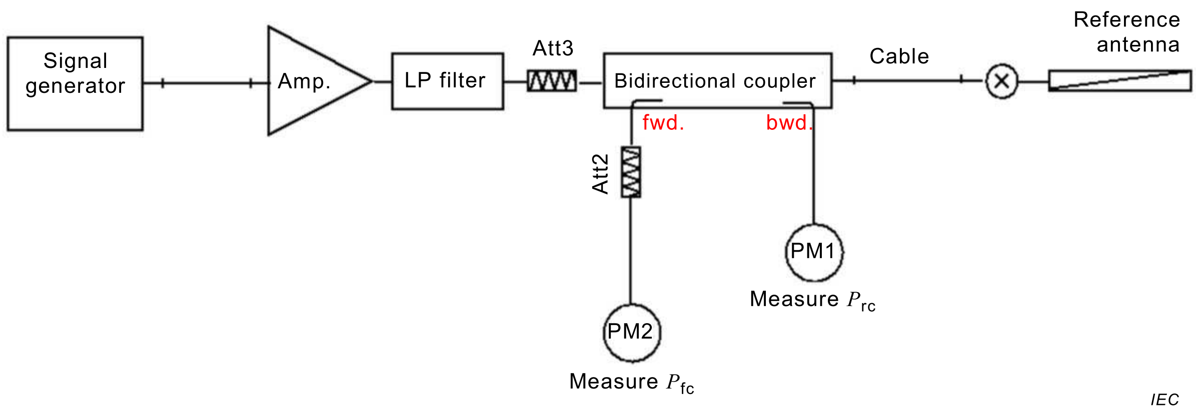

Figure D.4 – Equipment setup for measuring the power with the Reference antenna connected

j) Read the reverse coupled power P_{rc} at power meter PM1.

k) Measure the 1 g and 10 g peak spatial-average SAR, $SAR_{1g,m}$ and $SAR_{10g,m}$, at the phantom test position.

l) Calculate the return loss of the reference antenna in dB: $RL = P_{rcs} - P_{rc}$, where P_{rcs} and P_{rc} are in dBm.

m) Normalize the measured SAR by the forward power P_f.

$$SAR_{1g,NORM} = \frac{SAR_{1g,m}}{P_f} \tag{D.1}$$

$$SAR_{10g,NORM} = \frac{SAR_{10g,m}}{P_f} \tag{D.2}$$

where

$SAR_{1g,m}$ and $SAR_{10g,m}$ are the 1 g and 10 g peak spatial-average SAR measured at the forward power P_f.

$SAR_{1g,NORM}$ and $SAR_{10g,NORM}$ are the 1 g and 10 g peak spatial-average SAR normalized to 1 W forward power.

n) Record $SAR_{1g,NORM}$, $SAR_{10g,NORM}$, P_f, and RL.

o) Compare the measured SAR values with the appropriate target values, as described in D.3.2 (system check) and D.4.4 (system validation).

p) Check that the return loss, RL, is in accordance with the requirements of D.3.1.

D.2.4 Power measurement uncertainty

Figure D.2 describes the power measurement setup used to determine forward power (P_f) at the end of the cable. P_f is measured by PM1 and related to the coupled forward power (P_{fc}) measured by PM2. Return loss of the reference antenna (S_{11}) is determined by the power measurement setup shown in Figure D.3, where the shorted reverse coupled power (P_{rcs}) is measured at the reverse power port of the directional coupler by PM1. When the reference antenna is connected to the cable as shown in Figure D.4, the reverse coupled power (P_{rc}) is measured by PM1. The uncertainty contributions for P_f, P_{fc}, P_{rc} and P_{rcs} are as follows:

a) The contributors to P_f are: u_1(PM1), u_1(cable), u_1(att1), $u_1(\Gamma_{GE}, \Gamma_e, S_{11})$.

NOTE The uncertainty of the attenuator could be excluded if both the power meter PM1 and attenuator ATT1 are calibrated together

b) The contributors to P_{fc}: no uncertainty, because the signal generator output is adjusted to maintain an exact constant value for P_f at the output of the cable (reference plane).

c) The contributor to P_{rc}, P_{rcs} are: u_2(PM1), 2 × u_1(cable).

d) Error by approximation: u_1(F), this contributor is included if the measurement method with bidirectional coupler is used (the mismatch is included in this error) without VNA.

e) The mismatch error $u_1(\Gamma_{GE}, \Gamma_e, S_{11})$, this contributor is included if a measurement method with directional coupler and a VNA (for the S_{11} measurement) is used

where:

u_1(PM1) is dependent on instrument accuracy, sensor linearity, noise, zero setting, zero drift, calibration factor, reference power accuracy, reference power mismatch.

u_1(cable) is the maximum deviation resulting from cable movement (rectangular distribution).

u_1(attenuator) is the uncertainty on the attenuator value.

u_2(PM1) is dependent on instrument accuracy, sensor linearity, noise, zero setting, zero drift, calibration factor, reference power accuracy, reference power mismatch.

Γ_{GE} is the equivalent source reflection, when a directional coupler is used:

$$\Gamma_{GE} = \frac{S_{32} + S_{21}}{S_{31}} - S_{22} \qquad \text{(D.3)}$$

The S parameters for the directional coupler can be obtained from manufacturer specifications, or measured with a VNA.

f) $u_1(\Gamma_{GE}, \Gamma_e, S_{11})$ is expressed as:

$$u(\delta\Gamma) = \sqrt{2} \times |D_d| \times \sqrt{(|\Gamma_e|^2 + |S_{11}|^2} \qquad \text{(D.4)}$$

where

Γ_e is the reflection coefficient of the PM1 power sensor with attenuator attn. 1;

S_{11} is the reflection coefficient of the reference antenna.

D.3 *System check*

D.3.1 *System check* antennas and test conditions

The antennas used for *system check* can be different from those required for the *system validation* (see Annex F). *System check* antennas shall have excellent repeatability (less than 10 % variation) and therefore underpin good positioning repeatability (< 0,2 mm with respect to distance from the shell which shall be established with a low-loss spacer and < 1 mm in tangential directions in case of the head phantoms), mechanical stability, and impedance matching for the measurement conditions.

System check antennas can have two pairs of target values:

a) absolute targets $SAR_{1g,cal}$ and $SAR_{10g,cal}$ (e.g., see Tables D.2 and D.3). These target values shall be determined by numerical modeling that is compliant with IEC/IEEE 62704-1 or IEC 62704-4 standard requirements (including the low-loss spacer in the model). The target values shall also be validated experimentally using a traceable calibration standard (e.g., according to Annex G). Proper application of these conditions according to the requirements of this PAS shall be demonstrated.

b) The system check shall be performed within two weeks of the recalibration of the SAR measurement system by calibration lab and the $SAR_{1g,sys}$ and $SAR_{10g,sys}$ shall be provided.

The *system check* antennas should have a return loss greater than 12 dB at each location on the flat and SAM head phantoms. The return loss shall be measured annually during *system validation* using a network analyzer, to ensure that SAR measurement uncertainty due to power reflection remains as low as possible. Such uncertainty shall be assessed and documented.

For single probe systems, the tests are performed in one section of the same phantom only (e.g., in the flat section of the TwinSAM), following the requirements of IEC 62209-1 and IEC 62209-2.

For array systems, *system check* antennas for at least four frequencies (e.g., 835 MHz, 1 950 MHz, 2 450 MHz and 5 800 MHz) shall be used to cover system operating frequency range. At each selected frequency, SAR shall be measured in all flat and SAM phantoms for at least four locations. The antenna locations and target values for the head and flat phantoms are provided by the manufacturer.

NOTE If only one frequency is tested, the *system check* only needs to be performed at the specific frequency or at two closest frequencies.

D.3.2 System check acceptance criteria

System check is a complete 1 g and/or 10 g peak spatial-average SAR measurement. The measured 1 g and/or 10 g SAR is normalized to 1 W forward power to the *system check* antenna and compared to the appropriate target values. The required RF power measurement setup and SAR normalization procedure are described in D.2.

The *system check* is successful if:

- the measured values are within two standard deviations of the system standard uncertainty u_s of the absolute targets $SAR_{1g,cal}$ and $SAR_{10g,cal}$, and
- the measured values are repeatable within ± 10 % of the measured reference values ($SAR_{1g,sys}$ and/or $SAR_{1g,sys}$) for that measurement system.

In case this criterion cannot be met, the reasons for failure shall be investigated and corrected before starting DUT SAR testing in the failed frequency and phantom configuration.

D.4 *System validation*

D.4.1 Requirements for *system validation* antennas and test conditions

Validation test conditions shall be selected based on system specifications defined by the manufacturer as compliant with the requirements of this PAS and according to measurement requirements for the system at the testing laboratory.

NOTE For example, if a laboratory only performs WLAN tests for body-worn devices, validation is required only for the flat phantom in the 2,45 GHz and 5 GHz range for the subsets of tests defined below.

The validation antennas and procedure shall meet the following requirements:

a) *System validation* shall cover the range of frequencies used by the system for testing. Every DUT test frequency shall be within ±100 MHz or ±10 % (whichever is greater) of a validation frequency supported by the SAR system. A typical set of validation frequencies for a system used in the 700 MHz to 6 000 MHz range may include 750 MHz, 835 MHz, 900 MHz, 1 450 MHz, 1 750 MHz, 1 950 MHz, 2 450 MHz, 2 600 MHz, 3 700 MHz, 5 200 MHz, 5 500 MHz and 5 800 MHz.

b) System validation shall be done for the modulation, multiplexing scheme the duplexing method that represent the set of signals that the DUTs are using. In Table D.1, both modulations of group G1 and all modulations in each of groups G2 and G3 shall be tested. The tests can be reduced to one per group if it is demonstrated and documented that the system provides accurate results independent of modulation by design. These modulations are based on the recommendation that the system is tested for the modulations, multiplexing schemes, and duplex schemes for which the DUT generates the various peak-to-average ratios, in order to validate that the system accurately measures the signal.

c) SAR distributions shall be dominated by field components normal to the surface of phantoms (evanescent components).

d) SAR distributions shall be dominated by field components parallel to the surface of phantoms (propagating components) with various polarizations.

e) The antennas and RF measuring equipment used for the validation shall be an independent set of equipment from those used for system calibration. Using different sets of equipment avoids any calibration biases being passed on to the validation.

f) The measured 1 g SAR levels shall correspond to the dynamic range of the SAR measurement system and the range of SAR expected from wireless devices, (e.g., from > 0,1 W/kg to < 10 W/kg)

g) Different locations (loc) (Figure D.5 and Figure D.6) are chosen to ensure that variations in the sensor locations and inhomogeneity of the tissue equivalent material are considered. The locations are chosen for reliable psSAR evaluation within the measurement region specified for the system, i.e., the manufacturer shall specify this region. Locations that are too close to the edges of the measurement region may introduce errors and uncertainties that are unacceptable.

h) 1 g and 10 g SAR targets of the reference antennas shall be determined based on numerical assessments that are in compliance with IEC/IEEE 62704 series. The expanded uncertainty of the SAR targets shall not exceed 20 % and more than 60 % of the antennas shall be below 10 % (k = 2). The reference antennas shall be verified by calibration traceable to ISO/IEC 17025. The reference antennas used for *system validation* are defined in Annex F.

Table D.1 – Modulations and multiplexing methods used by radio systems

Group	No.	Group denomination	Modulation Type	Transmission method / Multiplexing	Duplex	Example	Description
G1	M1	Reference non modulated – Low PAPR	CW	n/a	n/a	CW	Unmodulated carrier
	M14	Reference non modulated – High PAPR	CW	n/a	n/a	Pulse	Pulse signal with a period of 10ms and a duty cycle of 10 % (1ms ON – 9ms OFF)
G2	M2	High PAPR	GFSK, PSK	TDMA	FDD	GSM	EDGE-FDD (TDMA, 8PSK, TN 0)
	M6	High PAPR	QAM	OFDM	TDD	WLAN	IEEE 802.11g WiFi 2.4 GHz (DSSS/OFDM, 54 Mbps)
	M5	High PAPR	QAM	OFDM	TDD	WLAN	IEEE 802.11a/h WiFi 5 GHz (OFDM, 54 Mbps)
	M10	High PAPR	64-QAM	SC-FDMA	TDD	LTE-TDD	LTE-TDD (SC-FDMA, 1 RB, 1.4 MHz, 64-QAM)
	M8	High PAPR	64-QAM	SC-FDMA	TDD	LTE-TDD	LTE-TDD (SC-FDMA, 100 RB, 10 MHz, 64-QAM)
G3	M4	Low PAPR	QAM	OFDM	TDD	WLAN	IEEE 802.11a/h WiFi 5 GHz (OFDM, 6 Mbps)
	M9	Low PAPR	16-QAM	SC-FDMA	FDD	LTE-FDD	LTE-FDD (SC-FDMA, 1 RB, 20 MHz, 16-QAM)
	M7	Low PAPR	QPSK	SC-FDMA	FDD	LTE-FDD	LTE-FDD (SC-FDMA, 100 RB, 20 MHz, QPSK)
	M3	Low PAPR	GFSK	TDMA	TDD	Bluetooth	IEEE 802.15.1 Bluetooth (GFSK, DH1)
	M12	Low PAPR	QPSK	DSSS	TDD	WLAN	IEEE 802.11b WiFi 2.4 GHz (DSSS, 11 Mbps)
	M13	Low PAPR	GFSK, PSK	TDMA	FDD	GSM	GPRS-FDD (TDMA, GMSK, TN 0-1-2-3)
	M11	Low PAPR	QPSK	CDMA	FDD	UMTS	WCDMA, 12.2 kbps RMC, IS-2000

D.4.2 Test positions for *system validation*

The test positions for head phantoms are selected such that the projected area of a large wireless device that can be operated at the ear is covered by the test positions within the measurement region. The selected dimensions are 80 mm × 160 mm. Given that the antennas can be located anywhere on the wireless device and that curved devices cannot be excluded, the antenna may be in close proximity to the user’s face anywhere within this area. The maximum measurement area specified by the system manufacturer shall be marked on the phantom or otherwise indicated to the user.

The test positions for flat phantoms are selected such that the largest wireless device to be tested by the system is covered by the test positions within the measurement region. Maximum device size (maximum length L, maximum width W) shall be marked on the phantom or otherwise indicated to the user. The validation locations shall be proportionally scaled to the maximum device size within the measurement region defined in Figure D.5.

The selected test positions for the flat and head phantoms are defined in the following:

– Flat phantom: the locations of positioning for the reference antennas are defined in Figure D.5 whereby the 0 degree orientation is defined as parallel to the D1-A1 line.
– Head phantom: the locations of positioning the reference antennas are defined in Figure D.6a and Figure D.6b, whereby the 0 degree orientation is the mouth-ear line. The rotation around the axis normal to the surface is defined in Figure D.7.

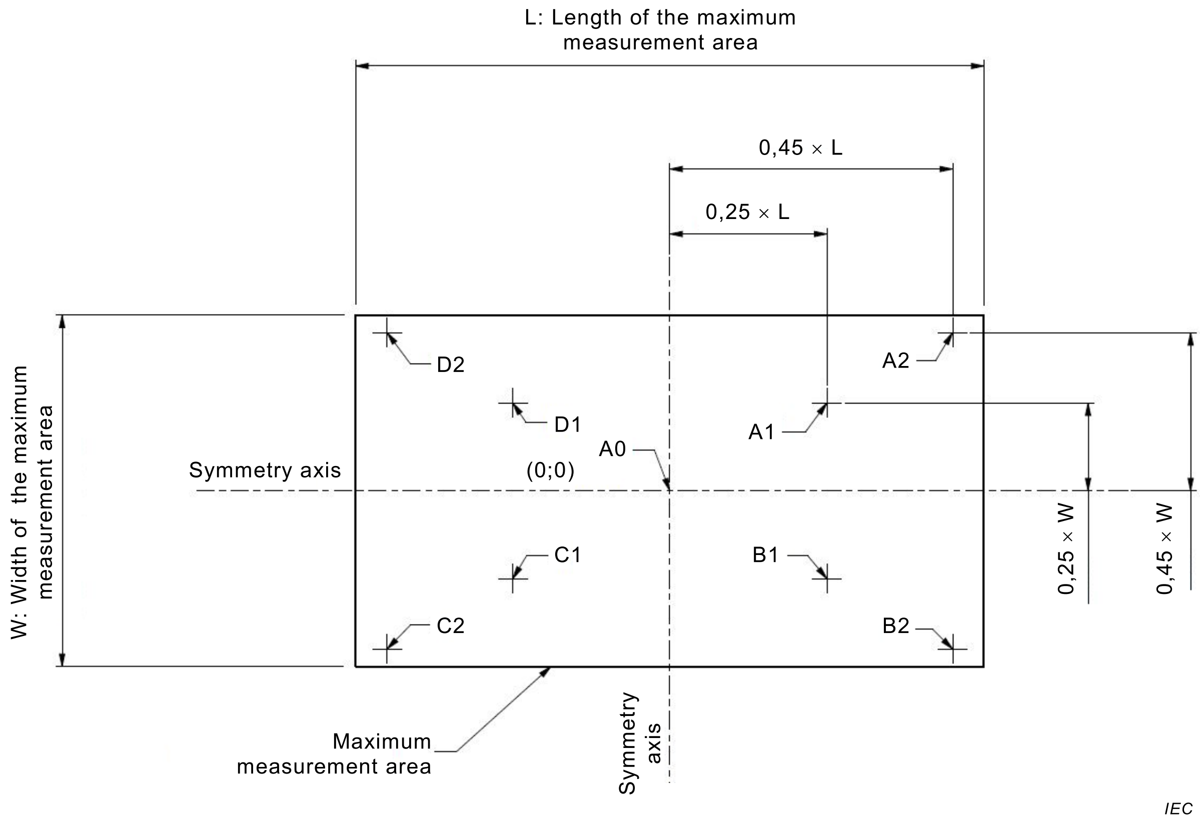

NOTE 1 The zero degree orientation is in the D1 to A1 direction with clockwise rotation to achieve the different orientation defined in Tables D.2 to D.3. The rotational axis z is normal to phantom surface and points inside the phantom.

NOTE 2 If the active measured area is larger, the measurement locations can be extended proportionally. Point A0 is aligned with the centre of the flat phantom.

Figure D.5 – *System check* and validation locations for the flat phantom for minimal device specs (the minimal L and W shall be 160 mm x 80 mm)

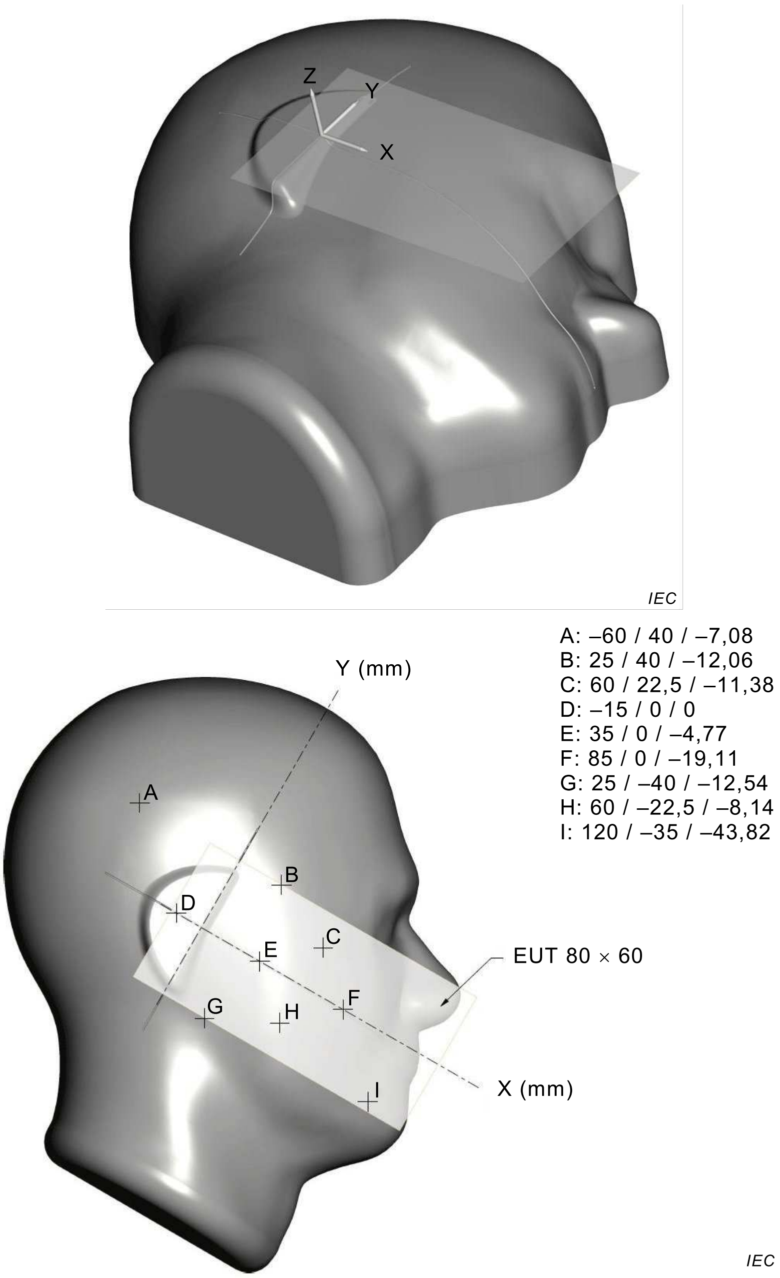

NOTE 1 The points correspond to the projected points from the planar phone on the head.

NOTE 2 The points are illustrated here for the right head but the mirror points shall be taken for the left head. Measurement location A can be omitted if the system is declared not suitable for testing devices with external stub or whip antennas. Measurement location I can be omitted if the system is declared not suitable for devices with bottom antenna or curved surface in close proximity to this location.

Figure D.6 – *System check* and validation locations for the head phantom

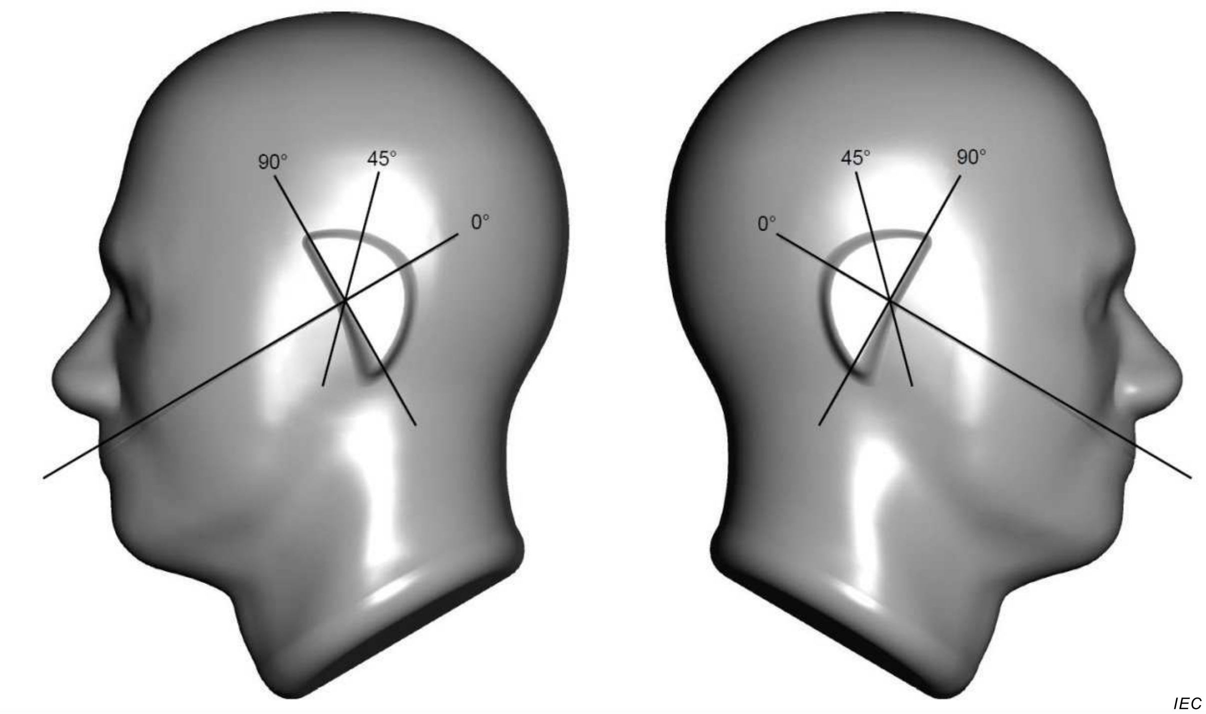

NOTE The z axis points normal to the surface and positive direction into the medium for the right head (and opposite for the left head). The 0° angle is parallel to the line from the mouth to the ear reference point (i.e., the x axis in Figure D.6). For the right head, the other angles are defined with clockwise rotation from 0°.

Figure D.7 – Definition of rotation angles for dipoles

D.4.3 *System validation* procedure based on peak spatial-average SAR

The *system validation* procedure is performed for each phantom system using the reference antennas as defined in Annex F and by sequentially measuring the spatial peak SAR 1 g and 10 g of all the test conditions as defined in Table D.2 to Table D.3. Additional tests can be performed to increase the rigidness of the evaluations. The target values have been determined numerically with a standard uncertainty of U_{saj} of 0,2 dB for the dipoles and 0,3 dB for the VPIFAs and 2-peak CPIFA. All values have been verified using the calibration procedure as defined in Annex F and the difference between numerical target and the calibration value was found well within the combined uncertainty of the calibration procedure.

Table D.2a – Peak spatial SAR (psSAR) averaged over 1g and 10g values for the flat phantom filled with tissue simulating material for the antennas defined in Annex F. Modulations are as defined in Table D.1

No	Antenna Annex F	f_1 [MHz]	P_f [dBm]	Modulation	Loc Deg	d [mm]	SAR 1g,cal	SAR 10g,cal	U_{saj} (k = 1) dB
1	D750	750	20	M1	A0/A1/A2/B1/B2 C1/C2/D1/D2 0/ 45/ 90	15	0,849	0,555	0,2
2	D750	750	13	M1, M9, M10	A0/A1/A2 0/ 67,5/ 90	15	0,169	0,111	0,2
4	D750	750	20	M2, M13, M14	C1/C2 22,5	25	0,515	0,359	0,2
5	D1950	1950	10	M1, M7, M8, M11	B1/B2 0/67,5/90	10	0,405	0,209	0,2
6	D1950	1950	24	M1	A 1/A2 0/ 45/ 90	10	10,17	5,25	0,2
7	D1950	1950	3	M1	A0/D1/D2 0/22,5/90	5	0,13	0,059	0,2
8	D1950	1950	30	M1, M14	D1/D2 22,5	25	6,91	4,15	0,2
9	D2450	2450	10	M1, M3, M6	C1/C2 0/45/90	10	0,514	0,238	0,2
11	D2450	2450	30	M3, M12	D1/D2 0/45/90	10	51,4	23,80	0,2
11	D2450	2450	3	M1	A0/A1/A2 0/67,5/90	5	0,188	0,078	0,2
12	D2450	2450	20	M3, M6, M14	B2 22,5	25	0,717	0,393	0,2
13	D5800	5800	10	M4, M5	D1/D2 0/67,5/90	10	0,78	0,219	0,2
15	D5800	5800	0	M1	A0/A1/A2 0/45/90/	5	0,274	0,057	0,2
16	D5800	5800	20	M1, M14	A0 22,5	25	1,48	0,57	0,2
17	D835	835	30	M1	A2 22,5/ 67,5	15	9,56	6,22	0,2
18	D900	900	17	M1	A1 0/ 90	15	0,547	0,350	0,2

No	Antenna Annex F	f_1 [MHz]	P_f [dBm]	Modulation	Loc Deg	d [mm]	SAR 1g,cal	SAR 10g,cal	U_{saj} (k = 1) dB
19	D1450	1450	13	M1	A0 0/ 90	10	0,583	0,324	0,2
20	D1750	1750	10	M1	B1 22,5/ 67,5	10	0,364	0,193	0,2
21	D2300	2300	20	M1	B2 0/ 90	10	4,87	2,33	0,2
22	D2600	2600	20	M1	C1 0/ 90	10	5,53	2,46	0,2
23	D3700	3700	10	M1	C2 22,5/ 67,5	10	0,674	0,242	0,2
24	D5000	5200	7	M1	D1 0/ 90	10	0,379	0,107	0,2
25	D5000	5500	7	M1	D2 22,5/ 67,5	10	0,417	0,117	0,2
26	D5000	5600	27	M1	A1 0/ 90	10	40,1	11,3	0,2
27	VPIFA-750	750	24	M1	A0/A1/A2/B1/B2/ C1/C2/D1/D2 0/ 90 0	0	3,25	0,97	0,3
28	VPIFA-835	835	24	M1	A0/A1/A2/B1/B2/ C1/C2/D1/D2 0/ 90	0	3,32	0,96	0,3
29	VPIFA-1950	1950	24	M1	A0/A1/A2/B1/B2/ C1/C2/D1/D2 0/ 90	0	2,18	0,90	0,3
30	VPIFA-3700	3700	24	M1	A0/A1/A2/B1/B2/ C1/C2/D1/D2 0/ 90	0	2,48	1,04	0,3

Table D.2b – Peak spatial SAR (psSAR) averaged over 1g and 10g values for antenna generating two peaks on the flat phantom filled with tissue simulating material for the antennas defined in Annex F. Modulations are as defined in Table D.1

No	**Antenna Annex F**	f_1 [MHz]	P_f dBm	**Mod UID**	**Loc Pos Deg**	d [mm]	SAR_1 **1g,cal**	SAR_1 **10g,cal**	SAR_2 **1g,cal**	SAR_2 **10g,cal**	U_{tij} **(k=1)** dB
1	2-PEAK CPIFA	2450	24	M1	A0/A1/A2/B1/B2/C1/C2/D1/D2 0/ 45/ 90	5	1,7	0,806	1,34	0,661	0,3

Table D.3a – Peak spatial SAR (psSAR) averaged over 1g and 10g values on the head left and right phantom for the antennas defined in Annex F. Modulations are as defined in Table D.1

	Antenna Annex F	f_1 [MHz]	P_f [dBm]	**Mod UID**	**Loc Pos Deg**	d [mm]	$SAR_{1g,cal}$	$SAR_{10g,cal}$	U_{sai} **(k=1)** dB
1	D750	750	30	M1, M9, M10, M14	A/ B/ D/ F 0/ 45/ 90	15	A(0/45/90)=(7,55/7,28/7,58); B(0/45/90)=(8,32/8,90/8,24); D(0/45/90)=(7,13/7,17/6,78); F(0/45/90)=(7,48/8,48/8,43)	A(0/45/90)=(4,98/4,91/5,09); B(0/45/90)=(5,51/5,85/5,44); D(0/45/90)=(4,85/4,90/4,62); F(0/45/90)=(5,03/5,72/5,60)	0,2
2	D750	750	15	M2, M13	C/ E/ G/ H/ I 0/ 45/ 90	15	C(0/45/90)=(0,243/0,278/0,266); E(0/45/90)=(0,278/0,288/0,259); H(0/45/90)=(0,243/0,288/0,266); I(0/45/90)=(0,256/0,247/0,225)	C(0/45/90)=(0,161/0,183/0,177); E(0/45/90)=(0,183/0,190/0,171); H(0/45/90)=(0,168/0,190/0,177); I(0/45/90)=(0,171/0,164/0,149)	0,2
3	D1950	1950	20	M1, M7, M8, M11	A/ B/ D/ F 0/ 45/ 90	10	A(0/45/90)=(4,22/3,98/4,10); B(0/45/90)=(4,23/4,27/4,17); D(0/45/90)=(2,91/2,87/2,85); F(0/45/90)=(4,00/4,14/4,22)	A(0/45/90)=(2,13/2,05/2,11); B(0/45/90)=(2,16/2,17/2,12); D(0/45/90)=(1,57/1,56/1,56); F(0/45/90)=(2,05/2,11/2,15)	0,2
4	D1950	1950	3	M1, M14	C/ E/ G/ H/ I 45	10	C(45)=(0,087); E(45)=(0,084); H(45)=(0,087); I(45)=(0,081)	C(45)=(0,044); E(45)=(0,043); H(45)=(0,044); I(45)=(0,042)	0,2
5	D1950	1950	14	M1	A-I 0/ 90	5	A(0/90)=(2,05/1,94); B(0/90)=(1,90/1,94); C(0/90)=(1,97/1,95); D(0/90)=(1,35/1,15); E(0/90)=(1,59/1,91); F(0/90)=(2,05/1,96); H(0/90)=(1,93/2,07); I(0/90)=(1,84/2,02)	A(0/90)=(0,90/0,87); B(0/90)=(0,85/0,86); C(0/90)=(0,87/0,86); D(0/90)=(0,67/0,58); E(0/90)=(0,74/0,86); F(0/90)=(0,90/0,87); H(0/90)=(0,86/0,92); I(0/90)=(0,85/0,88)	0,2
6	D1950	1950	24	M1	A-I 0/ 45/ 90	25	A(0/45/90)=(1,79/1,68/1,75); B(0/45/90)=(1,77/1,85/1,74); C(0/45/90)=(1,75/1,91/1,84); D(0/45/90)=(1,39/1,38/1,37); E(0/45/90)=(1,78/1,87/1,72); F(0/45/90)=(1,62/1,76/1,84); G(0/45/90)=(1,69/1,75/1,87); H(0/45/90)=(1,68/1,99/1,87); I(0/45/90)=(2,05/1,85/1,57)	A(0/45/90)=(1,08/1,03/1,07); B(0/45/90)=(1,07/1,11/1,05); C(0/45/90)=(1,06/1,14/1,10); D(0/45/90)=(0,85/0,85/0,84); E(0/45/90)=(1,07/1,12/1,04); F(0/45/90)=(1,00/1,08/1,12); G(0/45/90)=(1,05/1,07/1,14); H(0/45/90)=(1,03/1,18/1,11); I(0/45/90)=(1,27/1,15/0,96)	0,2
7	D2450	2450	20	M1, M3, M6, M12, M14	A/ B/ D/ F 0/ 90	10	A(0/90)=(5,46/5,35); B(0/90)=(5,40/5,38); D(0/90)=(3,39/3,22); F(0/90)=(5,32/5,48)	A(0/90)=(2,46/2,40); B(0/90)=(2,51/2,43); D(0/90)=(1,65/1,60); F(0/90)=(2,40/2,49)	0,2

	Antenna Annex F	f_1 [MHz]	P_f [dBm]	**Mod UID**	**Loc Pos Deg**	d [mm]	$SAR_{1g,cal}$	$SAR_{10g,cal}$	U_{cal} **(k=1)** dB
8	D2450	2450	10	M1	C/ E/ G/ H/ I 0/ 90	10	C(0/90)=(0,53/0,55); E(0/90)=(0,52/0,52); G(0/90)=(0,46/0,49); H(0/90)=(0,51/0,56); I(0/90)=(0,56/0,53)	C(0/90)=(0,24/0,25); E(0/90)=(0,24/0,24); G(0/90)=(0,23/0,23); H(0/90)=(0,24/0,27); I(0/90)=(0,26/0,24)	0,2
9	D5000	5800	24	M1, M4, M5, M14	A/ B/ D/ F 0/ 45/ 90	10	A(0/45/90)=(21,1/19,7/20,1); B(0/45/90)=(21,1/21,2/20,4); D(0/45/90)=(15,5/15,7/16,1); F(0/45/90)=(20,8/20,9/20,8)	A(0/45/90)=(5,2/51/5,1); B(0/45/90)=(5,4/5,3/5,2); D(0/45/90)=(5,0/5,1/5,3); F(0/45/90)=(5,2/5,2/5,2)	0,2
10	D5000	5800	5	M5	C/ E/ G/ H/ I 0/ 45/ 90	10	C(0/45/90)=(0,253/0,262/0,266); E(0/45/90)=(0,269/0,266/0,250); G(0/45/90)=(0,256/0,262/0,266); H(0/45/90)=(0,250/0,250/0,272); I(0/45/90)=(0,269/0,266/0,269)	C(0/45/90)=(0,063/0,066/0,066); E(0/45/90)=(0,070/0,066/0,063); G(0/45/90)=(0,070/0,073/0,073); H(0/45/90)=(0,063/0,060/0,066); I(0/45/90)=(0,066/0,066/0,066)	0,2
11	D5000	5800	24	M1	A/ B/ D/ F 0/ 45/ 90	5	A(0/45/90)=(69/5/69/7/67/4); B(0/45/90)=(63/9/73/9/74/9); D(0/45/90)=(25/2/27/8/25/8); F(0/45/90)=(67/4/75/0/75/0)	A(0/45/90)=(13,2/13,2/13,1); B(0/45/90)=(13,0/14,0/14,1); D(0/45/90)=(7,2/7,8/7,4); F(0/45/90)=(13,1/13,9/14,0)	0,2
12	D5000	5800	14	M1	C/ E/ G/ H/ I 0/ 45/ 90	25	C(0/45/90)=(0,41/0,43/0,43); E(0/45/90)=(0,41/0,40/0,38); G(0/45/90)=(0,37/0,39/0,40); H(0/45/90)=(0,38/0,41/0,42); I(0/45/90)=(0,39/0,39/0,39)	C(0/45/90)=(0,15/0,15/0,15); E(0/45/90)=(0,15/0,14/0,14); G(0/45/90)=(0,14/0,15/0,15); H(0/45/90)=(0,14/0,14/0,15); I(0/45/90)=(0,15/0,14/0,14)	0,2
13	D835	835	20	M1	A/ B/ D/ F 0/ 90	15	A(0/90)=(0,91/0,90); B(0/90)=(0,98/0,97); D(0/90)=(0,82/0,78); F(0/90)=(0,89/0,98)	A(0/90)=(0,595/0,602); B(0/90)=(0,644/0,637); D(0/90)=(0,557/0,528); F(0/90)=(0,597/0,649)	0,2
14	D900	900	30	M1	C/ E/ H/ I 0/ 90	15	C(0/90)=(10,34/11,15); E(0/90)=(11,46/10,86); H(0/90)=(10,40/11,12); I(0/90)=(11,09/9,26)	C(0/90)=(6,74/7,25); E(0/90)=(7,39/7,06); H(0/90)=(6,91/7,21); I(0/90)=(7,20/6,03)	0,2
15	D900	900	30	M1	G 0/ 90	25	G(0/90)=(5,76/7,10);	G(0/90)=(4,0/4,80);	0,2
16	D1450	1450	10	M1	A/ B/ D/ F 0/ 90	10	A(0/90)=(0,29/0,29); B(0/90)=(0,30/0,30); D(0/90)=(0,23/0,23); F(0/90)=(0,28/0,30)	A(0/90)=(0,16/0,16); B(0/90)=(0,17/0,16); D(0/90)=(0,13/0,13); F(0/90)=(0,16/0,17)	0,2

	Antenna Annex F	f_1 [MHz]	P_f [dBm]	**Mod UID**	**Loc Pos Deg**	d [mm]	$SAR_{1g,cal}$	$SAR_{10g,cal}$	U_{cal} **(k=1)** dB
17	D1750	1750	30	M1	C/ E/ H/ I 0/ 90	10	C(0/90)=(37,69/39,26); E(0/90)=(37,18/37,89); H(0/90)=(36,72/39,63); I(0/90)=(39,50/34,40)	C(0/90)=(19,70/ 20,52); E(0/90)=(19,59/19,93); H(0/90)=(19,35/20,57); I(0/90)=(21,03/17,92)	0,2
18	D2300	2300	10	M1	A/ B/ D/ F 0/ 90	10	A(0/90)=(0,51/0,50); B(0/90)=(0,51/0,50); D(0/90)=(0,33/0,33); F(0/90)=(0,49/0,51)	A(0/90)=(0,24/0,23); B(0/90)=(0,24/0,24); D(0/90)=(0,17/0,17); F(0/90)=(0,23/0,24)	0,2
19	D2600	2600	20	M1	C/ E/ G/ H/ I 0/ 90	10	C(0/90)=(5,63/5,88); E(0/90)=(5,72/5,56); G(0/90)=(5,21/5,52); H(0/90)=(5,41/5,95); I(0/90)=(6,02/5,58)	C(0/90)=(2,42/2,53); E(0/90)=(2,48/2,43); G(0/90)=(2,40/2,51); H(0/90)=(2,32/2,53); I(0/90)=(2,64/2,39)	0,2
20	D3700	3700	10	M1	A/ B/ D/ F 0/ 90	10	A(0/90)=(0,72/0,68); B(0/90)=(0,72/0,70); D(0/90)=(0,44/0,41); F(0/90)=(0,71/0,72)	A(0/90)=(0,24/0,24); B(0/90)=(0,25/0,24); D(0/90)=(0,17/0,16); F(0/90)=(0,24/0,25)	0,2
21	D5000	5200	10	M1	C/ E/ G/ H/ I 0/ 90	10	C(0/90)=(0,839/0,889); E(0/90)=(0,893/0,829); G(0/90)=(0,847/0,884); H(0/90)=(0,827/0,898); I(0/90)=(0,889/0,893)	C(0/90)=(0,216/0,227); E(0/90)=(0,232/0,219); G(0/90)=(0,235/0,244); H(0/90)=(0,209/0,224); I(0/90)=(0,231/0,229)	0,2
22	D5000	5400	5	M1	A/ B/ D/ F 0/ 90	10	A(0/90)=(0,273/0,261); B(0/90)=(0,276/0,266); D(0/90)=(0,190/0,193); F(0/90)=(0,272/0,272)	A(0/90)=(0,069/0,068); B(0/90)=(0,070/0,068); D(0/90)=(0,062/0,063); F(0/90)=(0,069/0,059)	0,2
23	D5000	5500	24	M1	C/ E/ G/ H/ I 0/ 90	10	C(0/90)=(20,6/21,8); E(0/90)=(21,9/20,4); G(0/90)=(20,8/21,7); H(0/90)=(20,4/22,1); I(0/90)=(21,8/21,8)	C(0/90)=(5,2/5,5); E(0/90)=(5,6/5,3); G(0/90)=(5,7/5,9); H(0/90)=(5,1/5,4); I(0/90)=(5,6/5,5)	0,2
24	D5000	5600	14	M1	A/ B/ D/ F 0/ 90	10	A(0/90)=(2,14/2,04); B(0/90)=(2,15/2,07); D(0/90)=(1,53/1,57); F(0/90)=(2,12/2,12)	A(0/90)=(0,54/0,52); B(0/90)=(0,55/0,53); D(0/90)=(0,49/0,52); F(0/90)=(0,53/0,53)	0,2

	Antenna Annex F	f_1 [MHz]	P_f [dBm]	**Mod UID**	**Loc Pos Deg**	d [mm]	$SAR_{1g,cal}$	$SAR_{10g,cal}$	U_{cal} **(k=1)** dB
25	VPIFA-750	750	24	M1	A…I 0/ 90	0	A(0/90)=(3,39/3,28); B(0/90)=(3,27/3,30); C(0/90)=(3,25/ 3,31); E(0/90)=(3,33/ 3,33); F(0/90)=(3,28/3,35); G(0/90)=(3,34/3,37); H(0/90)=(3,26/3,46); I(0/90)=(2,87/ 3,01)	A(0/90)=(0,91/ 0,88); B(0/90)=(0,89/ 0,90); C(0/90)=(0,87/ 0,89); E(0/90)=(0,92/ 0,91); F(0/90)=(0,89/ 0,91); G(0/90)=(0,96/ 0,96); H(0/90)=(0,88/ 0,92); I(0/90)=(0,81/ 0,84)	0,3
26	VPIFA-835	835	24	M1	A…I 0/ 90	0	A(0/90)=(3,39/ 3,27); B(0/90)=(3,26/ 3,28); C(0/90)=(3,20/ 3,22); E(0/90)=(3,23/ 3,23); F(0/90)=(3,21/ 3,23); G(0/90)=(3,24/ 3,31); H(0/90)=(3, 14/ 3,36); I(0/90)=(2,85/ 2,98)	A(0/90)=(0,93/ 0,90); B(0/90)=(0,91/ 0,92); C(0/90)=(0,88/ 0,88); E(0/90)=(0,91/ 0,90); F(0/90)=(0,90/ 0,90); G(0/90)=(0,96/ 0,97); H(0/90)=(0,87/ 0,92); I(0/90)=(0,83/ 0,86)	0,3
27	VPIFA-1950	1950	24	M1	A…I 0/ 90	0	A(0/90)=(2,27/ 2,23); B(0/90)=(2,23/ 2,25); C(0/90)=(2,29/ 2,27); E(0/90)=(2,27/ 2,26); F(0/90)=(2,24/ 2,28); G(0/90))=(2,24/ 2,22); H(0/90)=(2,26/ 2,32); I(0/90)=(2,14/ 2,16)	A(0/90)=(0,90/ 0,89); B(0/90)=(0,90/ 0,90); C(0/90)=(0,90/ 0,90); E(0/90)=(0,92/ 0,91); F(0/90)=(0,90/ 0,90); G(0/90)=(0,96/ 0,97); H(0/90)=(0,88/ 0,91); I(0/90)=(0,88/ 0,87)	0,3
28	VPIFA-3700	3700	24	M1	A…I 0/ 90	0	A(0/90)=(2,50/ 2,30); B(0/90)=(2,25/ 2,21); C(0/90)=(2,23/ 2,27); E(0/90)=(2,45/ 2,31); F(0/90)=(2,09/ 2,33); G(0/90)=(2,32/ 2,72); H(0/90)=(2,09/ 2,46); I(0/90)=(2,44/ 2,09)	A(0/90)=(1,02/ 1,00); B(0/90)=(0,96/ 0,97); C(0/90)=(0,98/ 0,98); E(0/90)=(1,01/ 1,00); F(0/90)=(0,97/ 0,99); G(0/90)=(0,99/ 1,05); H(0/90)=(0,97/ 1,00); I(0/90)=(0,98/ 0,96)	0,3

Table D.3b – Peak spatial SAR (psSAR) averaged over 1g and 10g values for antenna generating two peaks on the head left and right phantom for the antennas defined in Annex F. Modulations are as defined in Table D.1

No	**Antenna Annex F**	f_1 [MHz]	P_f dBm	**Mod UID**	**Loc Pos Deg**	d [mm]	SAR_1 **1g,cal**	SAR_1 **10g,cal**	SAR_2 **1g,cal**	SAR_2 **10g,cal**	U_{tij} **(k=1)**
1	2-PEAK CPIFA	2450	24	M1	Phone position R/L	0	3,00/4,80	1,41/1,96	2,12/2,91	0,94/1,45	0,3

D.4.4 Validation acceptance criteria

The validation criteria have been defined to meet the objectives as defined in D.1.2, i.e., to verify that the SAR measurement system is operating within its range of specified use and corresponding uncertainty as determined in clause 8 will not give erroneous measurement results for the DUT. Each single subsystem(s) or phantom (head left, head right, flat, etc.) is validated separately.

NOTE The acceptance criteria is an adaption of ISO 3611:2010, “Geometrical product specifications (GPS) – Dimensional measuring equipment: Micrometers for external measurements – Design and metrological characteristics”.

All validation antennas and configurations from Table D.2 and Table D.3 which are within the operating frequency range and surface area of the measuring system (as specified by the manufacturer), shall be tested according to the procedure defined in Annex D.2. The relative differences $r_{\mathrm{s,1g,j}}$ and $r_{\mathrm{s,10g,j}}$ in %, between the numerical targets $SAR_{\mathrm{1g,cal,j}}$ and $SAR_{\mathrm{10g,cal,j}}$ and the measured values, $SAR_{\mathrm{1g,m,j}}$ and $SAR_{\mathrm{10g,m,j}}$, is defined as:

$$r_{s,1g,j} = 100\% \times \left(\frac{SAR_{1g,m,j} - SAR_{1g,cal,j}}{SAR_{1g,cal,j}}\right) \quad \text{(D.5a)}$$

$$r_{s,10g,j} = 100\% \times \left(\frac{SAR_{10g,m,j} - SAR_{10g,cal,j}}{SAR_{10g,cal,j}}\right) \quad \text{(D.5b)}$$

whereby the maximum $r_{\mathrm{sj,max}}$ and the minimum $r_{\mathrm{sj,min}}$ over all $r_{\mathrm{s,1g,j}}$ and all $r_{\mathrm{s,10g,j}}$ shall be determined. The maximum permitted error (MPE) is the smallest tolerance (+O, -U) which encompasses ALL of the calculated differences.

Therefore, the system passes the criteria if the following conditions are met:

$$r_{\mathrm{sj,max}} < 2 \times u_{\mathrm{s}} + 15\ \% = +O \quad \text{(D.6)}$$

$$r_{sj,\mathrm{min}} > -100 \times \frac{2 \times u_s + 15\%}{100 + 2 \times u_s + 15\%} = -U \quad \text{(D.7)}$$

where

u_{s} is the standard system uncertainty for k = 1 in % as determined in clause 8 and

15 % is the maximum expanded uncertainty for k = 2 for the validation antennas as provided in Table D.2 and D.3.

NOTE Equation (D.6) limits the degree the system over-reads, and equation (D.7) limits the degree that the system under-reads. The 15% is the maximum target uncertainty of the validation antennas (k = 2). Because of conservative reasons in favor for the array systems these uncertainties are considered linearly additive. If the system uncertainty is 15%, +O = 45% and –U = -31 %.

If a system fails this validation test, the measurements corresponding to the points that failed shall be repeated at least 10 times in order to preclude measurement outliers. Calculate the average μ_{sj} and standard deviation σ_{sj} from the 10 r_{sj} values. If μ_{sj} is greater than one, replace r_{sj} with μ_{sj} + 2 σ_{sj}. If μ_{sj} is less than one, replace r_{sj} with μ_{sj} – 2 σ_{sj}.

The MPE values (+O, –U) obtained from the system validation procedure shall be reported in all measurement certificates, together with the uncertainty estimate for the measurements system.

NOTE This additional repetition ensures that 95 % of the values will be within the acceptance criteria and the acceptance criteria is not failed by chance.

Annex E
(informative)

Interlaboratory comparisons

E.1 Purpose

The purpose of the interlaboratory comparison is to compare the results from several laboratories in order to evaluate the performance of SAR measurement systems, their reported measurement uncertainties and measurement protocols defined in this PAS. The principle is to use reference devices and fully validated measurement systems defined in this PAS. The SAR assessment methodologies described in Clause 7 are used.

The measured data from all participating laboratories shall be compared. Also, each participating laboratory shall submit a full measurement uncertainty budget in accordance with Clause 8. If the deviations in the measured data between laboratories can be attributed to the measurement uncertainties (see E.5), the interlaboratory comparison is deemed to be successful. If not, all uncertainty sources shall be re-evaluated per the recommendations of Clause 8. Also, other possible sources of uncertainties different from those defined in Clause 8 shall be considered.

E.2 Monitor laboratory

A monitor laboratory shall be designated that is responsible for the maintenance of the reference devices (i.e., to check that they meet the requirements given in the following sections) and the circulation of the devices to the participating laboratories. The monitor laboratory is also responsible for collecting the measurement data.

If deemed necessary, the reference devices should be returned to the monitor laboratory periodically during the comparison campaign to verify the SAR level, output power (see E.5), frequency and battery condition.

NOTE General guidelines for accomplishing interlaboratory comparison tests are given for example in [50, 96].

E.3 Phantom set-up

The required phantoms and device holders are defined in this PAS. Metallic parts closer than 50 cm from the structure shall be avoided. The phantom shall be irradiated using a reference device mounted according to the test positions described in Clause 7.

E.4 Reference devices

Reference devices are commercial wireless devices that are maintained and distributed in accordance with ISO/IEC Guide 17043. The set of reference devices may also be extended to include non-commercial sources. Each reference device shall have evaluated target SAR values with associated uncertainty less than 30 % for $k = 2$. The designation of the supplier is based on the agreement between the participating parties.

E.5 Power set-up

If the reference device has an accessible antenna port, the forward power to the antenna should be measured by the monitor laboratory and each participating laboratory. The power set-up is dependent on the precision of the output power measurement of the reference device used for the interlaboratory comparison. Each device is checked by the participating laboratory so that the conducted output power of each reference device is in the range of

± 0,3 dB of the reference value reported by the monitor laboratory. The measured output power shall be reported to the monitor laboratory. The device battery shall be fully charged.

E.6 Interlaboratory comparison – Procedure

Measurement procedures for SAR assessment used in the interlaboratory comparison are the same as those used for compliance testing in accordance with Clause 7. Each participating laboratory shall provide a full test report in accordance with the requirements of Clause 9 including system check (see 7.1.2), system validation (see Annex D), tissue-equivalent media parameters (see Clauses 6 and 7.1.1), system uncertainty data (see Clause 8), and measured output power data (see E.5).

Results of the interlaboratory comparison shall be compared to their respective target values. Each result shall fall within the combined expanded uncertainty of the measured value and target value, i.e., the root-sum-squared of the expanded (k = 2) measurement uncertainty and the expanded (k = 2) target value uncertainty. The reports from different laboratories are to be evaluated and compared by the designated monitor laboratory.

Annex F
(normative)

Validation antennas

F.1 Introduction

The following subclauses define the antennas that shall be used for the system validation of vector measurement-based systems, as defined in Annex D. These antennas define a minimum set of antennas based on the criteria provided in Annex D. Antennas defined here shall not be removed from the validation protocol, as this would compromise the ability of the system validation to test the accuracy of the vector measurement-based system. However, additional antennas can be added to the list. The requirements for additional antennas are defined in F.5.

F.2 Standard dipole antenna

As specified in Annex D, standard dipoles well represent one category of antennas and can be easily specified and calibrated for the required frequencies. The reference dipoles are defined for the specific dielectric parameters and thickness of the phantom shell indicated in Table F.1. The reference dipole shall have a return loss better than –20 dB at the test frequency to reduce the uncertainty in the power measurement in the case of the flat phantom at a defined test distance. The return loss requirements can be reduced to better than –15 dB at the head and/or at closer and larger distances to not being required to use different sets of dipoles.

To meet this requirement, it is acceptable to fine-tune the reference dipoles by using low-loss dielectric or metal tuning elements at the ends of the dipole (Figure F.1). The standard dipole antennas of Figure F.1 with mechanical dimensions given in Table F.1 will produce the SAR values given in Table D.2a and Table D.3a when the *system validation* test of Annex D is followed. If dipole antennas are used that have different dimensions than those given in Table F.1, or if dipole antennas are used at frequencies other than those listed in Table F.1, the reference SAR values for those antennas shall be documented and independently verified using procedures that are consistent with the methodologies described in this PAS.

Table F.1 – Mechanical dimensions of the reference dipoles

Frequency (MHz)	**Phantom shell thickness** (mm)	***L*** (mm)	***h*** (mm)	**d_1** (mm)
D300	6,3	396,0	250,0	6,35
D300	2,0	420,0	250,0	6,35
D450	6,3	270,0	166,7	6,35
D450	2,0	290,0	166,7	6,35
D750	2,0	176,0	100,0	6,35
D835	2,0	161,0	89,8	3,6
D900	2,0	149,0	83,3	3,6
D1450	2,0	89,1	51,7	3,6
D1500	2,0	86,2	50,0	3,6
D1640	2,0	79,0	45,7	3,6
D1750	2,0	75,2	42,9	3,6
D1800	2,0	72,0	41,7	3,6
D1900	2,0	68,0	39,5	3,6
D1950	2,0	66,3	38,5	3,6
D2000	2,0	64,5	37,5	3,6
D2100	2,0	61,0	35,7	3,6
D2300	2,0	55,5	32,6	3,6
D2450	2,0	51,5	30,4	3,6
D2600	2,0	48,5	28,8	3,6
D3000	2,0	41,5	25,0	3,6
D3500	2,0	37,0	26,4	3,6
D3700	2,0	34,7	26,4	3,6
D5000 – 6000	2,0	20,6 [a]	40,3 [a]	3,6

[a] These dimensions are applicable for a coaxial diameter at the balun of d_2 = 2,1 mm (see Figure G.1).

NOTE The *L*, *h*, and d_1 dimensions shall be within ±2 % tolerance.

The reference dipole arms shall be parallel to the flat surface of the phantom within a tolerance of ± 2° or less (see Figure F.1). This can be assured by carefully positioning the empty phantom and the reference dipole to horizontal level using a spirit level.

The numerical target values above 3 GHz cannot be universally given as for below 3 GHz due to the greater effect from the spacer, phantom bottom and mechanical uncertainties. Thus, the numerical target values may be different from one dipole to another. It is important that for each dipole used for *system validation* a fully documented analysis is provided based on both numerical simulations and experimental validation.

Dimensions in millimetres

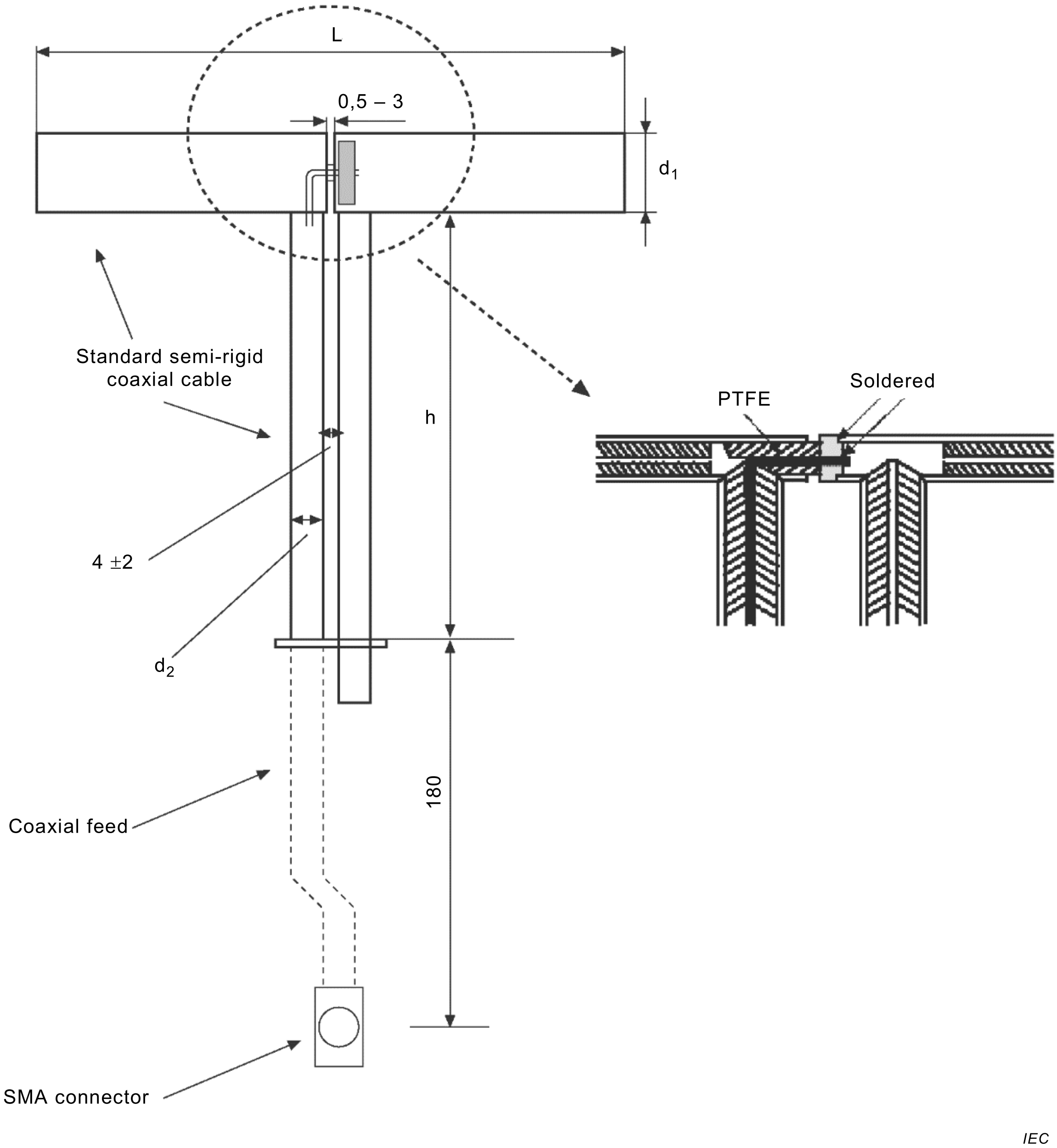

Key

L	Length of the dipole
d_1	Diameter of the dipole
d_2	Diameter of the coaxial cable at the balun
h	Length of the balun choke section
PTFE	polytetrafluoroethylene

Figure F.1 – Mechanical details of the standard dipole

F.3 VPIFA

These single band antennas are designed to be placed at a wide range of locations on the curved surface of the SAM head or on a flat phantom. The design is chosen to provide a predominantly E–field coupling, as seen in a range of antenna structures where antenna metallization extends beyond the ground plane. The structure is that of a PIFA antenna. The main resonant metallic ribbon is orthogonal to the surface of the phantom. It is short-circuited on one side and open-ended on the side that is close to the phantom, where a capacitive coupling is generated. The distance between the conductor and the phantom and its position are fixed by using a plastic separator, which is part of the antenna. The device should be held orthogonal to the surface. The SAR pattern is localized with a dominant orthogonal component. Four frequency versions for VPIFA-750, VPIFA-835, VPIFA-1950, and VPIFA-3 700 MHz are provided. At higher frequencies, the normal components dominate for $d \geq 2$ mm. Figure F.2(a) shows the basic structure of the antenna, seen from the PCB1 side. Figure F.2(a) shows the antenna as seen from the PCB2, here the flat mask has been removed to easily see the integrated spacer. The critical dimensions are shown in Figure F.2(c). Two PCB substrates are used for etching the metallic ribbon and the ground plane, respectively and have a thickness of 0,508 mm each one. Both substrates are mechanically separated by an FR4 frame. One end of this frame is used to fix the antenna to a holder. The antenna is designed to be matched to a 50 Ω coaxial connection. The dimensions for each frequency and the material properties are provided in Table F.2 and Table F.3, respectively. In order to compensate for the manufacturing errors, the antenna includes a tuning structure and a matching screw. In the first case, a dielectric bar is adjusted to tune the resonant frequency, while in the second case a brass screw integrated in the short circuit can be adjusted to change the distance between the feed point and the short-circuit, and therefore, improve the matching. The screw implementation requires a 0,3 mm prism with a hole in order to mechanically position and fix the screw. Additionally, a lock nut is used to secure the screw position. Once the antenna is fine-tuned, both elements should be fixed. The SMA connector requires a bending section to place the connection cable parallel to the antenna axis. To reduce the twisting force (torque), which can break the connector, it is recommended to first connect the bend to the cable and then connect the other side of the bend to the connector. The flat mask (cross shape with central hole for placing the integrated spacer) can be removed to use the same antenna in the SAM mask, see Figure F.3 (b) and Figure F.3 (c).

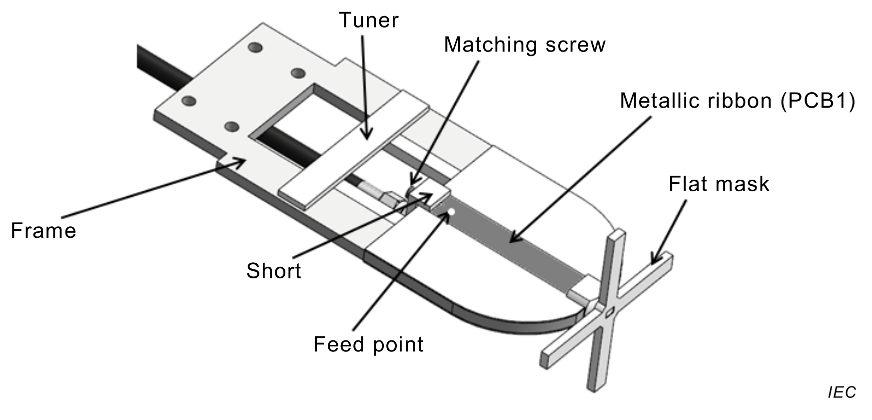

(a)

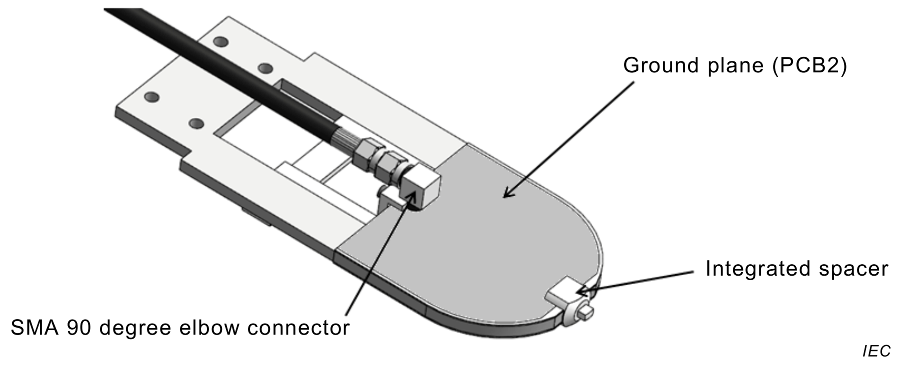

(b)

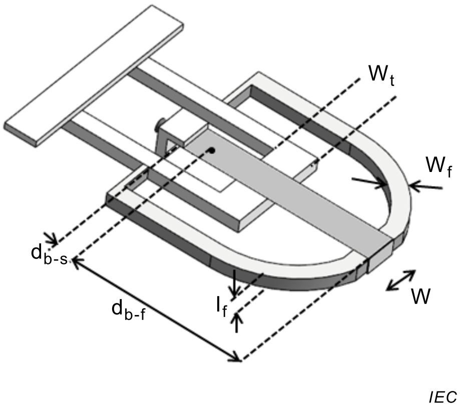

(c)

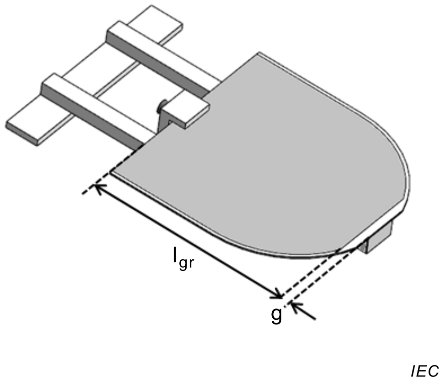

(d)

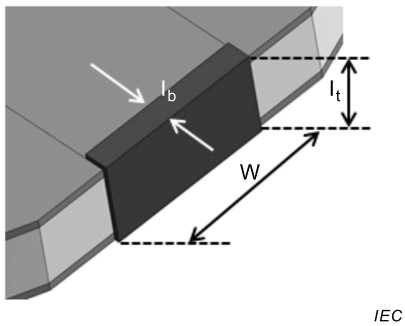

(e)

Key:

(a) General schematic of the antenna viewed from the metallic ribbon side.

(b) General schematic of the antenna viewed from the ground plane side.

(c) Critical dimensions for the antenna from the front side.

(d) Critical dimensions for the antenna from rear side.

(e) Detailed view of the bent segment.

Figure F.2 – VPIFA validation antenna

Key

(a) Flat mask.

(b) Right-head mask (0 deg and 90 deg).

(c) Left-head mask (0 deg and 90 deg).

NOTE The recommended tolerances for the 3D printed masks are ± 0,10 mm.

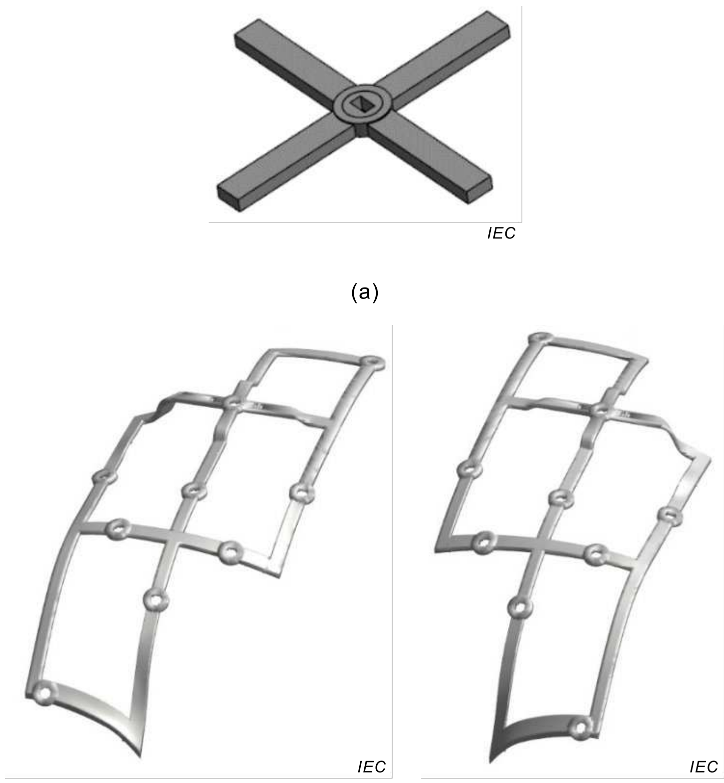

(b) (c)

Figure F.3 – Masks for positioning VPIFAs

The positioning tolerance using these masks are dominated by the mask uncertainty and the corresponding SAR uncertainty is already considered in the uncertainty of the target values.

Table F.2 – Dimensions for VPIFA antennas at different frequencies

Freq. (MHz)	**Ribbon & bent width,** W (mm)	**Length of bent width,** l_b (mm)	**Frame thickness,** l_f **/ radiator thickness,** l_t (mm)	**Frame width,** W_f (mm)	**Matching screw diameter/ length** (mm)	**Tuner width,** W_t (mm)	d_{b-f} (mm)	d_{b-s} (mm)	l_{gr} (mm)	**g** (mm)
750	10,00 ± 0,05	1,50 ± 0,10	4,00 ± 0,05 / 5,35 ± 0,05	5,00 ± 0,05	4,00 ± 0,05 / 12,00 ± 0,10	10,00 ± 0,10	58,00 ± 0,10	5,50 ± 0,10	59,90 ± 0,10	2,50 ± 0,05
835	10,00 ± 0,05	1,50 ± 0,10	4,00 ± 0,05 / 5,35 ± 0,05	5,00 ± 0,05	4,00 ± 0,05 / 12,00 ± 0,10	3,50 ± 0,10	51,70 ± 0,10	5,55 ± 0,10	53,70 ± 0,10	2,50 ± 0,05
1 950	10,00 ± 0,05	1,50 ± 0,10	4,00 ± 0,05 / 5,35 ± 0,05	5,00 ± 0,05	4,00 ± 0,05 / 12,00 ± 0,10	3,00 ± 0,10	77,70 ± 0,10	4,55 ± 0,10	78,45 ± 0,10	2,50 ± 0,05
3 700	3,00 ± 0,05	1,50 ± 0,10	4,00 ± 0,05 / 5,35 ± 0,05	5,00 ± 0,05	4,00 ± 0,05 / 12,00 ± 0,10	2,00 ± 0,10	36,7 ± 0,10	5,77 ± 0,10	38,75 ± 0,10	2,50 ± 0,05

Table F.3 – Electric properties for the dielectric layers for VPIFA antennas

	750 MHz		**835 MHz**		**1 950 MHz**		**3 700 MHz**	
	ε_r	σ [S/m]	ε_r	σ [S/m]	ε_r	σ [S/m]	ε_r	σ [S/m]
Frame (FR4)	4,38	3,49e-3	4,38	3,84e-3	4,37	8,45e-3	4,34	15,7e-3
Mask (3D print)	2,22	1,74e-3	2,22	1,83e-3	2,22	3,09e-3	2,22	5,06e-3
PCB_1 (RO4350B)	3,75	463e-6	3,75	517e-6	3,75	1,24e-3	3,74	2,46e-3
PCB_2 (RO4350B)	3,75	463e-6	3,75	517e-6	3,75	1,24e-3	3,74	2,46e-3
Spacer (PET)	2,97	7,52e-3	2,96	8,05e-3	2,90	14,5e-3	2,84	22,6e-3
Tuner (FR4)	4,38	3,49e-3	4,38	3,84e-3	4,37	8,45e-3	4,34	15,7e-3

F.4 2-PEAK CPIFA

This antenna generates two field peaks at 2450 MHz in order to test the algorithm capable of distinguishing two peaks. This feature is not frequency dependent and does not require tests at different frequencies. Its geometry is similar to a large cellular phone (150 mm × 75 mm) with thickness 10 mm. The antenna is fed by means of a semi-rigid coaxial connected to the 50 Ω point of the main radiator (Figure F.4 (a)). The antenna has 4 dielectric layers, all of them made of FR4, with a ground plane between layer 1 and layer 2. The labels for each layer are shown in Figure F.4(b). The antenna has been designed to have similar amplitude of the reflection coefficient in both flat and head phantoms. For this reason, a foam spacer with thickness 5 mm has to be placed between the antenna and the flat phantom shell. The radiation mechanism is similar to that of a planar inverted-F antenna (PIFA), where a metallic conductor is open-ended in one extreme and short-circuited in the other extreme. The feed point has to be chosen at the right distance from the short. In the specific case of the 2-peak CPIFA, the metallic conductor or ribbon has a T-shape, with two branches open-ended and the third one short-ended. The open-ended are bent. With the aim of generating peaks with different amplitude one of the bent segments is slightly shorter than the other (2 mm shorter). Two screws with variable position have been included. One screw in the short-circuit section is used to improve the matching of the antenna, while with the aim of tuning the antenna and compensating the manufacturing tolerances the second screw is inserted through the common part of the ribbon in the dielectric layer 2. The ribbon has a thickness of 300 μm which has to be considered, while the ground plane conductor has a thickness of only 34 μm. Three rectangular and one cross-shaped cavities have been included to serve as reference when positioning the antenna. The cross center coincides with the ear point of head phantoms. Those cavities cut across the four FR4 layers. Their dimensions are shown in Figure F.4(c), with l_i = 12 mm and w_i = 3 mm. The cross is formed by two rectangular cavities. In the same drawing the slot made in the Layer 4 to allow inserting the semi-rigid coaxial is shown. Layer 1 and Layer 4 are identical, except that Layer 4 has the slot for the coaxial and the hole for the tuning screw. Layer 2 has the hole for the tuning screw.

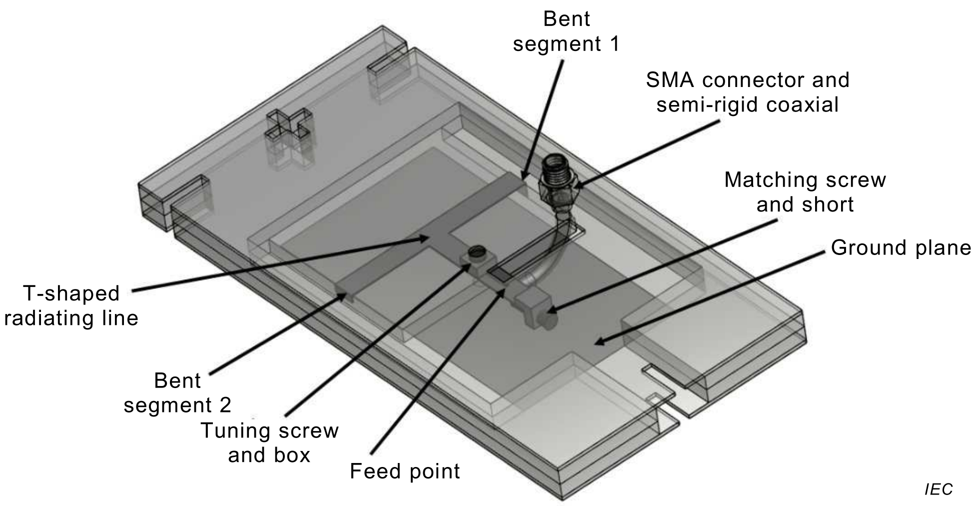

(a)

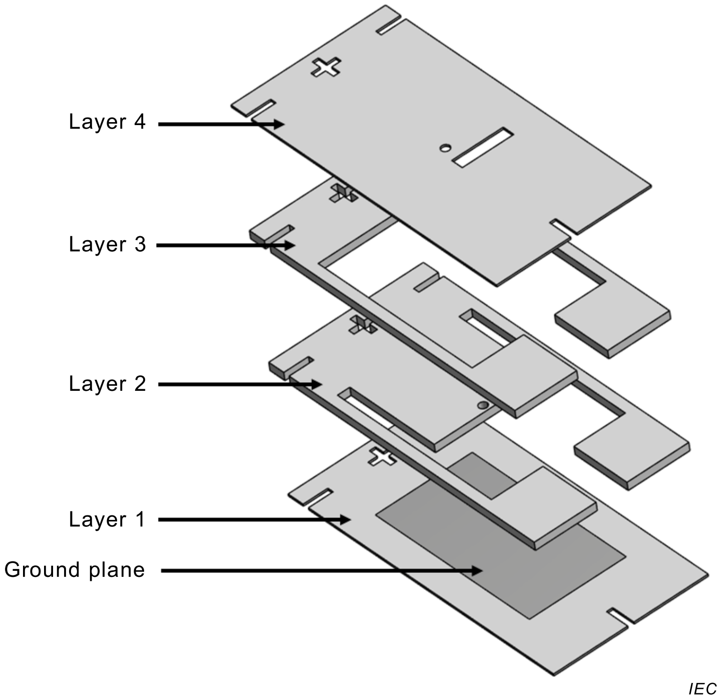
Layer 4
Layer 3
Layer 2
Layer 1
Ground plane
IEC

(b)

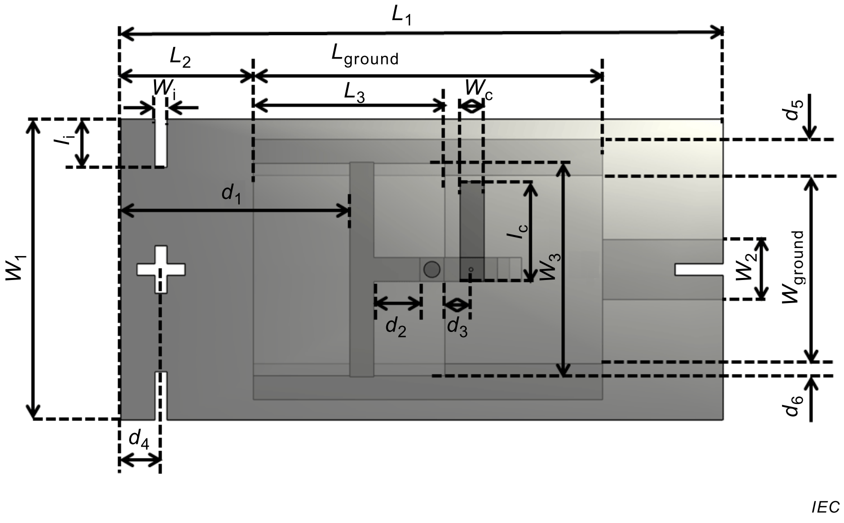
L1
L2
Lground
Wi
L3
Wc
d5
li
d1
lc
W1
W3
W2
Wground
d2
d3
d6
d4
IEC

(c)

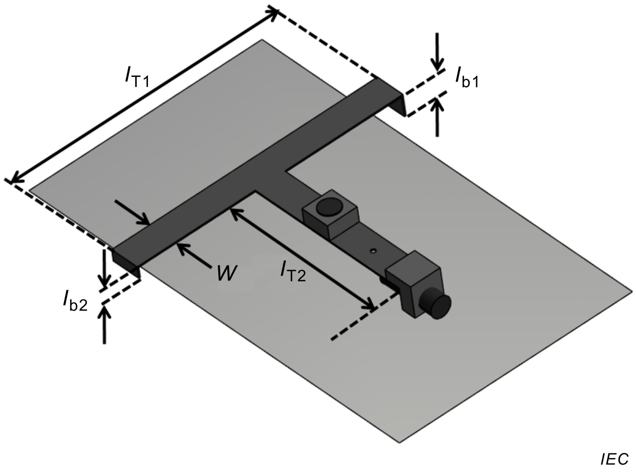

(d)

Key

(a) full model with connecting elements
(b) expanded view of the substrates
(c) upper view
(d) radiating

Figure F.4 – Peak CPIFA at 2450 MHz

The details of the different components are shown in Figure F.4(c), including relative position of each component. The T-shaped split ribbon made of copper is shown in Figure F.4(d). Figure F.5(a) shows in detail the brass structure for inserting the matching screw, in the short. Its lower side is soldered to the ground plane. The ribbon must be inserted just in the upper part of the screw and soldered to the structure in the upper side. As a reference, the figure of the matching structure shows a point named A_R to which the ribbon must be attached. Figure F.5(b) shows in detail the structure for introducing the tuning screw, that is also made of brass. This must be soldered to the ribbon in the upper side. In both cases, the diameter of the screw is 4 mm, with maximum length of 12 mm for the matching screw and 5 mm for the tuning screw.

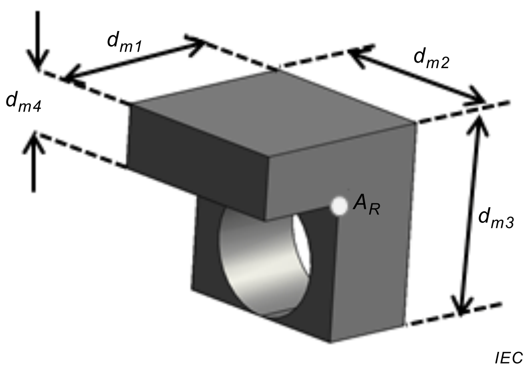

(a) Detail of the matching structure

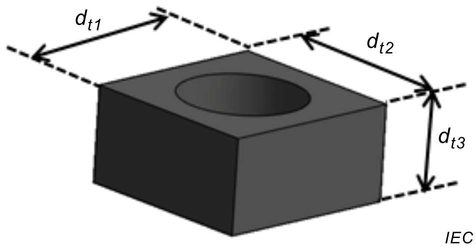

(b) Detail of the tuning structure

Figure F.5 – Tuning structure and matching structure

Table F.4 – Thickness of substrates and planar metallization

Dielectrics	**Thickness** (mm)	**PEC**	**Thickness** (mm)
Layer 1 = Layer 4 (FR4)	1,00 ± 0,10	Ground plane	0,035 ± 0,003 (negligible in simulation)
Layer 2 = Layer 3 (FR4)	4,00 ± 0,10	T-shaped radiating line	0,30 ± 0,05

Table F.5 – Dielectric properties for FR4

	2 450 MHz	
	ε_r	σ [S/m]
FR4	4,36	0,0105

Table F.6 – Lengths for the different components

Item	**length** (mm)	**Item**	**length** (mm)
L_1	150,00 ± 0,10	l_{T1}	53,60 ± 0,05
W_1	75,00 ± 0,10	l_{T2}	33,80 ± 0,05
L_{ground}	87,00 ± 0,05	w	6,00 ± 0,05
w_{ground}	47,00 ± 0,05	l_{b1}	4,30 ± 0,05
L_2	33,00 ± 0,10	l_{b2}	2,30 ± 0,05
W_2	15,00 ± 0,10	d_{m1}	6,00 ± 0,10
d_1	57,00 ± 0,10	d_{m2}	6,00 ± 0,10
d_2	11,50 ± 0,10	d_{m3}	6,30 ± 0,10
d_3	6,74 ± 0,50	d_{m4}	2,00 ± 0,10
d_4	10,00 ± 0,10	d_{t1}	6,00 ± 0,10
d_5	9,00 ± 0,10	d_{t2}	6,00 ± 0,10
d_6	3,00 ± 0,10	d_{t3}	3,00 ± 0,10
l_i	12,00 ± 0,10	Foam spacer	5,00 ± 0,25
w_i	3,00 ± 0,10	matching screw diameter	4,00 ± 0,05
L_3	47,90 ± 0,10	matching screw length	12,00 ± 0,10
W_3	53,00 ± 0,10	tuning screw diameter	4,00 ± 0,05
l_c	25,00 ± 0,10	tuning screw length	5,00 ± 0,10
w_c	6,00 ± 0,10		

F.5 Additional antennas

The antennas defined in the previous clauses of this Annex shall be used for the system validation. They define a minimum set of antennas to test the accuracy of the vector measurement-based system to evaluate if the system is acceptable for measurement of DUTs according to this PAS. Antennas cannot be removed from the system validation, as this would compromise the ability of the system validation to evaluate the accuracy and uncertainty of the system. However, other antennas can be added to the list.

The following are minimum requirements for any antenna added to the validation protocol.

- Justification shall be provided for the inclusion of an antenna and how its use strengthens the validation section;

- The test configurations (e.g., frequencies, locations on the phantom, distance, rotation angle) shall be provided;
- Detailed drawings, including all dimensions and tolerances, shall be provided. CAD files of the antennas shall be made available with sufficient detail of the construction and parameters so that the numerical targets can be independently verified;
- Target SAR values shall be provided from high-resolution numerical simulations of the CAD file of the antenna. These shall be available for all defined test configurations on the phantoms;
- Physical antennas shall be measured using a SAR measurement system that has an ISO/IEC 17025 accredited calibration to validate the numeric target values and generate a certificate of traceability;
- Annex G shows an example of a procedure to calibrate those additional antenna.

Annex G
(normative)

Calibration of Reference Antennas

G.1 Introduction

The purpose of this Annex for the calibrator of reference antennas is to define the calibration procedure and calibration uncertainty of reference antennas that are used to validate the SAR measurement system. Since this PAS includes several different measurement principles, validation of the measurement system is important for checking the measurement reliability of these systems. The use of well-characterized reference antenna which are described in Annex F is important, since the users of these systems are not able to examine the system-embedded parameters by themselves, e.g. evaluate the effect of sensor displacement within the array.

The target SAR values of the reference antennas shall be determined, and the uncertainty of the target values should be low (typically below 0,3 dB for k = 1) to ensure reliability of the validation tests. A typical means of reducing the uncertainty is to use the same equipment (tissue-equivalent liquid, dielectric spacer, power sensors and couplers) as used for waveguide probe calibration. For example, it results in low uncertainty for determining the input power to the reference antenna. In case the same equipment is not used for the calibration of the reference antenna, related uncertainty should be considered. The average of two measurements with a 90-degree probe rotation between the two measurements would significantly reduce the uncertainty due to the axial isotropy of the probe. These tests should be performed for phantom shell material that is well characterized by measurements and for which sensitivity on SAR is determined by simulations or mathematical analysis. In all cases, the forward power and reflected power during the tests and the tuned frequency should be recorded.

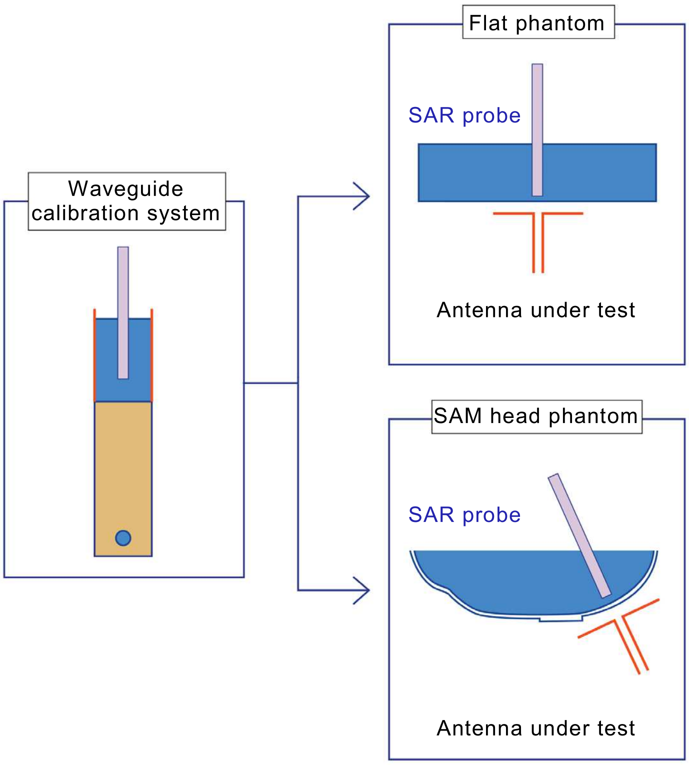

Figure G.1 – Measurement setup for waveguide calibration of dosimetric probe, and similar setup (same tissue-equivalent liquid, dielectric spacer, power sensors and coupler) for antenna calibration

G.2 Parameters or quantities and ranges to be determined by calibration method

The reference antenna is placed in the defined position below the flat or SAM-head phantom. Parameters to be determined include peak 1 g and 10 g averaged SAR values measured inside the medium when exposed with the reference antenna. This is performed at the central operating frequency of the reference antenna. These values can be considered as the "calibrated" or "target" quantities. Additionally, they should comply with the theoretical results, within a given uncertainty (typically within 0,3 dB). This agreement demonstrates the correct performance of the reference antenna.

Furthermore, transmission, electrical delay of the reference antenna, reference antenna impedance and return loss when positioned at the standardised calibration distances from the lossy medium shall be assessed.

G.3 Reference Antenna Calibration Setup

The uncertainty of the power to the reference antenna shall be as low as possible. This requires the use of a test set-up with bi-directional coupler, calibrated power meters. The recommended set-up is shown in Figure G.2.

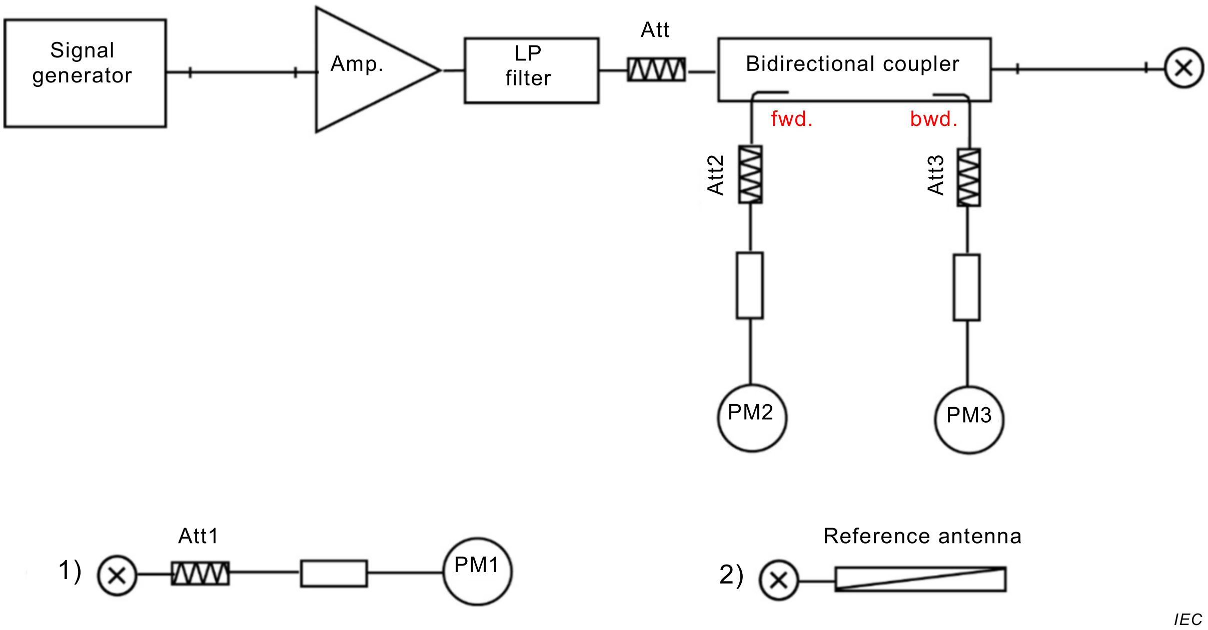

Figure G.2 – Setup for calibration of a reference antenna

The calibrated power meter PM1 (including calibrated attenuator Att1) is connected to the cable to measure the forward power at the location of the connector (X) to the *system check* antenna. Desired input power level to the reference antenna (Pin) is defined as a sum of a reference attenuator Att1 and power meter PM1 reading.

Power meter PM2 is used as a monitor of the input power. Power meter PM3 monitors the reflected power level. After manual check (setup under 1) and verification of values, the cable is disconnected from the power meter PM1 and connected to the reference antenna (setup see Figure G.2).

G.4 Reference Antenna Calibration procedure

G.4.1 Verification of Return Loss

The following electrical circuit parameters of the reference antenna are measured with a VNA (vector network analyser) in order to verify the functionality and the respective requirements: Transmission loss and delay between connector and feed point (e.g., values determined from S_{11} with the feed point shorted or by other techniques) and return loss when positioned under the phantom.

G.4.2 Calibration of Reference Antennas: Step-by-Step Procedure

The reference antenna shall be placed below the flat or SAM head phantom at the defined distance and position. The phantom shall be filled with tissue simulating medium with appropriate parameters (TSL parameters shall be measured within 24 hours of the calibration).

The following requirements of the phantom shall be observed in order to reduce the measurement uncertainty:

a) The thickness shall be 2,00 mm ± 0,05 mm at the location of the antenna. Calibrated instrumentation suitable for measuring directly at the phantom having an accuracy of better than 0,05 mm shall be used to determine the thickness.

b) The dielectric parameters of the shell material shall comply with the nominal targets between 3,0 and 3,5.

c) The dielectric parameters of the liquid shall be measured with an uncertainty of less 2 % and a deviation from the targets within ±3 %.

d) The liquid temperature during SAR measurements shall be within ±1 °C of the liquid temperature during dielectric parameter measurements. Preferably the same liquid as for the probe calibration are used.

The measurement system selected shall be appropriate for the reference antenna under test; including choice of 1) dosimetric probe with valid calibration parameters for the calibration frequency, calibrated electronics, and medium parameters and 2) the power setup including calibrated power meters, couplers and attenuators. Preferably, the same power antenna, coupler and power meter as during the calibration of the probe is used.

The measurement protocol shall include the following procedures as described in IEC 62209-2:

a) Power reference;
b) Area Scan with appropriate grid settings;
c) Zoom Scan with appropriate grid settings;
d) Power drift.

Verify the measurement setup using the measurement software (e.g. verification of phantom location, alignment of the probe).

Connect the cable as in Figure G.2 and turn the RF power on. Verify that the reference antenna is still placed as required in step 1.

When the measurements are completed, prepare and issue the calibration document.

G.4.3 Uncertainty Budget of Reference Antenna Calibration

Each component contributing to uncertainty that is frequency-dependent is evaluated in the frequency band where SAR assessment is performed. Below are listed the main uncertainty contributions and reduced tolerances that would be practically achievable in order to obtain calibrated or target values with minimal uncertainties. The methods described in this Annex enable the determination of the 1 g and 10 g spatial peak SAR target values with an uncertainty of smaller than 10 %.

– The incident power measurement tolerance is derived from the calibration certificate of the power sensor, power meter and reference attenuator (Att1). This item includes: power sensor calibration uncertainty, calibration uncertainty of the reference attenuator (Att1), and mismatch uncertainties on the important junctions.
– The power uncertainty includes: mismatch between a reference attenuator and reference antenna, bi-directional coupler error (directivity error) and error due to the mismatch of the reference antenna in the setup and the uncertainty of net power delivered to the reference antenna, arising from the uncertainty of the reference antenna reflection factor.
– The probe calibration uncertainty can be lowered if the same power measurement setup is used for reference antenna calibration as for probe calibration.
– The dielectric parameters and the temperature shall be measured before the first measurement and last measurements. The deviation shall be as small as achievable; typically < ±0,2 °C in a controlled environment and not more than ±3 % from the target value.
– The axial isotropy tolerance accounts for probe rotation around its axis. For the calibration of reference antennas, axial isotropy error of a dosimetric probe shall not exceed ±0,1 dB.
– The hemispherical isotropy error includes all probe orientations and field polarizations. For the calibration of reference antennas, hemispherical isotropy error of a dosimetric probe shall not exceed ±0,3 dB (preferably much smaller).

- Linearity error of the dosimetric probe is determined as the maximum deviation of the measured and actual field strength. For reference antenna calibration, the input power to the antenna shall be chosen to be well above the noise level of the probe (i.e., S/N: > 20 dB) and for minimal linearity error (typically < 0,05 dB).
- Sufficient power shall be used to feed the reference antennas, typically at 0,5 W to 1 W, such that the detection limit error becomes negligible.
- The probe boundary effect is an enhanced sensitivity in the immediate vicinity of medium boundaries, due to a capacitive coupling effect between the probe and the medium boundary at the medium and phantom shell surfaces. As probe calibration procedure includes also boundary-effect compensation parameters remaining error is reduced to 1 %.
- Readout electronics uncertainty is as stated on the corresponding calibration certificate.
- Response time/Integration time set to 0 (CW signal used).
- Probe positioner error: The absolute accuracy for short distance movements depends on the robot but can be considerably better than ±0,1 mm and can be approximated as normally distributed. A typical number of points in a Zoom Scan is 343 for frequencies below 3 GHz and 448 points for frequencies above 3 GHz. Therefore, the randomness of the position error can be used to calculate the uncertainty.
- Probe positioning error: The surface detection shall have a precision of better than 0,2 mm. As the surface is detected for each z-grid-line of the cube (typical number of grid lines is 47 for frequencies below 3 GHz and 64 for frequencies above 3 GHz), the uncertainty can be reduced as the distance is measured multiple times.
- Extrapolation/interpolation: the maximum evaluated tolerance for the variety of zoom scan shifts and probe types shall be determined for the specific antenna.
- The antenna to medium distance tolerance can be kept below 1 % as reference antennas have well defined (low loss) spacers to establish correct distance between the top surface of the antenna and the bottom surface of the phantom.
- RF ambient can be nullified as calibration is done in well-controlled environment with no external disturbance.
- Phantom uncertainty should be kept as small as possible.
- Medium conductivity/permittivity errors are evaluated as per IEC 62209-1 and IEC 62209-2.

Table G.1 – Example uncertainty budget for reference antenna (DIPOLE) calibration for 1g and 10g averaged SAR (750 MHz – 3 GHz)

Uncertainty Description	Uncert. value ±%	Probab. distr.	div	c_i [1] (1g)	Std. unc. (1g)	Std. unc. (1g)	c_i [1] (10g)	Std. unc. (10g)	v_i [2] or v_{eff}
Incident power:						1,4		1,4	
Power reference of 50 MHz antenna	0,5	N	2	1	0,3				
Sensor calibration factor at 1mW	0,7	N	2	1	0,4				
Sensor linearity at 50 MHz	0,4	R	1,73	1	0,2				
Mismatch sensor & reference attn.	0,3	U	1,41	1	0,2				
Mismatch reference attn. & coupler	0,3	U	1,41	1	0,2				
S_{21} of reference attn.	2,3	N	2	1	1,2				
Antenna power:						1,8		1,8	
Mismatch antenna & coupler	2,0	U	1,41	1	1,4				
Cable attenuation variation	1,2	R	1,73	1	0,7				
Coupler uncertainty (S_{11})	1,1	U	1,41	1	0,8				
Net power uncertainty	0,2	N	2	1	0,1				
Measurement System Related:									
Probe calibration	3,4	N	1	1		3,4	1	3,4	
Axial isotropy	1,6	R	1,73	1		0,9	1	0,9	
Hemispherical isotropy	7,3	R	1,73	0		0,0	0	0,0	
Linearity	1,2	R	1,73	1		0,7	1	0,7	
Detection limit	0,0	R	1,73	1		0,0	1	0,0	
Boundary effect	1,0	R	1,73	1		0,6	1	0,6	
Readout electronics	0,3	N	1	1		0,3	1	0,3	
Response time (CW)	0,0	R	1,73	1		0,0	1	0,0	
Integration time (CW)	0,0	R	1,73	1		0,0	1	0,0	
Probe positioner	0,02	R	1,73	1		0,01	1	0,01	
Probe positioning	0,4	R	1,73	1		0,2	1	0,2	
Extrapolation/Interpolation	1,0	R	1,73	1		0,6	1	0,6	
Antenna and phantom related:									
Distance antenna-medium	1,0	R	1,73	1		0,6	1	0,6	
RF ambient condition	3,0	R	1,73	1		0,0	1	0,0	
Phantom uncertainty	2,0	R	1,73	1		1,2	1	1,2	
Temp, unc – Conductivity	1,7	R	1,73	0,78		0,8	0,71	0,7	
Medium conductivity (mea.)	2,0	N	1,73	0,78		1,6	0,71	1,4	
Temp. unc – Permittivity	0,2	R	1,73	0,23		0,0	0,26	0,0	
Medium permittivity (mea.)	2,0	N	1,73	0,23		0,5	0,26	0,5	
Combined Standard Uncertainty						± 4,9		± 4,8	
Expanded Standard Uncertainty (k=2)						± 9,7		± 9,6	

[1] c_i is the sensitivity coefficient

[2] v_i or v_{eff} are the degrees of freedom in the standard uncertainty $u(x_i)$ for the input estimate (x_i); and the degree of effective freedom in combined uncertainty $u_c(x_i)$, used to obtain $t_{tp}(v_{eff})$, respectively.

Table G.2 – Example uncertainty budget for reference antenna calibration (PIFA) for 1 g and 10 g averaged SAR (750 MHz – 3 GHz)

Uncertainty Description	Uncert. value ±%	Probab. distr.	div	c_i [1] (1g)	Std. unc. (1g)	Std. unc. (1g)	c_i [1] (10g)	Std. unc. (10g)	v_i [2] or v_{eff}
Incident power:						1,4		1,4	
Power reference of 50 MHz antenna	0,5	N	2	1	0,3				
Sensor calibration factor at 1 mW	0,7	N	2	1	0,4				
Sensor linearity at 50 MHz	0,4	R	1,73	1	0,2				
Mismatch sensor & reference attn.	0,3	U	1,41	1	0,2				
Mismatch reference attn. & coupler	0,3	U	1,41	1	0,2				
S_{21} of reference attn.	2,3	N	2	1	1,2				
Antenna power:						1,8		1,8	
Mismatch antenna & coupler	2,0	U	1,41	1	1,4				
Cable attenuation variation	1,2	R	1,73	1	0,7				
Coupler uncertainty (S_{11})	1,1	U	1,41	1	0,8				
Net power uncertainty	0,2	N	2	1	0,1				
Measurement System Related:									
Probe calibration	3,4	N	1	1		3,4	1	3,4	
Axial isotropy	1,6	R	1,73	0,7		0,6	0,7	0,6	
Hemispherical isotropy	7,3	R	1,73	0,7		2,9	0,7	2,9	
Linearity	1,2	R	1,73	1		0,7	1	0,7	
Detection limit	0,0	R	1,73	1		0,0	1	0,0	
Boundary effect	1,0	R	1,73	1		0,6	1	0,6	
Readout electronics	0,3	N	1	1		0,3	1	0,3	
Response time (CW)	0,0	R	1,73	1		0,0	1	0,0	
Integration time (CW)	0,0	R	1,73	1		0,0	1	0,0	
Probe positioner	0,02	R	1,73	1		0,01	1	0,01	
Probe positioning	0,4	R	1,73	1		0,2	1	0,2	
Extrapolation/Interpolation	5,0	R	1,73	1		2,9	1	2,9	
Antenna and phantom related:									
Distance antenna-medium	1,0	R	1,73	1		0,6	1	0,6	
RF ambient condition	3,0	R	1,73	1		0,0	1	0,0	
Phantom uncertainty	2,0	R	1,73	1		1,2	1	1,2	
Temp. unc – Conductivity	1,7	R	1,73	0,78		0,8	0,71	0,7	
Medium conductivity (mea.)	2,0	N	1,73	0,78		1,6	0,71	1,4	
Temp. unc – Permittivity	0,2	R	1,73	0,23		0,0	0,26	0,0	
Medium permittivity (mea.)	2,0	N	1,73	0,23		0.5	0.26	0.5	
Combined Standard Uncertainty						± 6,3		± 6,3	
Expanded Standard Uncertainty (k=2)						± 12,7		± 12,6	

[1] c_i is the sensitivity coefficient.

[2] v_i or v_{eff} are the degrees of freedom in the standard uncertainty $u(x_i)$ for the input estimate (x_i); and the degree of effective freedom in combined uncertainty $u_c(x_i)$, used to obtain $t_{tp}(v_{eff})$, respectively.

Table G.3 – Example uncertainty budget for reference antenna (DIPOLE) calibration for 1g and 10g averaged SAR (3 – 6 GHz)

Uncertainty Description	Uncert. value ±%	Probab. distr.	div	c_i [1] (1g)	Std. unc. (1g)	Std. unc. (1g)	c_i [1] (10g)	Std. unc. (10g)	v_i [2] or v_{eff}
Incident power:						1,5		1,5	
Power reference of 50 MHz antenna	0,5	N	2	1	0,3				
Sensor calibration factor at 1mW	0,8	N	2	1	0,4				
Sensor linearity at 50 MHz	1,1	R	1,73	1	0,6				
Mismatch sensor & reference attn.	0,6	U	1,41	1	0,4				
Mismatch reference attn. & coupler	0,6	U	1,41	1	0,4				
S_{21} of reference attn.	2,3	N	2	1	1,2				
Antenna power:						2,0		2,0	
Mismatch antenna & coupler	2,0	U	1,41	1	1,4				
Cable attenuation variation	2,0	R	1,73	1	1,2				
Coupler uncertainty (S_{11})	1,0	U	1,41	1	0,8				
Net power uncertainty	0,2	N	2	1	0,1				
Measurement System Related:									
Probe calibration	4,6	N	1	1		4,6	1	4,6	
Axial isotropy	1,6	R	1,73	1		0,9	1	0,9	
Hemispherical isotropy	7,3	R	1,73	0		0,0	0	0,0	
Linearity	1,2	R	1,73	1		0,7	1	0,7	
Detection limit	0,0	R	1,73	1		0,0	1	0,0	
Boundary effect	1,0	R	1,73	1		0,6	1	0,6	
Readout electronics	0,3	N	1	1		0,3	1	0,3	
Response time (CW)	0,0	R	1,73	1		0,0	1	0,0	
Integration time (CW)	0,0	R	1,73	1		0,0	1	0,0	
Probe positioner	0,04	R	1,73	1		0,02	1	0,02	
Probe positioning	0,8	R	1,73	1		0,5	1	0,5	
Extrapolation/Interpolation	2,0	R	1,73	1		1,2	1	1,2	
Antenna and phantom related:									
Distance antenna-medium	2,0	R	1,73	1		1,2	1	1,2	
RF ambient condition	3,0	R	1,73	1		0,0	1	0,0	
Phantom uncertainty	2,0	R	1,73	1		1,2	1	1,2	
Temp. unc – Conductivity	1,7	R	1,73	0,78		0,8	0,71	0,7	
Medium conductivity (mea.)	2,0	N	1,73	0,78		1,6	0,71	1,4	
Temp. unc – Permittivity	0,2	R	1,73	0,23		0,0	0,26	0,0	
Medium permittivity (mea.)	2,0	N	1,73	0,23		0,5	0,26	0,5	
Combined Standard Uncertainty						± 6,1		± 6,0	
Expanded Standard Uncertainty (k=2)						± 12,2		± 12,1	

[1] c_i is the sensitivity coefficient

[2] v_i or v_{eff} are the degrees of freedom in the standard uncertainty $u(x_i)$ for the input estimate (x_i); and the degree of effective freedom in combined uncertainty $u_c(x_i)$, used to obtain $t_{tp}(v_{eff})$, respectively

Annex H
(normative)

General considerations on uncertainty estimation

H.1 Concept of uncertainty estimation

The concepts of uncertainty estimation in the measurement of the SAR from wireless devices are based on the general rules provided by the ISO/IEC Guide 98-3. Nevertheless, uncertainty estimation for complex measurements remains as a difficult task and requires high-level and specialized engineering knowledge. In order to facilitate this task, guidelines and approximation formulas are provided in this Clause, enabling the estimation of each individual uncertainty component. The concept is designed to provide the system uncertainty for the entire frequency range of 30 MHz to 6 GHz and for any device under test within the scope of the document. Different uncertainty budgets for different frequency bands or other conditions may be assessed as long as the user can easily comply with these conditions. As an example, if a system is made of several independent sections, e.g. sealed hermetic phantoms with embedded probe-arrays, an uncertainty budget may be defined for each individual phantom.

The uncertainty evaluation described in this Clause is designed to be broadly applicable to SAR measurement systems that comply with the normative clauses of this PAS. However, some measurement systems may require additional uncertainty analysis.

It is not sufficient to provide only Table 2 and Table 3. Detailed documentation shall be provided of the estimation of each influence quantity including methodology, assessment of data for each component, as well as how the uncertainty was derived from the data set.

Dosimetric assessment systems utilizing vector probe or vector probe-array technologies falling in the scope of this PAS require additional considerations as compared to techniques covered by IEC 62209−1 and IEC 62209-2. To properly evaluate the uncertainty budget for such approaches, two main aspects have to be taken into account:

1) The tolerance on some of the components has to be assessed in amplitude and in phase, before being transferred into an uncertainty on peak spatial-average SAR.
2) The sensitivity coefficients c_i of the uncertainty components have to be carefully revised by feeding the tolerances into the processing algorithms, so that these coefficients will generally be method-dependent.

Technological implementations of dosimetric assessment systems covered by this PAS as well as their calibration setups and procedures also differ from IEC 62209-1 and IEC 62209-2 ones. As a result, the list of uncertainty components and the uncertainty evaluation methods had to be specifically revised. The list of uncertainty components is provided in Annex G, Annex H and Annex I.

For systems and technologies covered by this PAS, some uncertainty components may be correlated, so that certain combined uncertainties evaluations have to be carried out. As an example, for a single vector probe or probe-array system, the resulting uncertainty from probe positioning tolerance will actually depend on post-processing uncertainties. In addition, for probe-array systems, depending on the system technology and implemented method, the probe-array will be characterized during the calibration by either looking at each single probe transfer function or by taking into account the complete response of the array as a whole. Whether one or the other approach is taken will result in differences in uncertainty evaluation. In the latter case, for instance, it may be more relevant to assess multiple uncertainty components altogether instead of separating them.

The uncertainty assessment shall be consistent with the validation results of Annex D. Otherwise the stated uncertainty is not valid.

To define the procedures and requirements for a Type A and B evaluation that are consistent with ISO/IEC Guide 98-3 is complex. Nevertheless, there is a need for fast array systems, the performance of which must be fully understood when used for demonstrating compliance with safety limits. In order to achieve this goal, this clause provides essential requirements and guidance for ensuring that the uncertainty evaluation is thorough and conservative. In addition, the approach proposed in subclause D.4 defines a series of test to evaluate the relevance and conservativeness of the reported uncertainty budget.

Guidance for assessing the uncertainty budget is provided in Clause 8. The procedure of validation is defined in Annex D using the antennas of Annex F.

The details how the uncertainty is determined is described in 8.3.

H.2 Type A and Type B evaluation

Both Type A and Type B evaluations of the standard uncertainty shall be used. The evaluation of uncertainty by the statistical analysis of a series of observations is termed a Type A evaluation of uncertainty. The evaluation of uncertainty by means other than the statistical analysis of a series of observations is termed a Type B evaluation of uncertainty. Each component of uncertainty, however evaluated, is represented by an estimated standard deviation, termed standard uncertainty, which is determined by the positive square root of the estimated variance.

When a Type A analysis is performed, the standard uncertainty u_i shall be derived using the estimated standard deviation from statistical observations. When a Type B analysis is performed, u_i comes from the upper a_+ and lower a_- limits of the quantity in question, depending on the probability distribution function defining $a = (a_+ - a_-)/2$, then:

- rectangular distribution: $u_i = a/\sqrt{3}$
- triangular distribution: $u_i = a/\sqrt{6}$
- normal distribution: $u_i = a/k$
- U-shaped (asymmetric) distribution: $u_i = a/\sqrt{2}$

  where;

  a is the half-length of the interval set by limits of the influence quantity

  k is the coverage factor

  u_i is the standard uncertainty

Predetermined standard deviations based on a larger number of repeat tests can be used to estimate uncertainty components in cases where the system, method, configuration and conditions, etc., are representative of the specific DUT.

H.3 Degrees of freedom and coverage factor

When the degrees of freedom are less than 30, a coverage factor of two is not the appropriate multiplier to achieve a 95 % confidence level. A simple but only approximately correct method is to use t in place of the coverage factor k, where t is the Student's-t factor. Standard deviations of t-distributions are narrower than normal (Gaussian) distributions, but the curves approach the Gaussian shape for large numbers of degrees of freedom. The degrees of freedom for most standard uncertainties based on Type B evaluations can be assumed to be infinite. Then the effective degrees of freedom of the combined standard uncertainty, u_C, will most strongly depend on the degrees of freedom of the Type A contributions and their magnitude relative to the Type B contributions. The coverage factor (k_p) for small sample populations shall be determined by equation (H.1):

$$k_p = t_p(\nu_{eff}) \quad \text{(H.1)}$$

where;

k_p is the coverage factor for a given probability p

$t_p(\nu_{eff})$ is the t-distribution

ν_{eff} is the effective degrees of freedom estimated using the Welch-Satterthwaite formula:

$$\nu_{eff} = \frac{u_c^4}{\sum_{i=1}^{m} \frac{c_i^4 u_i^4}{\nu_i}} \quad \text{(H.2)}$$

c_i is the sensitivity coefficient of each uncertainty component u_i

ν_i is the number of degrees of freedom for each uncertainty component u_i

The subscript p refers to the approximate confidence level, e.g., 95 %. Tabulated values of $t_p(\nu_{eff})$ are available, for example in [116].

NOTE As an example, assume that the combined standard uncertainty calculated from all the quantities for the 1g SAR in Table H.1 with an assumed positioning uncertainty of 7 % is u_c = 14,2 %. Assume also that the number of samples or tests is equal to 5, so ν_i = 4 and the degrees of freedom for all of the other components are $\nu_i = \infty$. From the equation $\nu_{eff} = u_c^4 \Big/ \sum_{i=1}^{m} \frac{c_i^4 u_i^4}{\nu_i}$, the effective degrees of freedom for the combined standard uncertainty is ν_{eff} = 68, so k = 2 does apply in this case, and the expanded uncertainty is U = 29 %. If the standard uncertainty for positioning variations goes to 9 % and the number of tests is reduced to 4 (ν_i = 3), then ν_c = 15,3 %, ν_{eff} = 25, $k = k_p = k_{95} = t = t_{95}$ = 2,06, and the expanded uncertainty becomes U = 2,06 × 15,6 % = 31,4 %.

H.4 Combined and expanded uncertainties

The contributions of each component of uncertainty shall be recorded with description, probability distribution, sensitivity coefficient, c_i, and uncertainty value, $u(x_i)$ of the uncertainty component, x_i. A recommended tabular form is shown in Table H.1.

If all uncertainty components, x_i, are statistically independent, the combined standard uncertainty $u_c(y)$ for SAR measurement (y) shall be estimated according to the following formula (H.3):

$$u_c(y) = \sqrt{\sum_{i=1}^{m} c_i^2 \cdot u^2(x_i)} \quad \text{(H.3)}$$

The variable y is either the 1-gram or 10-gram peak-spatial average SAR. Therefore, the above equation can be written specifically for the estimation of the combined standard uncertainty for the 1-gram and 10-gram peak spatial-average SAR, $u_{c,1g}$ and $u_{c,10g}$, respectively:

$$u_{c,1g} = \sqrt{\sum_{i=1}^{m} c_{i,1g}^2 \cdot u^2(x_i)} \quad \text{(H.4)}$$

$$u_{c,10g} = \sqrt{\sum_{i=1}^{m} c_{i,10g}^{2} \cdot u^{2}(x_i)} \tag{H.5}$$

If there is some significant non-linearity then higher-order terms, C_{ij}, in the Taylor series expansion used to derived the equation shall be used to calculate the combined standard uncertainty. Further description is provided in ISO/IEC Guide 98-3. The sensitivity coefficients $c_{i,1g}$ and $c_{i,10g}$ describe how the combined uncertainty for the 1-gram and 10-gram peak spatial-average SAR vary with changes in the values of the uncertainty component x_i.

If some uncertainty components are statistically dependent on others, the following general formula shall be applied to calculate the combined standard uncertainty:

$$u_c(y) = \sqrt{\sum_{i=1}^{m} c_i^2 \cdot u^2(x_i) + 2\sum_{i=1}^{m-1}\sum_{j=i+1}^{m} c_i c_j u(x_i) u(x_j) r(x_i, x_j)} \tag{H.6}$$

In the above equation, $r(x_i, x_j)$ is the correlation coefficient which is calculated from the estimated covariance $u(x_i,x_j)$ associated with the two components x_i and x_j.

$$r(x_i, x_j) = \frac{u(x_i, x_j)}{u(x_i)u(x_j)} \tag{H.7}$$

In the special case where all uncertainty terms are completely correlated (i.e., $r(x_i, x_j) = 1$), the uncertainty is a linear sum of the individual components:

$$u_c(y) = \sum_{i=1}^{m} c_i \cdot u(x_i) \tag{H.8}$$

Further description and examples of evaluating uncertainty is provided in ISO/IEC Guide 98-1 and ISO/IEC Guide 98-3.

The expanded uncertainty U shall be estimated by multiplying the standard uncertainty by a coverage factor of $k = 2$ representing a confidence interval of 95 %.

The evaluation of several uncertainty components can be combined and assessed by Monte-Carlo-method or more advanced methods. In such a case, the calculation of the correlation coefficient may not be needed.

H.5 Analytical reference functions

IEC 62209-1 and IEC 62209-2 standards describe three reference evaluation functions used to create artificial SAR data for testing the accuracy of post-processing algorithms. These functions are defined analytically and allow an accurate peak spatial-average SAR calculation. These mathematical objects are however made of real values taken by the function at the different locations in space. This is hence not enough to support the evaluation of uncertainty contributions involving near-field reconstruction techniques. Indeed, such approaches require field distribution inputs which satisfy Maxwell equations and verify laws of electromagnetic field propagation within the tissue-simulating material contained in the phantom.

In this PAS, a new form of analytical reference functions is introduced which have the required properties. The general analytical formula for the reference complex vector electric field distributions is defined as follows as a sum of electric dipole moments:

$$E(\boldsymbol{x}) = \mathbb{G}(\boldsymbol{p})(\boldsymbol{x}) := \sum_{i=1}^{80}\sum_{j=1}^{80}\left(\nabla^2 G_k(\boldsymbol{x}-\boldsymbol{y}_{ij})\boldsymbol{p} + k^2 G_k(\boldsymbol{x}-\boldsymbol{y}_{ij})\boldsymbol{p}_{ij}\right) \tag{H.9}$$

where

x is a $\mathbb{R}^3$ vector made of spatial coordinates at which the field is observed.

$$G_k(x) = e^{ik|x|}/4\pi|x|,$$

k is the unique solution of $k = \omega\mu_0(\omega\varepsilon_0\varepsilon' - i\sigma)$

$Im(k) > 0$ and $\nabla^2 G_k(x) = \partial G_k(x)/\partial x_i \partial x_j$ is the Hessian matrix of $G_k(x)$.

y_{ij} is a $\mathbb{R}^3$ vector containing x, y and z spatial coordinates indicating the location of the dipole.

p_{ij} is the dipole moment belonging to $\mathbb{C}^3$ space with coordinates, p_x, p_y and p_z.

Files containing tables of y_{ij} and p_{ij} are provided with this PAS. Each provided set defines a particular solution. The provided reference functions have been determined so that the analytical complex electric field distribution is at a minimum distance (in the sense of the L^2 norm) from numerical results obtained in FDTD-computed realistic exposure conditions with flat and head phantoms meeting the requirements of this PAS.

The reference functions are used hereafter to evaluate several uncertainty contributions which involve a propagation of the error through the reconstruction algorithms.

Table H.1 shows the list of available reference functions provided with this PAS. All the functions are normalized so that the reference peak spatial-average 1g SAR equals 1 W/kg.

Table H.1 – Parameters of analytical reference functions and associated reference peak 10g SAR value. Reference peak 1g SAR value is 1 W/kg for every function

Function ID	**Frequency** (MHz)	**Antenna description**	**Phantom and test position**	**Medium relative permittivity**	**Medium conductivity** ($S.m^{-1}$)	**Reference peak 10g SAR** (W/kg)
001	850	Ultra wide-band (UWB) coplanar strip-fed monopole fitting handset-like casing of 11,5cm x 74cm (called UWBA here after) at 0mm from flat phantom	Flat phantom – UWBA casing in contact	42,234	0,892	0,570
002	1 800	Ultra wide-band antenna (UWBA)	Flat phantom – UWBA casing in contact	40,451	1,391	0,472
003	1 900	UWBA	Flat phantom – UWBA casing in contact	40,287	1,458	0,464
004	2 450	UWBA	Flat phantom – UWBA casing in contact	39,376	1,873	0,415
005	5 500	UWBA	Flat phantom – UWBA casing in contact	33,304	5,185	0,269
006	5 800	UWBA	Flat phantom – UWBA casing in contact	32,648	5,555	0,263
007	750	VPIFA-750	Flat phantom – VPIFA-750 flat mask in contact	42,477	0,855	0,262
008	1 950	VPIFA-1950	Flat phantom – VPIFA-1950 flat mask in contact	40,205	1,492	0,392
009	750	Validation dipole	Flat phantom – *system validation* position	42,477	0,855	0,638
010	835	Validation dipole	Flat phantom – *system validation* position	42,269	0,887	0,633
011	1 750	Validation dipole	Flat phantom – *system validation* position	40,534	1,358	0,507

Annex I
(normative)

Evaluation of the measurement system uncertainty

I.1 Measuring system uncertainties to be specified by the manufacturer

I.1.1 Calibration *CF*

The standard uncertainty *CF* for calibration of the vector system is determined by the system calibration laboratory or manufacturer.

Example protocols for calibration of vector measurement-based systems are given in Annex B. The protocols depend on each technological implementation and hardware. Calibration uncertainty shall be assessed and documented by the system manufacturer. The radiating antenna used for calibration of the vector measurement-based system should be traced according to national standards. The system calibration uncertainty should be documented and appropriate to the calibration method applied. The uncertainty includes the antenna uncertainty.

Depending on the system implementation, the probe or probe-array may be directly calibrated together with its readout electronics or the readout electronics may be calibrated separately. In the latter case, additional uncertainties resulting from the connection of the two blocks after calibration shall be taken into account, e.g. mismatch uncertainty for a RF probe and RF readout having different impedances.

The assessed tolerance valid at the sensor location needs to be translated to the uncertainty for the peak spatial SAR and filled into Table 2. The translation is a function of the actual implemented 3D reconstruction and can only be performed by the manufacturer. All steps shall be documented.

I.1.2 Vector probe or vector probe-array isotropy *ISO*

Probe or probe-array isotropy is a measure of the deviation in probe response to arbitrary field polarization and incidence. In general, fields emitted by a handset are of arbitrary polarization and incidence. For single probe systems, this uncertainty component can be evaluated following IEC 62209-1 and IEC 62209-2 appropriate procedures. For systems using vector probe-arrays, technology-specific considerations have to be taken into account. The manufacturer shall evaluate this contribution during the calibration.

If algorithms are applied to compensate for the deviation from isotropic response, then the SAR uncertainty shall be determined with the same evaluation hardware and software as is used for performing the SAR measurements.

To evaluate the isotropy, the SAR measurement system shall be exposed to reference fields containing waves with varying angles of incidences with respect to the line normal to the phantom surface. The SAR gradients in the direction normal to the phantom shell shall be low enough that probe positioning tolerance does not significantly influence the isotropy assessment.

The isotropy shall be characterized for at least one frequency in each frequency band of interest.

The assessed tolerance valid at the sensor location needs to be translated to the uncertainty for the peak spatial SAR and filled into Table 2. The translation is a function of the actual implemented 3D reconstruction and can only be performed by the manufacturer. All steps shall be documented.

I.1.3 Mutual sensor coupling *MSC*

I.1.3.1 General

For systems using probe-arrays, coupling between the probe sensors may exist, due to imperfect isolation of the sensors. This uncertainty term is caused by port-to-port coupling where the readout at a given sensor port is influenced by the voltage and/or current at another sensor port. Mutual sensor coupling may be evaluated and compensated during calibration. However, this coupling is in principle dependent on the polarization, distribution and angle of incidence of the impinging field and is therefore difficult to remove completely during calibration.

The assessed tolerance valid at the sensor location needs to be translated to the uncertainty for the peak spatial SAR and filled into Table 2. The translation is a function of the actual implemented 3D reconstruction and can only be performed by the manufacturer. All steps shall be documented.

Two methods are described below.

In order to isolate this uncertainty contribution from other components:

- The probe or probe-array shall be immersed in tissue-simulating material complying with the requirements of this PAS.
- The reference antennas used shall have a polarization purity of more than 10 dB.
- The reference antennas shall be far enough from the phantom so that the interaction with the probe or probe-array can be neglected.
- The fields shall be sufficiently above the noise floor.

I.1.3.2 Evaluation of mutual sensor coupling for independently-calibrated probes

In the case of probe arrays with probes that are calibrated independently prior to assembly or in the case of probe arrays that are calibrated together in its final operating condition without compensation for mutual coupling, the mutual sensor coupling uncertainty shall be evaluated by computing the difference between the single point SAR measured using one probe in isolation and the SAR measured by the same probe surrounded by the other probes. Several antennas with different polarizations and angles of incidence are required. The antennas are moved to the required positions so that each sensor is actually exposed to a field intensity compatible with the dynamic range of the measurement system. For each test condition, the calibration coefficients and post-processing are applied on the measured data to evaluate the vector field over the measurement surface. It shall be documented how the error propagates and how the uncertainty is coupled to other uncertainty terms.

I.1.3.3 Evaluation of mutual sensor coupling for probe arrays using compensation

For probe-arrays where the probes are calibrated together in its final operating condition and the mutual coupling between the sensors is characterized as a scattering matrix and compensated (e.g., during the probe-array calibration), mutual coupling will be reduced. However, the remaining mutual sensor coupling error shall be assessed. Also, the uncertainty on the compensation is taken into account as an additional contribution to the measurement system calibration uncertainty. It shall be documented how the error propagates and how the uncertainty is coupled to other uncertainty terms.

I.1.4 Scattering within the array *AS*

I.1.4.1 General

Scattering of the electromagnetic fields in the phantom due to the presence of the array cause distortion of the impinging field distribution captured by the sensors. These reflections are strongly dependent on the distribution, polarization and angle of incidence of the incident fields. Therefore, they cannot be fully calibrated out. This uncertainty term is correlated with the uncertainty due to mutual coupling between the sensors.

In order to characterize this uncertainty component and minimize the influence from other components:

- The probe or probe-array shall be immersed in tissue-simulating material complying with the requirements of this PAS.
- The reference antennas used shall have a polarization purity of more than 10 dB.
- The reference antennas shall be far enough from the phantom so that the interaction with the probe or probe-array can be neglected.
- The probe or probe-array shall be far enough from the phantom shell so that the boundary effect can be neglected.
- The fields shall be sufficiently above the noise floor.
- The incident angles of the propagating field with respect to the orientation of the array shall cover 0° to 45°.
- The polarizations of the propagating field shall include parallel and normal polarization with respect to the array.

Reference antennas with different polarizations and angles of incidence are required. The antennas are moved at as many needed positions so that each sensor is exposed to a field intensity compatible with the dynamic range of the measurement system. For each test condition, the calibration coefficients and post-processing are applied on the measured data to evaluate the vector field over the measurement surface. This can also be evaluated by computational analysis that is validated experimentally.

The assessed tolerance valid at the sensor location needs to be translated to the uncertainty for the peak spatial SAR and filled into Table 2. The translation is a function of the actual implemented 3D reconstruction and can only be performed by the manufacturer. All steps shall be documented.

I.1.4.2 Evaluation of array scattering for independently-calibrated probes

In the case of probe-arrays that are calibrated independently prior to assembly or in the case of probe arrays that are calibrated together in its final operating condition without compensation for scattering, the scattering within the array uncertainty shall be evaluated by computing the difference between the single point SAR measured using one probe in isolation and the SAR measured by the same probe surrounded by the other probes but without the sensing element connected. This ensures to minimize the influence of port-to-port mutual coupling.

I.1.4.3 Evaluation of array scattering for systems using compensation

For probe-arrays where the probes are calibrated together in its final operating condition and the mutual coupling between the sensors is characterized as a scattering matrix and compensated (e.g., during the probe-array calibration), the effect of the scattered field on the received signal by each sensor may be evaluated from a time-domain analysis of the probe-array response. The contribution from the scattered field shall be isolated using a time-gating approach. The uncertainty shall then be evaluated as the maximum relative difference between the SAR obtained using the original signals to the one obtained with time-gated signals. If a time-filtering compensation is applied during measurements, this compensation shall be included for the uncertainty evaluation and its uncertainty contribution characterized.

It is also possible to assess altogether the isotropy (I.1.2), sensor mutual coupling (I.1.3) and scattering within the array (I.1.4) uncertainty components. This can be done with a setup respecting the requirements of this sub-clause. In this case, the obtained vector field for each measurement in conditions of the defined set is projected on the reference vector field for the corresponding antenna and test condition. Ideally this projection shall equal the squared norm of the reference vector field at every point. In practice however, this projection deviates from the squared norm by a relative residual error. The maximum relative residual error obtained for all test conditions within a space region compatible with system dynamic range is reported as the uncertainty for this component with a rectangular distribution.

I.1.5 System linearity LIN

The evaluation of system linearity must be performed such that all components of the system introducing potential non-linearities are assessed. For instance, if a vector probe contains no non-linear element but its readout electronic does, then the tests to evaluate this uncertainty contribution shall include the readout electronics. The uncertainty term is evaluated as described in IEC 62209-1.

This evaluation may be done either in free space or in the tissue-equivalent medium. This is performed by a power sweep covering a local SAR in the range of 0,12 W/kg to 100 W/kg (rms for CW signals) in steps of 3 dB or less. The linearity uncertainty is defined as the maximum deviation in the SAR vs. power characteristic from the best-fit straight reference line going through zero ($SAR = a \times P$, where a is the best-fit slope of the line, using the method of least-squares) defined over the interval 0,12 W/kg to 100 W/kg.

The assessed tolerance valid at the sensor location needs to be translated to the uncertainty for the peak spatial SAR and filled into Table 2. The translation is a function of the actual implemented 3D reconstruction and can only be performed by the manufacturer. All steps shall be documented.

I.1.6 Sensitivity limit SL

System sensitivity limit is evaluated according to relevant clauses of IEC 62209-1 in such a way that the signal to noise ratio (determined at the measurement time) is at the lower bound of the system dynamic range as specified by the manufacturer. The sensitivity limit uncertainty is defined as the difference between the measured SAR and the SAR vs. power characteristic from the best-fit straight reference line going through zero ($SAR = a \times P$, as described in I.1.5).

The assessed tolerance valid at the sensor location needs to be translated to the uncertainty for the peak spatial SAR and filled into Table 2. The translation is a function of the actual implemented 3D reconstruction and can only be performed by the manufacturer. All steps shall be documented.

I.1.7 Boundary effect BE

A change in sensitivity of the probe can occur when it is in close proximity to a dielectric interface (i.e. the interface between the phantom and the phantom shell). This is caused by distortion of the scattered field at the probe tip by the proximity of the dielectric interface. For a given phantom and probe, the magnitude of the error will depend on the separation and orientation of the probe with respect to the interface and also the frequency.

This effect is negligible if:

- The closest distance between the probe tip and the boundary is greater than the diameter of the probe tip.
- The sensor or sensor array is calibrated *in-situ* within the phantom and remains at the same separation and orientation with respect to the dielectric interface during subsequent measurements.

If these conditions are not met the boundary effect shall be determined by the manufacturer and an uncertainty term, BE, included to account for the boundary error, or residual error in any compensation applied to correct for it.

The assessed tolerance valid at the sensor location needs to be translated to the uncertainty for the peak spatial SAR and filled into Table 2. The translation is a function of the actual implemented 3D reconstruction and can only be performed by the manufacturer. All steps shall be documented.

I.1.8 Readout electronics *RE*

The readout electronics are used to process the signals read by the sensors. The readout electronics may have non-linear components (e.g., amplifiers) and may load the sensors causing distortion. One method to determine these uncertainty components is by replacing the probe with an equivalent antenna having the same antenna impedance as the probe under consideration according to the manufacturer's specifications for the probe. This is generally performed by the system manufacturer. Each uncertainty shall be converted to a standard uncertainty using normal probability distribution. The RSS value of these uncertainties shall then be used to determine the overall readout electronics uncertainty.

The assessed tolerance valid at the sensor location needs to be translated to the uncertainty for the peak spatial SAR and filled into Table 2. The translation is a function of the actual implemented 3D reconstruction and can only be performed by the manufacturer. All steps shall be documented.

I.1.9 Response time *RT*

The response time uncertainty is the measurement error caused by movement of the probe during measurement. For systems having fixed probes, this uncertainty is zero.

For systems having moveable probes, response time uncertainty is evaluated by exposing the probe to an E-field step response producing at least 100 W/kg near the phantom surface. The signal response time is evaluated as the time required by the probe and its readout electronics to reach 90 % of the expected final value produced by the step response by switching the RF power on and off. During the SAR measurement, the probe shall remain stationary at each measurement location for at least twice the assessed response time so that the probe signal response time uncertainty is negligible. Under these measurement conditions, a tolerance value of zero may be entered in the appropriate uncertainty table. Otherwise, the SAR uncertainty due to signal response-time uncertainty shall be assessed, using the signal characteristics of the test device. In this case, the signal step-response time uncertainty is equal to the percentage difference between the SAR measured at the chosen measurement time and the SAR measured at twice the chosen measurement time. A rectangular probability distribution shall be assumed.

The assessed tolerance valid at the sensor location needs to be translated to the uncertainty for the peak spatial SAR and filled into Table 2. The translation is a function of the actual implemented 3D reconstruction and can only be performed by the manufacturer. All steps shall be documented.

I.1.10 Probe positioning *PP*

The mechanical restrictions of the field probe or probe-array positioner can introduce deviations in the accuracy and repeatability of probe positioning which add to the uncertainty of the measured SAR. The uncertainty is due to mechanical uncertainties in the sensor location during manufacturing. The actual distance of the sensor from the phantom surface is different from the assumed (nominal) distance, and each sensor location varies in a certain tolerance range. The impact of these deviations cannot be assessed in the same way as for systems covered by IEC 62209-1 and IEC 62209-2, because of the existence of multiple probes and the potential use of phase information and field reconstruction algorithms. The uncertainty is evaluated using a set of numerically generated vector field reference distributions covering the performance requirements of Annex D (e.g., generated using the formulation in Annex H.5). The procedure is as follows:

i) For each numerical distribution, the field is sampled at points and in polarizations which correspond to the measurement grid applied by the physical system.

ii) From these original sampled data, the peak spatial-average SAR is computed using the same processing as used for measurements with this particular system. In this process, step (i) gives the reference SAR, $SAR_{ref,i}$, for each field distribution case i (a number of i distributions is supposed per frequency).

iii) The known tolerance on probe or probe-array positioning is used to generate measurement scan grids G_j (j = 1 to J) affected by mechanical errors. The manufacturer shall make a model to represent such mechanical errors. For example, each tolerance may have a rectangular or triangular distribution if the manufacturer defines maximum acceptable deviations from nominal locations. In the case of moving probes, the repeatability uncertainty of the probes positioning must be included in the mechanical error. J sampled distributions of each reference vector field are then created by using the G_j sampling grids.

iv) For each reference field i and each grid j, the reconstruction algorithms of the measurement system are applied to compute the peak spatial-average SAR, $SAR_{i,j}$. The software shall assume ideal positions of the points in the grid. As a consequence, the algorithms are used as if sampled field values were obtained from a probe or probe-array with perfectly known position, whereas the probe or probe-array is actually sampling the field on a grid which deviates from the targeted locations.

v) For each (i, j) couple, the relative difference $\%SAR_{i,j} = (SAR_{i,j} - SAR_{ref,i})/ SAR_{ref,i}$ is computed.

U_i is then calculated for each reference field configuration i as the 95th percentile of the absolute value of $\%SAR_{i,j}$ for all J probe or probe-array grid locations. The uncertainty is then estimated as the RMS value of U_i across the applicable frequency range for all I exposure conditions. This value is calculated on I x J cases with I × J – 1 degrees of freedom. A normal distribution (k = 2) is assumed.

The assessed tolerance valid at the sensor location needs to be translated to the uncertainty for the peak spatial SAR and filled into Table 2. The translation is a function of the actual implemented 3D reconstruction and can only be performed by the manufacturer. All steps shall be documented.

I.1.11 Sampling error *SE*

The measured SAR distribution is estimated from the direct sampling of the field at a set of discrete points. If the sampling resolution is coarse compared to the gradients of the induced SAR distribution, the peak spatial-average may be inaccurate.

The evaluation of this uncertainty may be combined with the evaluation of the uncertainty of reconstruction algorithms.

The uncertainty is evaluated using a set of numerically generated vector field reference distributions covering the performance requirements of Annex D (e.g., generated using the formulation in Annex H.5).

Move each reference function over several points in X and Y directions surrounding the reference location. The points are defined for a 1 mm resolution with respect to the center point (A0 for flat phantoms, E for head phantoms), extending half of the sensor resolution in both directions. The values are evaluated at the sampling resolution of the SAR measurement equipment. The values are input to the SAR system software which computes the peak-spatial average SAR using the reconstruction algorithms as if they were actually measured. The resulting 1 g and 10 g SAR values are compared with reference SAR values. Record the maximum deviation of the SAR value from the target. A rectangular probability distribution is assumed.

The assessed tolerance valid at the sensor location needs to be translated to the uncertainty for the peak spatial SAR and filled into Table 2. The translation is a function of the actual implemented 3D reconstruction and can only be performed by the manufacturer. All steps shall be documented.

I.1.12 Array boundaries *AB*

In addition to SAR errors due to the spatial resolution and the locations of the sensors, there are errors at the boundary of the measurement area due to truncation of the field and extrapolation of the field distribution beyond the measurement area.

The evaluation of this uncertainty can be combined with the evaluation of the uncertainty of reconstruction algorithms.

The uncertainty is evaluated using a set of numerically generated vector field reference distributions covering the performance requirements of Annex D (e.g., generated using the formulation in Annex H.5). The reference distributions are applied close to the boundary of the measurement area. If the measurement system provides warnings or error messages to the user about the measurement error at locations near the boundary, the evaluation shall be performed inside of these locations. Compare the resulting 1-gram and 10-gram average SAR with the target values. The reference distributions shall be applied at the boundaries of the applicable measurement region defined by the manufacturer. The software shall clearly define the measurement region such that measurements outside this region provide warnings to the user. For each edge and each corner of the measurement region, the reference function shall be applied for the given point and other points toward the centre of the measurement region, in steps according to the sensor resolution. The maximum deviation for all cases shall be recorded. A rectangular probability distribution is assumed.

The assessed tolerance valid at the sensor location needs to be translated to the uncertainty for the peak spatial SAR and filled into Table 2. The translation is a function of the actual implemented 3D reconstruction and can only be performed by the manufacturer. All steps shall be documented.

I.1.13 Phantom shell *PS*

The evaluation of this uncertainty contribution shall be made on the flat phantom. This uncertainty contribution can be evaluated with a Type A approach, using numerical reference field distributions, as follows:

i) For each numerical field distribution, the peak spatial-average SAR is computed with the phantom shell having a target thickness as defined by the standard, and a target permittivity and conductivity as evaluated by the system manufacturer, complying with the requirements of this PAS. For each simulation i, the peak spatial-average $SAR_{\text{ref,i}}$ is then obtained.

ii) The known tolerances on thickness, permittivity and conductivity are used to generate J simulation models (j = 1 to J) with modified phantoms.

iii) For each reference exposure condition *i* and modified phantom model *j*, the field distribution is computed using IEC/IEEE 62704-1 compliant software. From the obtained results, the field is sampled at the system probe or probe-array locations and along the appropriate polarizations, prior to applying reconstruction algorithms. SAR averaging is applied on the reconstructed fields to calculate the peak spatial-average SAR, $SAR_{\text{i,j}}$, for each (i ,j) couple.

iv) For each reference exposure condition i, the relative deviation is then calculated as ($SAR_{\text{i,j}}$-$SAR_{\text{ref,i}}$)/ $SAR_{\text{ref,i}}$.

v) The uncertainty is estimated as the RMS value on the I × J cases, with a (I × 3) – 1 degree of freedom. Normal distribution is assumed.

The assessed tolerance valid at the sensor location needs to be translated to the uncertainty for the peak spatial SAR and filled into Table 2. The translation is a function of the actual implemented 3D reconstruction and can only be performed by the manufacturer. All steps shall be documented.

I.1.14 Tissue-equivalent material parameters MAT

I.1.14.1 Introduction

Details of dielectric parameter test methods are given in Annex J of IEC 62209-1:2016, and uncertainty estimation methods are given in ISO/IEC Guide 98-1. In this PAS, the same procedures and concepts as defined by IEC 62209-1 and IEC 62209-2 apply. However, the tissue-simulating material permittivity and conductivity may be parameters of the processing algorithms and therefore influence the calculations in a way which is specific to each processing approach. As a consequence, the system manufacturer shall demonstrate a proper evaluation of sensitivity coefficients relating to tolerances on tissue-equivalent parameters.

I.1.14.2 Material density

IEC 62209-1 and IEC 62209-2 apply.

The assessed tolerance valid at the sensor location needs to be translated to the uncertainty for the peak spatial SAR and filled into Table 2. The translation is a function of the actual implemented 3D reconstruction and can only be performed by the manufacturer. All steps shall be documented.

I.1.14.3 Material conductivity

The uncertainty due to the material conductivity arises from two different sources. The first source of uncertainty is the allowable tolerance from the Table A.3 target value and the second antenna of uncertainty arises from the measurement procedures used to assess conductivity. The uncertainty shall be estimated using a normal probability. Tissue equivalent materials shall yield conductivity values within ± 10 % of the target values at the frequencies at which the SAR is measured. Clause I.4.1 shall be used to correct the measured SAR for the deviations in conductivity.

The assessed tolerance valid at the sensor location needs to be translated to the uncertainty for the peak spatial SAR and filled into Table 2. The translation is a function of the actual implemented 3D reconstruction and can only be performed by the manufacturer. All steps shall be documented.

I.1.14.4 Material permittivity

The uncertainty due to the material relative permittivity arises from two different sources. The first source of uncertainty is the allowable tolerance from the Table A.3 target value and the second antenna of uncertainty arises from the measurement procedures used to assess relative permittivity. The uncertainty shall be estimated using a normal probability (I.4.1). Tissue equivalent materials shall yield relative permittivity values within ± 10 % of the target values at the frequencies at which the SAR is measured. Clause I.4.1 shall be used to correct the measured SAR for the deviations in permittivity.

The assessed tolerance valid at the sensor location needs to be translated to the uncertainty for the peak spatial SAR and filled into Table 2. The translation is a function of the actual implemented 3D reconstruction and can only be performed by the manufacturer. All steps shall be documented.

I.1.14.5 Material temperature

The measurements of both SAR and tissue dielectric parameters shall be carried out at an ambient temperature between 18 °C and 25 °C inclusively. These two measured temperatures must not differ by more than 2 °C. The following evaluation shall be conducted for each recipe to determine the uncertainty caused by the temperature uncertainty. This evaluation is typically done only once per recipe at the frequencies of interest. This evaluation shall be performed for every new or modifications to a recipe.

Measurements of the dielectric parameters at material temperatures T_{low} = 18 °C and T_{high} = 25 °C shall be computed according to the equations (I.1):

$$\varepsilon\_\text{temp\_liquid}_{\text{uncertainty}}[\%] = 100\times\left|\frac{2\times\left[\varepsilon_r(\mathrm{T_{high}})-\varepsilon_r(\mathrm{T_{low}})\right]}{\varepsilon_r(\mathrm{T_{high}})+\varepsilon_r(\mathrm{T_{low}})}\times\frac{2\ ^{\circ}\mathrm{C}}{\mathrm{T_{high}}-\mathrm{T_{low}}}\right|$$
$$\sigma\_\text{temp\_liquid}_{\text{uncertainty}}[\%] = 100\times\left|\frac{2\times\left[\sigma(\mathrm{T_{high}})-\sigma(\mathrm{T_{low}})\right]}{\sigma(\mathrm{T_{high}})+\sigma(\mathrm{T_{low}})}\times\frac{2\ ^{\circ}\mathrm{C}}{\mathrm{T_{high}}-\mathrm{T_{low}}}\right| \quad \text{(I.1)}$$

where;

ε_temp_material$_{uncertainty}$	is the temperature uncertainty for the material permittivity in percent;
σ_temp_material$_{uncertainty}$	is the temperature uncertainty for the material conductivity in percent;
$\varepsilon_r(T_{high})$	is the relative permittivity at temperature T_{high};
$\varepsilon_r(T_{low})$	is the relative permittivity at temperature T_{low};
$\sigma(T_{high})$	is the conductivity at temperature T_{high};
$\sigma(T_{low})$	is the conductivity at temperature T_{low};
T_{high}	is the highest temperature in °C at which the dielectric parameters were measured;
T_{low}	is the lowest temperature in °C at which the dielectric parameters were measured.

These equations can be used to derive the temperature uncertainty for the particular material. The uncertainty of the measurements of T_{low} and T_{high} shall be less than 0,1 °C. Note that ± 1 °C tolerance is applicable only for this uncertainty evaluation. They do not affect the temperature requirements during testing.

The values of ε_temp_material$_{uncertainty}$ and σ_temp_material$_{uncertainty}$ are entered into column c of the appropriate rows in Table 2. A rectangular probability distribution has been assumed for the material temperature uncertainty in Table 2. The sensitivity coefficients for the material temperature uncertainty are c_σ for conductivity and c_ε for permittivity. They are calculated using the procedure described in I.2.6.1.

The assessed tolerance valid at the sensor location needs to be translated to the uncertainty for the peak spatial SAR and filled into Table 2. The translation is a function of the actual implemented 3D reconstruction and can only be performed by the manufacturer. All steps shall be documented.

I.1.14.6 Spatial variation in tissue equivalent material parameters

The dielectric parameters of the tissue-simulating material can vary spatially. The spatial variation in the dielectric parameters can be assessed on a production sample of the material by making dielectric parameter measurements at multiple regions (at least 10) in a dielectric sample across the frequency range of interest. This evaluation shall be performed after a period corresponding to the minimum maintenance period recommended by the manufacturer. The methods of Annex J in IEC 62209-1:2016 can be used to measure the dielectric parameters, if appropriate. The dielectric measurement methods shall be appropriate to the material being tested. The uncertainty term is calculated from the highest percent difference in each of the permittivity and conductivity from the average value, and a rectangular distribution is assumed. This uncertainty term is only taken into account in the uncertainty budget if larger than the respective permittivity and conductivity measurement uncertainties.

The assessed tolerance valid at the sensor location needs to be translated to the uncertainty for the peak spatial SAR and filled into Table 2. The translation is a function of the actual implemented 3D reconstruction and can only be performed by the manufacturer. All steps shall be documented.

I.1.15 Phantom Homogeneity *HOM*

A conservative exposure assessment had been determined and validated for the defined phantom shell homogeneously filled with the specified tissue simulating material to a depth of 150 mm. In case of array systems, a significant proportion of the head is filled with low loss dielectric and/or conductive materials. The medium depth may also deviate from 150 mm. The uncertainty with respect to the specified homogeneous phantoms as defined in Annex A shall be determined by numerical simulations comparing the homogeneous phantom with the physical head including the array. The worst-case effect on the peak spatial SAR shall be determined by plane wave antennas or dipoles at distances to the phantom shell larger than 50 mm and different incident angles and polarizations and considered as rectangular distribution.

This uncertainty contribution is correlated with *MSC*, *AS* and *ISO* components and may be evaluated in conjunction with these three contributions by using the approach used in I.1.6.

The assessed tolerance valid at the sensor location needs to be translated to the uncertainty for the peak spatial SAR and filled into Table 2. The translation is a function of the actual implemented 3D reconstruction and can only be performed by the manufacturer. All steps shall be documented.

I.2 Uncertainty of post-processing algorithms

I.2.1 Introduction

This subclause describes the estimation of the uncertainty resulting from the post-processing of the discrete measured data to determine the 1 g and 10 g peak spatial-average SAR, i.e., the combined uncertainty of interpolation, extrapolation, averaging and maximum finding algorithms. The developed uncertainty concept assumes that there are no errors in location of the grid points: probe and probe-array positioning and measurement uncertainties are not included.

This uncertainty is evaluated by applying the post-processing algorithms, including reconstruction and averaging, to the analytical reference electromagnetic field distributions as introduced in Annex H. This uncertainty is then obtained from evaluating the relative difference from the obtained peak spatial-average SAR to defined targets.

I.2.2 Evaluation of uncertainty due to reconstruction *REC*

This subclause describes the method to evaluate the uncertainty contribution due to reconstruction algorithms, excluding peak spatial SAR averaging. The following procedure shall be applied:

i) Sample reference analytical field distributions provided with this PAS at grid points and using polarizations corresponding to the measurement scan performed by the actual system.

ii) Process the sampled data by utilizing system reconstruction and peak spatial-averaging algorithms.

iii) For each distribution, compute the relative difference between the peak spatial-average SAR obtained in step (ii) to the reference SAR targets for the provided analytical functions.

The uncertainty is obtained as the RMS of the values obtained in step (iii) for all the appropriate distributions. Normal distribution and a degree of freedom of N – 1 are assumed, N being the number of considered analytical reference functions.

This approach naturally takes into account the actual sampling and truncation of the fields resulting from measurement system implementation. In order to ensure a complete evaluation for sampling and array boundaries uncertainties, the set of reference vector field distributions at a flat phantom shall include: (i) reference vector field distributions translated by half of the scan grid resolution (half of probe-to-probe distance in the case of an array) at least along two axes in both positive and negative directions (4 translations per field distribution); (ii) reference vector field distributions translated so that the expected peak spatial SAR is located at all relevant edges of the measurement area as recommended by the manufacturer (at least 4 translations if the measurement area is rectangular). If such an approach is taken to include sampling and truncation effects, uncertainty contributions for sampling, array boundaries, reconstruction algorithms are evaluated in a combined fashion so that only one combined uncertainty value shall be reported in Table 2.

I.2.3 Impact of noise on interpolation and extrapolation *POL*

This is the influence of signal noise on the accuracy of the measurement. The impact of measurement noise being fed into processing algorithms can be estimated by the following procedure:

i) Add white Gaussian noise to reference 3-D vector field distributions and create X noisy sets for each initial condition. The standard deviation of the noise on the amplitude and phase data shall be aligned with the actual system measurement noise.
ii) Sample noisy field distributions of the set at grid points and using polarizations corresponding to the measurement scan performed by the actual system.
iii) Process the sampled data by utilizing system interpolation, extrapolation, and integration algorithms as if they were actually measured.
iv) For each distribution affected with noise, calculate the relative standard deviation of the peak spatial-average SAR.
v) For each phantom and frequency, the uncertainty is estimated as the RMS of the values obtained in step (iv) for all the appropriate distributions affected by noise. Normal distribution is assumed. A degree of freedom of N-1 is assumed, supposing N initial noiseless distributions are involved at a given frequency. The maximum uncertainty across the applicable frequency range and used phantoms shall be reported.

I.2.4 SAR Averaging *SAV*

Uncertainty due to SAR averaging shall be evaluated based on test functions as defined in Clause 7.2.10.2 of IEC 62209-1:2016.

I.2.5 SAR scaling *SARS*

The same procedure as described by IEC 62209-1 and IEC 62209-2 applies.

I.2.6 SAR correction for deviations in permittivity and conductivity *SC*

I.2.6.1 Assessment of tissue-equivalent material dielectric parameter measurement uncertainties

The measurement procedures described in Annex J of IEC 62209-1:2016 use vector network analysers for dielectric property measurements. Network analysers require calibration in order to account for and remove inherent losses and reflections. The uncertainty budget for dielectric measurement derives from inaccuracies in the calibration data, analyser drift, and random errors. Other sources of errors are the uncertainties of the sample holder hardware, and deviations from the optimal dimensions for the specified frequencies, and sample properties. This applies regardless of the type of sample holder and the nature of the scattering parameters being measured. Uncertainties due to the straight-line fit in the slotted-line method can be evaluated using a least-squares analysis.

In Table 2 to Table 5, the sensitivity coefficients c_i in columns *f* and *g* for the measurement uncertainties of the conductivity and permittivity of tissue-equivalent materials are needed. These sensitivity coefficients shall be determined for each specific processing technique used by the system. In setting up the parameters of the algorithms, target values shall be assumed for the dielectric properties. The sensitivity coefficients are then obtained numerically using the following procedure:

i) Calculate the peak spatial-average SAR on reference numerical vector field distributions representing various exposure conditions and obtained with tissue-equivalent material parameters set as target values. The same sampling grid and processing algorithms shall be as in the actual system.

ii) Calculate the peak spatial-average SAR on a modified set of reference distributions based on the same conditions as in step (i) but with dielectric parameters varied to mesh the space of tolerances on permittivity and conductivity, e.g., all the couples composed of target permittivity and conductivity ± 2 %. In this step, the reference field distributions are actually modified due to deviations of permittivity and conductivity values from targets. However, the processing algorithms are supposed not to have the information on this deviation and hence are configured to operate with dielectric parameters set as targets.

iii) Calculate the relative differences ΔSAR in peak spatial-average SAR values determined in step (ii) with respect to peak spatial-average SAR determined in step (i) for each condition.

iv) For each frequency, calculate the slopes of best-fit linear regressions relating ΔSAR expressed in percent to $\Delta\varepsilon_r'$ and $\Delta\sigma$ expressed in percent. These slopes are respectively the sensitivity coefficients on permittivity and conductivity measurement tolerances.

The largest sensitivity coefficients over the considered frequency range shall be entered into Table 2 to Table 5.

I.2.6.2 SAR correction formula for deviation from dielectric target values

The determination of SAR correction for the deviation of dielectric properties from target values shall be determined for each specific processing technique used by the system. In setting up the parameters of the algorithms, dielectric properties actually measured for the tissue-equivalent material used in the system shall be assumed. The corrections and their uncertainty are obtained numerically using the following procedure:

i) Calculate the peak spatial-average SAR on the reference numerical vector field distributions representing various exposure conditions and obtained with tissue-equivalent material parameters set as target values. The same sampling grid and processing algorithms as in the actual system shall be used.

ii) Calculate the peak spatial-average SAR on a modified set of reference distributions based on the same conditions as in step (i) but with dielectric parameters set as target dielectric properties ±10%. In this step, the reference field distributions are actually modified due to deviations of permittivity and conductivity values from targets. The processing algorithms are supposed to be fed with the information on this deviation and hence are set to operate with dielectric parameters corresponding to the measured values.

iii) Calculate the relative differences ΔSAR in peak spatial-average SAR values determined in step (ii) with respect to peak spatial-average SAR determined in step (i) for each condition.

iv) For each frequency f, calculate the slopes of best-fit linear regressions relating ΔSAR expressed in percent to $\Delta\varepsilon_r'$ and $\Delta\sigma$ expressed in percent. These slopes are respectively the sensitivity coefficients c_ε and c_σ on known deviations from permittivity and conductivity targets.

v) For each frequency f, the correction coefficient is obtained as $-c_{\varepsilon} \times \Delta\varepsilon_r' - c_{\sigma} \times \Delta\sigma$. The correction uncertainty is obtained as the RMS value of relative residuals (relative differences between the SAR calculated at step (ii) with applied correction for each relevant condition with respect to the SAR calculated at step (i)).

The largest uncertainty value over the considered frequency range shall be entered into Tables 2 to 5, with a normal probability distribution assumed. A degree of freedom of N-1 is assumed, supposing N distributions are involved at a given frequency.

I.3 Measuring system errors which are dependent on the DUT

I.3.1 Introduction

These errors include those relating to device position, separation distance to phantom, frequency, signal modulation, form factor, number and type of the antenna/s and backscatter/mutual coupling between the antenna and the sensor array. The corresponding standard may include a Type A uncertainty analysis based on measurements of a set of antennas whose relevance is clearly demonstrated. To limit the influence of systematic errors on the uncertainty, the uncertainty of the accepted power shall be no larger than 10 % of the total uncertainty of the target value of the antenna.

I.3.2 Probe or probe-array coupling with the DUT *PAC*

The probe or probe-array partly scatters the impinging power radiated by the DUT and transmitted into the phantom. This scattering phenomenon results in two different types of measurement uncertainty components: (i) the boundary effect, which relates to the part of the power which is back-scattered by the probe or probe-array to the interface, then back-scattered again at the impedance transition between tissue-material and shell-air interface; (ii) the modification of the DUT loading which causes a reaction of the power amplifier that may adjust its output power.

The boundary effect is addressed in Annex I.1.7. This Clause applies to the second type of impact relating to a modification of the DUT behaviour. The following procedure shall be applied:

i) Connect validation antenna or a set of reference antennas to port 1 of a VNA using RF coaxial cable.

ii) Measure the magnitude of S_{11} of the antennas at the applicable phantoms in the applicable frequency range. In this step, the phantoms contain no probe or probe-array. The antennas are positioned at each phantom in agreement with positions defined for the validation or at a relevant set of test positions.

iii) Measure the magnitude of S_{11} of the antennas in the same conditions with the phantoms containing the probe or probe-array.

iv) For each antenna and test position, compute

$$Power\_mismatch = |1-[1-|S_{11\_\mathrm{with\_probe}}|^2]/[1-|S_{11\_\mathrm{without\_probe}}|^2]| \quad \text{(I.2)}$$

v) For each phantom, compute the relative standard deviation of the $Power\_mismatch$ across applicable test conditions.

vi) Report the maximum between standard deviations calculated at (v) as the SAR measurement uncertainty contribution with assumed normal distribution.

The reported uncertainty following this approach will overestimate the actual uncertainty. Indeed, power amplifiers of modern DUT are usually designed to compensate for different loadings such that the PA will usually apply more power when its output impedance gets away from the optimal load-pull zone and less power when the matching is better. This is all the more true if the DUT uses dynamic antenna tuning.

I.3.3 Modulation Response *MOD*

The following uncertainty can be determined by using any antenna (e.g., dipole) or open-ended waveguide as a source with a setup equal or equivalent to a setup used for system verification. The signal generation setup shall simulate the modulation for which the uncertainty is determined according to the specification of the communication system standard. For a system with one or several probes, the power shall be increased such that a range of 0,1 W/kg local SAR or less to 10 W/kg or more is assessed by steps of 5 dB. At each power level, the SAR shall be measured with the modulated signal and with CW at the same rms power (verification that the power meter is a true rms detector and that the amplifier is sufficiently linear for the entire dynamic of the signal is required).

Equation (I.3) can be used to derive the modulation uncertainty for the particular modulation X.

$$\mathrm{SAR\_mod}X_{\mathrm{uncertainty}}[\%] = \underset{i=\{x,y,z\}}{\mathrm{MAX}}\left(\underset{P_i = P_0}{\overset{P_0+20\,\mathrm{dB}}{\mathrm{MAX}}}\left(100\times\left|\frac{\mathrm{SAR}(P_i)_{\mathrm{mod}X_i}}{\mathrm{SAR}(P_i)_{\mathrm{CW}_i}}-1\right|\right)\right) \quad \text{(I.3)}$$

where

$SAR\_\mathrm{mod}\ X_{\mathrm{uncertainty}}$	is the uncertainty for the particular modulation *X* in percent;
$SAR(P_i)_{\mathrm{mod}\ Xi}$	is the SAR measured with the modulated signal at a mean power;
$SAR(P_i)_{\mathrm{CWi}}$	is the SAR measured with CW at the same mean power.

The SAR uncertainty is determined as the maximum of all $SAR\_\mathrm{mod}X$ at each step. A rectangular probability distribution is assumed for probe modulation response uncertainty.

I.3.4 Integration time *IT*

Probe integration-time uncertainties may arise when test devices do not emit a continuous signal. When the integration time and discrete sampling intervals used in the probe electronics are not synchronized with the pulsed characteristics of the measured signal, the RF energy at each measurement location may not be fully or correctly captured. This uncertainty shall be evaluated according to the signal characteristics of the test device prior to the SAR measurement.

The probe integration time shall be determined from SAR measurements using a stable antenna with the same signal characteristics and the same probe type that is used for DUT measurements. Measurements at a single point (where the SAR is at least 1 W/kg) shall be made consecutively using the chosen integration time and progressively larger integration times. Double the integration time for each consecutive measurement until the last and next to last measurements are within 0,1 dB of each other. Each measurement at a given integration time shall be repeated several times to verify that the measurement result is stable, and the average SAR of the repeat measurements shall be used for that integration time. The probe integration time uncertainty is the percent difference between the average SAR at the chosen integration time and the RMS value at the last measurement step when growing the integration time. A rectangular probability is assumed.

I.3.5 Measurement system drift and noise *DN*

This subclause describes three uncertainty terms:

a) Noise in the SAR measurement system. This is typically due to component noise.
b) Short-term drifts (e.g., over a period of minutes or hours). This is due to equipment heating, electromagnetic interference or changes in ambient conditions.
c) Long-term drifts (over the calibration period). This may be caused by amplifier stability, changes in the dielectric parameters of the medium and component drift.

Uncertainty due to drift and noise is evaluated from trend analysis of the SAR measurement taken at several times on a measurement system as shown in Figure I.1. They are evaluated separately and combined as the root-sum-squared of the uncertainties assuming that they are statistically independent. Use a dipole antenna as an antenna, fed with a CW signal (to avoid modulation uncertainty) having an input power corresponding to a 1 g peak spatial-average SAR level of 1 W/kg. For the short-term drift, record the 1 g and 10 g peak spatial-average SAR at different times from initial power up of the SAR measurement system (after manufacturer-recommended warm-up time) and continuing as often as possible (defined by the measurement speed) for a period of 8 hours. Use the fastest stable scan rate of the system for these measurements. Use a sufficiently long integration time such that the integration time uncertainty is negligible for these tests.

Compute the moving average. The averaging window size shall be chosen such that the component noise is averaged out but not the influence of the change of ambient conditions (e.g., 5 seconds). Record the maximum deviation between the resulting points.

The measurement system drift and noise uncertainty is calculated as

$$u^2(drift + noise) = u^2(drift) + u^2(noise) \tag{I.4}$$

$$SAR_{uncertainy}\,[\%] = 100\times\left[\frac{\max(M_i) - \min(M_i)}{(\max(M_i) + \min(M_i))} + \frac{2\times M_{Noise}}{(\max(M_i) + \min(M_i))}\right] = 100\times\left[\frac{2\times M_{Noise} + \max(M_i) - \min(M_i)}{(\max(M_i) + \min(M_i))}\right] \tag{I.5}$$

The long-term drift uncertainty is evaluated in the same way, except that measurements are conducted over the calibration period (e.g., 1 year).

The uncertainty is assumed to have a rectangular distribution.

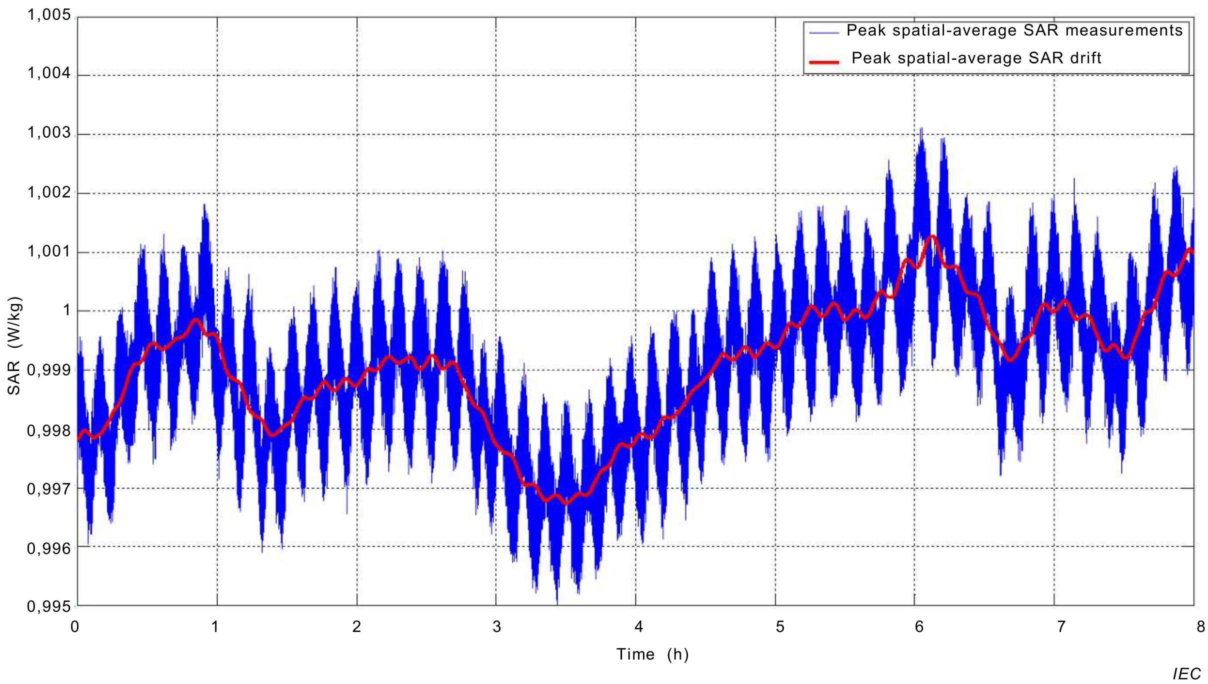

Figure I.1 – Illustration of the SAR measurements during 8 hours and the centered moving average

I.4 DUT-related errors or validation antenna related errors and environmental factors

I.4.1 Device holder DH

I.4.1.1 General

Some holders may still affect the antenna, so the uncertainty resulting from the holder (i.e. the deviation from a set-up without the holder) shall be estimated. The uncertainty of the device holder for testing a specific DUT shall be estimated according to the Type B method described below. Alternatively, the Type A method described below can be used to assess the uncertainty for a group of wireless devices having similar SAR characteristics and tested with the same device holder.

I.4.1.2 Device holder perturbation uncertainty for a specific DUT: Type B

The uncertainty for a specific handset operating in a specific device holder shall be estimated by performing the following two tests using a flat phantom:

a) assessment of the 1 g or 10 g peak spatial-average SAR ($SAR_{\text{w/ holder}}$) by placing the device in the holder in the same way it would be held when tested next to the head, then positioning the handset in direct contact with a flat phantom (horizontal and vertical centre line of the handset parallel to the bottom of the flat phantom);
b) assessment of the 1 g or 10 g peak spatial-average SAR ($SAR_{\text{w/o holder}}$) by placing the device in the same position as in a) but held in place using foamed polystyrene or equivalent low-loss and non-reflective material (permittivity no greater than 1,2 and loss tangent no greater than 10^{-5}).

The SAR uncertainty to be used is:

$$SAR_{\text{uncertainty}}\,[\%] = \left(\frac{SAR_{\text{w/ holder}} - SAR_{\text{w/o holder}}}{SAR_{\text{w/o holder}}} \right) \times 100 \tag{I.6}$$

where

$SAR_{\text{uncertainty}}$	is the uncertainty in percent;
$SAR_{\text{w/ holder}}$	is the SAR with device holder in W/kg;
$SAR_{\text{w/o holder}}$	is the SAR without device holder in W/kg.

This uncertainty has an assumed rectangular probability distribution and $v_i = \infty$ degrees of freedom.

I.4.1.3 Device holder perturbation uncertainty for a specific test device: Type A

The specific device holder disturbance uncertainty data evaluated according to the Type B method described above for a group of handsets with the same shape and with substantially equivalent SAR distribution characteristics shall be statistically compiled and applied to selected groups of devices tested in the same device holder and the same configurations. The statistical procedures shall include at least six devices, each evaluated according to the Type B method described above. As more handsets having similar SAR characteristics are evaluated with the same device holder, the perturbation error may be included in a Type A uncertainty analysis and applied to future SAR evaluations of similar device and holder configurations. Increasing the number of test devices will increase the degrees of freedom (v_i) and lower the coverage factor (k_p). The coverage factor (k_p) for such conditions should be determined as $k_p = t_p\,(v_{\text{eff}})$ where $t_p(v_{\text{eff}})$ is the coverage factor of the t-distribution, and v_{eff} is the effective number of degrees of freedom estimated using the Welch-Satterthwaite Formula. The effect of the device holder for N different models of handsets in the different configurations shall be estimated by performing the tests according to the Type B method described above for each model (N shall be at least 6).

The corresponding uncertainty shall be estimated by using the root-mean-square of the individual uncertainties, with degrees of freedom of $v_i = N - 1$. The database should be updated yearly in order to account for handset design changes.

I.4.2 Device Positioning *DP*

I.4.2.1 General

The deviation of the actual handset position from the positions described in the standard depends on the precision of the handset positioner as well as on the interpretation and handling of the person performing the test. In addition, the magnitude of this deviation on the peak spatial-average SAR values depends on the handset design. Since these parameters cannot be separated, the following Type A tests as described below shall be performed.

I.4.2.2 Positioning uncertainty of a specific handset in a specific device holder

The positioning uncertainty of a specific handset tested in a specific device holder is assessed by repeating measurements of the 1 g or 10 g peak spatial-average SAR. This positioning uncertainty shall be evaluated using the antenna position, frequency channel, and device position for the operating mode that produced the highest SAR among all frequency bands. In addition to the original SAR measurement, the handset shall be repositioned and the tests repeated at least four times. This minimum of five tests is sufficient to establish a reasonable value for the degrees of freedom. If the positioning uncertainty of an individual device is suspected to be large, more tests may need to be performed to reduce the impact on the total measurement uncertainty. Increasing the number of tests will increase the effective degrees of freedom (v_{eff}) and decrease the coverage factor. The average SAR for the total number of measurements (N) is used to determine the SAR uncertainty according to the standard deviation and degrees of freedom ($v_i = N - 1$) of the number of tests performed.

I.4.2.3 Positioning uncertainty of specific types of handsets in a specific device holder

A Type A uncertainty analysis can be applied for a group of handsets with predominantly the same shape and substantially equivalent dimensions and SAR distributions. The tests shall include at least six devices, each evaluated according to the procedures for a specific handset in a specific device holder described above. The number of tests n shall be at least 5, and each of the n tests shall be performed for all M devices). Half of the n tests shall be in the cheek position and the other half shall be in the tilt position. The corresponding uncertainty shall be estimated by applying the root-mean-square of the M individual standard deviations. The value to be filled in the uncertainty table shall be the standard uncertainty with $k = 1$. The degrees of freedom are determined according to the total number of tests $N = n \times M$. For the M devices included in the specific group of handsets, $v_i = N - 1$. If this procedure is applied to determine uncertainty, it may be unnecessary to apply the procedures for a specific handset in a specific device holder described above to individual handsets. The database should be updated yearly in order to account for handset design changes.

I.4.3 Measured SAR drift *SD*

This uncertainty term is evaluated as described in IEC 62209-1.

I.4.4 RF ambient conditions *AC*

Clause 7.2.3.7 of IEC 62209-1:2016 applies.

I.4.5 Measurement system immunity/secondary reception *MSI*

During measurement, the field radiated by the DUT may be picked up by parts of the measurement system other than the field sensors. This may result in undesirable effects susceptible to increase the measurement uncertainty. The assessment of this contribution is system specific and shall be documented by the manufacturer. It can be for example carried out by using the validation antennas in specified test positions and blocking the direct field reception from the probe or probe-array supposed to perform the measurement. SAR measurements shall be performed in these conditions at frequencies specified for the validation and for each phantom in case each phantom contains a dedicated probe or probe-array. The uncertainty shall be estimated assuming a rectangular probability distribution.

I.4.6 Deviation of experimental antennas DEX

Clause 7.2.12 of IEC 62209-1:2016 applies

I.4.7 Other uncertainty contributions when using validation antennas OVS

Clause 7.2.13 of IEC 62209-1:2016 applies.

Bibliography

[1] Aberbour L., Derat B., Cozza A., Analysis of vector E-field sensor array for real-time SAR assessment, Proc. of European Conference on Antenna and Propagation (EuCAP), 2013

[2] Álvarez, Yuri, Fernando Las-Heras, and Marcos Rodríguez Pino. "Reconstruction of equivalent currents distribution over arbitrary three-dimensional surfaces based on integral equation algorithms." IEEE Transactions on Antennas and Propagation 55.12 (2007): 3460-3468

[3] Álvarez, Yuri, Fernando Las-Heras, and Marcos R. Pino. "The sources reconstruction method for amplitude-only field measurements." IEEE transactions on Antennas and Propagation 58.8 (2010): 2776-2781

[4] Anderson A.P., Microwave holography, Proceedings of the IEE, vol. 124, n° 11R, pp. 946-962, 1977

[5] ARAI, M.J., BINNER, G.P., and CROSS, T.E. Estimating errors due to sample surface roughness in microwave complex permittivity measurements obtained using a coaxial probe. *Electron. Lett.*, Jan. 19, 1995, vol. 32, no. 2, pp. 115-117

[6] Balanis, Constantine A. Advanced engineering electromagnetics. John Wiley & Sons, 2012

[7] Balzano, Q., Garay, O., and Manning, T., "Electromagnetic energy exposure of the users of portable cellular telephones," *IEEE Transactions on Vehicular Technology,* Vol. 44, No. 3, pp. 390–403, Aug. 1995

[8] BAO, J.Z., SWICORD, M.L., and DAVIS, C.C. Microwave dielectric characterization of binary mixtures of water, methanol, and ethanol. *J. Chem. Phys.*, Mar. 12, 1996, vol. 104, no. 12, pp. 4441-4450

[9] Bit-Babik G., Faraone, A., Ballen M. and Chou C-K., "Sensitivity of the Spatial-Average Peak SAR to the Dielectric Parameters of Media Used for Compliance Testing in the Frequency Range 0.3 – 3 GHz," *Antennas and Propagation Society International Symposium Digest*, Vol. 3, pp. 722-725, June 2002

[10] BLACKHAM, D.V. and POLLARD, R.D. An improved technique for permittivity measurements using a coaxial probe. *IEEE Trans. Instrumen. Meas.,* Oct. 1997, vol. 46, no. 5, pp. 1093-1099

[11] Bolomey J. Ch., La méthode de diffusion modulée: une approche au relevé des cartes de champs micro- ondes en temps réel, L'Onde Electrique, vol.62, n°5, pp. 73-78, May 1982

[12] Bolomey J.Ch., Cown B.J., Fine G., Jofre L., Mostafavi M., Picard D., Estrada J.P., Friedrich P.G. and Cain F.L., Rapid near-field antenna testing via arrays of modulated scattering probes, IEEE Transactions on Antennas and Propagation, vol. 36, n°6, pp. 804-814, June 1988

[13] Bolomey J.Ch. and Gardiol F., Engineering applications of the modulated scattering technique, Artech House Ed., Norwood, MA, USA, ISBN 1-58053-147-4, 2001

[14] Bolomey J. C., "Efficient near-field techniques for human exposure evaluation: Applications to mobile and fixed antennas," presented at the Electromagnetic Environment and Human Exposure Evaluation Workshop of EMC, Sorrento, Italy, 2002

[15] Buchholz, B., Armstrong, T.J. and Goldstein, S.A., “Anthropometric data for describing the kinematics of the human hand,” Ergonomics vol. 35, no. 3, pp. 261-273, 1992

[16] Bugbee, W.D and Botte, M.J, “Surface Anatomy of the Hand: The Relationships Between Palmar Skin Creases and Osseous Anatomy,” Clinical Orthopaedics and Related Research, 296, 122-126, 1993

[17] Capdevila S., Bolomey J.Ch. and Romeu J., RFID array probe for EM-field measurements, AP-S / URSI Conference, pp.1 – 4 (ISSN :1522-3965), June 2009

[18] Capdevila S., Jofre L., Bolomey J.Ch. and Romeu J., RFID Multiprobe Impedance-Based Sensors, IEEE Transactions on Instrumentation and Measurement, vol.59, n°12, pp. 3093-3101, December 2010

[19] CHOU, C.K., CHEN, G.W., GUY, A.W. and LUK, K.H., Formulas for preparing phantom muscle tissue at various radiofrequencies. *Bioelectromag.*, 1984, vol.5, pp. 435-441

[20] CHRIST, A., CHAVANNES, N., POKOVIC, K, GERBER, H.U. and KUSTER, N. Numerical and Experimental Comparison of Human Head Models for SAR Assessment. *Proceedings of Millennium Workshop on Biological Effects of Electromagnetic Fields*, Heraklion, Kreta, Greece, Oct. 2000, pp. 234-240

[21] CLARKE, R.N., GREGORY, A.P., HODGETTS, T.E., and SYMM, G.T. Improvements in coaxial sensor dielectric measurement: relevance to aqueous dielectrics and biological tissue. in *Microwave Aquametry: Electromagnetic Wave Interaction With Water-containing Materials*, A. Kraszewski, ed., New York: IEEE Press, 1996, pp. 279-297

[22] Collignon G., Michel Y., Robin F., Saint J. and Bolomey J.Ch., Quick microwave field mapping for large antennas, Micowave Journal, vol. 25, n° 12, pp. 129-132, December 1982

[23] Cozza A., Merckel O., Bolomey J.-Ch., A new probe-array approach for fast SAR measurements, Proceedings of International Workshop on Antenna Technology (IWAT), 2007DAVIS, C.C. AND BALZANO, Q., ”THE INTERNATIONAL INTERCOMPARISON OF SAR MEASUREMENTS ON CELLULAR TELEPHONES," IEEE TRANS. ELECTROMAGNETIC COMPATIBILITY, VOL. 51, PP. 210-216, 2009

[24] DIECK, R.H. MEASUREMENT UNCERTAINTY: METHODS AND APPLICATIONS. NORTH CAROLINA, RESEARCH TRIANGLE PARK: INSTRUMENT SOCIETY OF AMERICA, 1992

[25] Derat B., Cozza A., Merckel O., Bolomey, J.-Ch., Numerical analysis of a printed E-field RF probe-array used for rapid SAR assessment, Proceedings 23rd Annual Review of Progress in Applied Computational Electromagnetics (ACES 2007), 2007

[26] DERAT, B., "IMPACT OF THE HAND ON THE AVERAGED SAR IN THE HEAD: SIMULATION OF A CAD PHONE MODEL," PRESENTATION TO IEC PT62209 MT-1, APRIL 22, 2009

[27] Derat et al., A novel technology for fast and accurate Specific Absorption Rate Measurement, Proceedings of International Workshop on Antenna Technology (IWAT), 2013

[28] Di Nallo, C., and Faraone, A., “Effect of amplitude modulation of the CDMA IS-95 signal on SAR measurements,” *IEEE Transactions on Electromagnetic Compatibility,* vol. 48, no. 3, pp. 552-562, August 2006

[29] Douglas, M.G., Kanda, M.Y., Luengas W.G., Ballen, M., Babij T.M. and Chou, C-K., “An Algorithm for Predicting the Change in SAR in a Human Phantom due to Deviations in its Complex Permittivity,” *IEEE Transactions on Electromagnetic Compatibility*, 2007, vol. 51, no 2, May 2009

[30] Douglas, M.G. and Chou, C-K., “Enabling the Use of Broadband Tissue Equivalent Liquids for Specific Absorption Rate Measurements,” *IEEE Electromagnetic Compatibility Symposium*, July 2007

[31] Douglas, M., Bucher, C., Ofli, E., Kuster, N., Derat, B. and Gabriel, S., " Investigation of the influence of the Hand on Head SAR,"presentation to IEC PT 62209 MT-1, March 22, 2010

[32] Douglas, M., Derat, B., Liao, X., Ofli, E., and Kuster, N., "Hand Phantom Models for the Assessment of SAR in the Head from Cellular Telephones," Asia-Pacific Symposium on Electromagnetic Compatibility, Beijing, China, April 12-16, 2010

[33] DROSSOS, A., SANTOMAA, V. and KUSTER, N. The dependence of electromagnetic energy absorption upon human head tissue composition in the frequency range of 300-3000 MHz. *IEEE Trans. Microwave Theory Tech.*, Nov. 2000, vol. 48, no. 11, pp. 1988-1995

[34] EA-2/07 (rev.01) EAL Strategy to Achieve Comparability of Results in Calibration and Testing, Mar

[35] EIA RS-261-B: 1979, “Rectangular Waveguides (WR3 to WR2300).” 1997

[36] EVANS, S. and MICHELSON, S.C. Intercomparison of dielectric reference materials available for the calibration of an open-ended probe at different temperatures. *Meas. Sci. Tech*., Dec. 1995, vol. 6, no. 12, pp. 1721-1732

[37] FARAONE, A., McCOY, D. O., CHOU, C. K., and BALZANO, Q. Characterization of miniaturized E-field probes for SAR measurements. *IEEE Intl. Symp. Electromag. Compat.*, Washington, DC, 2000, pp. 749-754

[38] Federal Communications Commission Office of Engineering and Technology Supplement C (Ed. 01-01) to OET Bulletin 65 (Ed. 97-01), *Evaluating Compliance with FCC Guidelines for Human Exposure to Radiofrequency Electromagnetic Fields, Additional Information for Evaluating Compliance of Mobile and Portable Devices with FCC Limits for Human Exposure to Radiofrequency Emissions,* Washington, DC, June 2001

[39] FERREIRA P.J.S.G. Non-iterative and fast iterative methods for interpolation and extrapolation. *IEEE Trans. Sig. Proc.*, Nov 1994, vol. 41, pp. 3278-3282

[40] FIEGUTH, P.W., KARL, W.C., WILLSKY, A.S. and WUNSCH, C. Multi-resolution optimal interpolation and statistical analysis of TOPEX/POSEIDON satellite altimetry. *IEEE Trans. Geosci. Remote Sens.*, Mar. 1995, vol. 33, pp. 280-292

[41] J. R. Fienup; Phase retrieval algorithms: a comparison; Applied Optics 21(15): 2758-2769, 1982

[42] Foged L.J., Scannavini A., Efficient Testing of Wireless Devices from 800 MHz to 18 GHz, RadioEngineering, vol. 18, n° 4, pp. 460-466, December 2009. available on http://www.radioeng.cz/fulltexts/2009/09_04_460_466.pdf

[43] FORD, C and ETTER, D.M. Wavelet basis reconstruction of non uniform sampled data. *IEEE Trans. Circuits Sys. II: Analog Dig. Sig. Proc.*, Aug. 1998, vol. 45, no. 8, pp. 1165-1168

[44] Francavilla, M., Schiavoni, A., Bertotto, P., and Richiardi, G., “Effect of the hand on cellular phone radiation,” *IEE Proceedings Microwaves, Antennas and Propagation,* Vol. 148, No. 4, pp. 247–253, Aug. 2001

[45] Francavilla, M. and Schiavoni, A., "Effect of the Hand in SAR Compliance Tests of Body Worn Devices," *Applied Computational Electromagnetic Society Conference*, Verona, Italy, March 21, 2007

[46] Francavilla, M. and Schiavoni, A., “New reference function for post – processing uncertainty evaluation in SAR compliance tests,” IEEE Microwave and Wireless Components Letters, Vol. 18, No. 5, May 2008

[47] A. Fresnel, Ann Chim et Phys, (2), 1 (1816), Oeuvres, Vol. 1, 89, 129

[48] FUKUNAGA, K., WATANABE, S., WAKE, K., and YAMANAKA, Y. Time dependence of tissue-equivalent dielectric liquid materials and its effect on SAR. *EMC Europe Symp.*, Sorrento, Italy, Sep. 2002

[49] GABRIEL, C., CHAN, T.Y.A., and GRANT, E.H. Admittance models for open ended coaxial probes and their place in dielectric spectroscopy. *Phys. Med. Biol.*, 1994. vol. 39, no.12, pp. 2183-2200

[50] GABRIEL, S., LAU, R.W. and GABRIEL, C. The dielectric properties of biological tissues: 3. Parametric models for the dielectric spectrum of tissues. *Phys. Med. Bio.*, 1996, vol. 41, no. 11, pp. 2271-2293

[51] Gabriel, S., Lau, R. W., and Gabriel, C., “The dielectric properties of biological tissues: II. Measurement in the frequency range 10 Hz to 20 GHz,” *Physics in Medicine and Biology,* Vol. 41, No. 11, pp. 2251–2269, 1996

[52] Gandhi, O. P., Lazzi, G., and Furse, C. M., “Electromagnetic absorption in the human head and neck for mobile telephones at 835 and 1900 MHz,” *IEEE Transactions on Microwave Theory and Techniques,* Vol. 44, No. 10, pp. 1884–1897, Oct. 1996

[53] R. W. Gerchberg and W. O. Saxton, “A practical algorithm for the determination of the phase from image and diffraction plane pictures,” Optik 35, 237 (1972)

[54] Ghasr M.T. and Zoughi R., A high-dynamic range heterodyne receiver for modulated scattering measurement, IEEE Transactions on Instrumentation and Measurement, vol. 61, pp. 811-816, 2012

[55] Ghasr M.T., Abou Khoussa M.A., Kharkowsky S. and Zoughi R., Portable real-time microwave camera at 24 GHz, IEEE Transactions on Antennas and Propagation, vol.60, n°2, pp. 1114-1125, February 2012

[56] Gimm Y-M., “Development of Fast Speed SAR Measurement System Which Can Be Installed on the Assembly Line of Mobile Devices,” Technical Report to Institute for Information Technology Advancement(IITA) of South Korean Government, 2003

[57] Gimm Y-M., Ju Y-J., Kahng S-T., Lee Y-R., and Lee S-B., "Quick SAR measurement system by 2D array E-field sensors," Proc. of 2013 APMC, Seoul, Korea, Nov. 5 – 8, 2013

[58] Gimm Y-M., Kwon D-H., "Fast SAR measurement system structure using E-field sensors array," Proc. of Asia-Pacific Radio Science Conference, Toyama, Japan, Sep. 25, 2010

[59] Gimm Y-M., Lee Y-R., Song Y-J., Kwon D-H., Park S-H., "Rapid SAR measurement by arraying E-field sensors in the phantom," Proc. of Korea-Japan EMT/EMC/BE Joint Conference, Seoul, Korea, May 18, 2012

[60] Gregory, A. P. and Clarke, R. N., *Tables of the Complex Permittivity of Dielectric Reference Liquids at Frequencies up to 5 GHz*, NPL Report MAT 23, National Physical Laboratory, Teddington, England, 2009

[61] GORDON, C.C., CHURCHILL, T., CLAUSER, C.E., BRADTMILLER, B., McCONVILLE, J.T., TEBBETTS I. and WALKER, R.A., 1988 *Anthropometric Survey of U.S. Army Personnel: Methods and Summary Statistics*. Technical Report NATICK/TR-89/044, U.S. Army Natick Research, Development and Engineering Center, Massachusetts: Natick, Sep. 1989

[62] GREGORY, A.P. and CLARKE, R.N. *Tables of the Complex Permittivity of Dielectric Reference Liquids at Frequencies up to 5 GHz*. NPL Report CETM 33, Centre for Electromagnetic and Time Metrology. Teddington, England: National Physical Laboratory, 2001

[63] GREINER, T.M. HAND ANTHROPOMETRY OF US ARMY PERSONAL, ARMY NATICK RESEARCH DEVELOPMENT AND ENGINEERING CENTER, TECHNICAL REPORT NATICK/TR-92/011, DEC. 1991

[64] Henriksson T., Joacimowicz N., Joisel A., Conessa C., Diet A. and Bolomey J.Ch., Quantitative Microwave Breast Phantom Imaging Using a Planar 2.45 GHz System, IEEE Transactions on Instrumentation and Measurement, vol. 59, n° 10, pp. 2691-2699, 2010

[65] HAMADA, L., Sato, K., IShii, N.*, Watanabe, S., Development of the SAR-probe calibration system using the reference dipole an*tenna in head-simulating liquid, 2008 Asia-Pacific Symposium on Electromagnetic Compatibility, Singapore, pp. 116-119, May, 2008

[66] HILL, N.E., VAUGHAN, W.E., PRICE, A.H., and DAVIES, M. Dielectric Properties and Molecular Behaviour. London: Van Nostrand Reinhold, 1969

[67] IEC 60050 (all parts), *International Electrotechnical Vocabulary (IEV)* (available at www.electropedia.org)

[68] EIA-261-B, Rectangular Waveguides (WR3 to WR2300) – TR-14.1, IEEE Standard Measurement Procedure for Field-Disturbance Sensors, 1979

[69] ICNIRP, "International Commission on Non-Ionizing Radiation Protection guidelines for limiting exposure to time-varying electric, magnetic and electromagnetic fields (Up to 300 GHz)," *Health Physics,* Vol. 74, No. 4, pp. 494–522, 1998

[70] IEEE Std 1528, Recommended Practice for Determining the Peak Spatial-Average Specific Absorption Rate (SAR) in the Human Head from Wireless Communications Devices: Measurement Techniques, New York: Institute Electrical and Electronics Engineers, Sep. 2013

[71] Ishii, N., Sato, K, Hamada, L, Watanabe, S., Gain calibration in near-field region of antenna in tissue-equivalent liquid for SAR assessment, 2008 Asia-Pacific Symposium on Electromagnetic Compatibility, Singapore, pp.112-115, May, 2008

[72] ISO/IEC DIR-2 (2001-7), IEC Directives – Part 2: Rules for the structure and drafting of International Standards. Geneva: International Electrotechnical Commission

[73] ISO/IEC Guide 43-1:1997, *Proficiency testing by interlaboratory comparisons – Part 1: Development and operation of proficiency testing schemes*

[74] ISO/IEC Guide 98-3:2008 *Guide to the Expression of Uncertainty in Measurement*

[75] Jackson, John D. (1998). Classical Electrodynamics (3rd ed.). Wiley. ISBN 0-471-30932-X

[76] Jensen, M. A., and Rahmat-Samii, Y., "Performance analysis of antennas for hand-held transceivers using FDTD," *IEEE Transactions on Antennas and Propagation,* Vol. 42, No. 8, pp. 1106–1113, Aug. 1994

[77] Jensen, M. A. and Rahmat-Samii, Y., "EM interaction of handset antenna and a human in personal communications", *Proceedings of the IEEE*, vol. 83, no.1, pp. 7-17, Jan. 1995

[78] JENKINS, S., HODGETTS, T.E., CLARKE, R.N., and PREECE, A.W. Dielectric measurements on reference liquids using automatic network analysers and calculable geometries. *Meas. Sci. Tech*., July 1990, vol. 1, no. 7, pp. 691-702

[79] JOKELA, K., HYYSALO, P. and PURANEN, L. Calibration of specific absorption rate (SAR) probes in waveguide at 900 MHz. *IEEE Trans. Instrumen. Meas.*, Apr. 1998, vol. 47, no. 2, pp. 432-438

[80] KAATZE, U. Complex permittivity of water as function of frequency and temperature. *J. Chem. Engin. Data*, 1989, vol. 34, no. 4, pp. 371–374

[81] KAATZE, U., POTTEL R., and SCHAFER M. Dielectric spectrum of dimethyl sulfoxide/water mixtures as a function of composition. *J. Phys. Chem.*, 1989, vol. 93, pp. 5623-5627

[82] KANDA, M.Y., BALLEN, M., CHOU, C.K. Formulation and characterization of tissue simulating liquids used for SAR measurement (500-2000 MHz). *Asia-Pacific Radio Science Conference*, Tokyo, Japan, Aug. 1-4, 2001, pp. 274

[83] KANDA KANDA, M, ANALYTICAL AND NUMERICAL TECHNIQUES FOR ANALYZING AN ELECTRICALLY SHORT DIPOLE WITH A NONLINEAR LOAD, IEEE TRANSACTIONS ON ANTENNAS AND PROPAGATION, JAN 1980, VOL. 28, ISSUE: 1, PP. 71- 78

[84] Kanda M.Y., Douglas M.G., Mendivil E.D., Ballen M., Gessner A.V. Chou C-K., "Faster Determination of Mass-Averaged SAR From 2-D Area Scans," IEEE Transactions on Microwave Theory and Techniques, vol. 52, no. 8, pp. 2013-2020, August, 2004

[85] Kim J-H., Gimm Y-M., "Implementation of SAR measurement system with stationary probes," Journal of the Korea Electromagnetic Engineering Society, vol. 17, no. 2, pp. 221 – 227, 2006

[86] Kiminami K., Iyama T., Onishi T., Uebayashi, S., Novel Specific Absorption Rate (SAR) Estimation Method based on 2-D Scanned Electric Fields, IEEE Transactions on Electromagnetic Compatibility, Volume 50, No. 5, p. 828-836; 2008

[87] King R.J., Microwave homodyne receivers, IEE Series, Peter Peregrinus, London, 1978

[88] Klemm M., Leendertz J.A., Gibbins D. and Craddock I.J., Microwave Radar-based breast cancer detection: imaging in inhomogeneous breast phantoms, IEEE Antennas and Wireless Propagation Letters, vol. 8, pp. 1349-1352, 2009

[89] Kuster, N. and Balzano, Q., “Energy absorption mechanism by biological bodies in the near field of dipole antennas above 300 MHz,” *IEEE Transactions on Vehicular Technology,* Vol. 41, No. 1, pp. 17–23, Feb. 1992

[90] KUSTER N., KÄSTLE, R., and SCHMID, T. Dosimetric evaluation of mobile communications equipment with known precision (invited paper). *IEICE Trans. Commun.*, May 1997, vol. E80-B, no. 5, pp. 645-652

[91] KUSTER, N., BALZANO, Q. and LIN, J.C., Eds. *Mobile Communications Safety.* London: Chapman & Hall, 1997

[92] LANCASTER, P. and SALKAUSKA, K. *Curve and Surface Fitting: An Introduction*. New York: Academic Press, 1986

[93] LADBURY, J.M., CAMELL, D.G., ELECTRICALLY SHORT DIPOLES WITH A NONLINEAR LOAD, A REVISITEDANALYSIS”, IEEE TRANSACTIONS ON ELECTROMAGNETIC COMPATIBILITY, FEB 2002, VOL. 44, ISSUE: 1, PP 38-44

[94] Le, D.T., Hamada, L., Watanabe, S., "Measurement procedure to determine SAR of multiple antenna transmitters using scalar electric field probes," 2014 International Conference on Advanced Technologies for Communications (ATC 2014), 15 October 2014

[95] LEE, A.K., and PACK, J.K. Effect of head size for cellular telephone exposure on EM absorption. *IEICE Trans. Commun*., Mar. 2002, vol. E85-B, no. 3, pp. 698-701

[96] LEE, A.K., CHOI, H.D., LEE, H.S., and PACK, J.K. Human head size and SAR characteristics for handset exposure. *ETRI J.*, Apr. 2002, vol. 24, no. 2, pp. 176-179

[97] LEISTEN, O., VARDAXAGLOU, Y., SCHMID, T., ROSENBERGER, B., AGBORAW, E., KUSTER, N., and NICOLAIDIS, G. Miniature dielectric-loaded personal telephone antennas with low user exposure. *Electron. Lett.*, Aug. 20, 1998, vol. 34, no. 17, pp. 1628-1629

[98] LEVIN, V.V. and PODLOVCHENKO, T.L. Dispersion of the dielectric permittivity of ethylene GLYCOL. ZHURNAL STRUKTURNOI KHIMII, 1970, VOL. 11, PP. 766-767

[99] LI, C.-H., OFLI, E., CHAVANNES, N., AND KUSTER, N., “EFFECTS OF HAND PHANTOM ON MOBILE PHONE ANTENNA PERFORMANCE,” IEEE TRANSACTIONS ON ANTENNAS AND PROPAGATION, VOL. 57, NO. 9, PP. 2763–2770, SEP. 2009

[100] LI, C.H., OFLI, E., CHAVANNES, N. AND KUSTER, N., "SAR AND EFFICIENCY PERFORMANCE OF MOBILE PHONE ANTENNA WITH DIFFERENT USER HAND POSITIONS," ANTENNAS AND PROPAGATION SOCIETY INTERNATIONAL SYMPOSIUM, CHARLESTON, USA, 2009

[101] LI, C-H., DOUGLAS, M., OFLI, E. DERAT, B. AND KUSTER, N., " INVESTIGATION OF THE INFLUENCE OF THE HAND ON HEAD SAR," REPORT TO IEC PT 62209 MT-1, APRIL, 2010

[102] Loader, B. G, Gregory A.P. Bownds, D. *Coaxial artefact standard for specific absorption rate100 kHz to 400 MHz*, Progress in Electromagnetic Research Symposium (PIERS), 23-27 March, 2009, Beijing, China

[103] Manning M. Massey P., “Rapid SAR testing of mobile phone prototype using a spherical test geometry,” in IEE Tech. on Antenna Measurements and SAR Seminar, Loughborough, U.K., May 28–29, 2002

[104] Merckel O., Fleury G., Bolomey J.-C., “Rapid SAR measurement via parametric modeling,” Proc. 5th International Congress of the European BioElectromagnetics Association (EBEA), p. 75-77, Helsinki, Finland, Sep. 2001

[105] Merckel O., Bolomey J.-Ch., Joisel A., “Near-field approach to Rapid SAR Measurement of Mobile Phones”, Symp. of the Association for Measurement and Testing of Antennas (AMTA 2003), Irvine, Denver, USA, Oct. 2003

[106] MEIER, K., BURKHARDT, M., SCHMID, T. and KUSTER, N. Broadband calibration of E-field probes in lossy media. *IEEE Trans. Microwave Theory Tech.*, Oct. 1996, vol. 44, no. 10, pp. 1954-1962

[107] Meyer, F. J. C., Palmer, K. D., and Jakobus, U., “Investigation into the accuracy, efficiency and applicability of the method of moments as numerical dosimetry tool for the head and hand of a mobile phone user,” *Applied Computational Electromagnetics Society Journal,* Vol. 16, No. 2, pp. 114–125, July 2001

[108] MIGLIORE, M.D. Partial self-calibration method for permittivity measurement using truncated coaxial cable. *Electron. Lett.*, July 20, 2000, vol. 36, no. 15, pp. 1275-1277

[109] MISRA, D. A quasi-static analysis of open-ended coaxial lines. *IEEE Trans. Microwave Theory Tech.*, Oct. 1987, vol. 35, no. 10, pp. 925-928

[110] MISRA, D., CHABBRA, M., EPSTEIN, B.R., MIROTZNIK, M., and FOSTER, K.R. Noninvasive electrical characterization of materials at microwave frequencies using an open-ended coaxial line: test of an improved calibration technique. *IEEE Trans. Microwave Theory Tech.*, Jan. 1990, vol. 38, no. 1, pp. 8-14

[111] MISRA, D. On the measurement of the complex permittivity of materials by an open-ended coaxial probe. *IEEE Microwave Guided Wave Lett.*, May 1995, vol. 5, no. 5, pp. 161-163

[112] MOSIG, J.R, BESSON, J.C.E, GEX-FABRY, M. and GARDIOL, F.E. Reflection of an open-ended coaxial line and application to non-destructive measurement of materials. *IEEE Trans.* INSTRUMEN. MEAS., 1981, IM-30, PP 46-51

[113] Montgomery, D.C., Design and Analysis of Experiments (4th edition), New York: John Wiley and Sons. (1997)

[114] NAHMAN, N.S., KANDA, M., LARSEN, E.B. and CRAWFORD, M.L. Methodology for standard electromagnetic field measurements. *IEEE Trans. Instrumen. Meas.*, Dec. 1985, vol. IM-34, no. 4, pp. 490-503

[115] NEVELS, R.D., BUTLER, C.M. and YABLON, W. The annular slot antenna in a lossy biological medium. *IEEE Trans. Microwave Theory Tech.*, 1985, MTT-30, pp 314-319

[116] NIST TN1297, *Guidelines for Evaluating and Expressing the Uncertainty of NIST Measurement Results*. Gaithersburg, MD: National Institute of Standards and Technology, 1994

[117] NYSHADHAM, A., SIBBALD, C.L., and STUCHLY, S.S. Permittivity measurements using open-ended sensors and reference liquid calibration – an uncertainty analysis. *IEEE Trans. Microwave Theory Tech.*, Feb. 1992, vol. 40, no. 2, pp. 305-314

[118] Onishi, T. and Uebayashi S., “Influence of phantom shell on SAR measurement in 3-6 GHz frequency range,” IEICE Trans. Commun., vol., E88-B, no. 8, pp. 3257 – 3262, 2005

[119] Loader B., Gregory A., Bownds D., and Johnson Y., “Non-toxic phantoms for SAR measurements (30 MHz to 6 GHz),” The 32nd Annual Meeting of the Bioelectromagnetics Society (BEMS 2010), Seoul, Korea, June 14-18, 2010

[120] Onishi, T. and Uebayashi S., “Influence of phantom shell on SAR measurement in 3-6 GHz frequency range,” IEICE Trans. Commun., vol., E88-B, no. 8, pp. 3257 – 3262, 2005.K. Park, H. Jun, K. Joyner, B. Lee, "Hand effect on Head SAR: Simulation and Additional Tests," Report to IEC PT 62209 MT-1, December, 2009

[121] Paris, D. T. and Hurd F.K., Basic Electromagnetic Theory, McGraw-Hill 1969, pg. 383–385

[122] Pelosi, M., Franek, O., Knudsen, M. B., Christensen, M., and Pedersen, G. F., “A grip study for talk and data modes in mobile phones,” IEEE Transactions on Antennas and Propagation, vol. 57, no. 4, pp. 856–865, Apr. 2009

[123] Pelosi, M., Franek, O., Pedersen, G.F., Knudsen, M., "User's Impact on PIFA Antennas in Mobile Phones," IEEE 69th Vehicular Technology Conference, Barcelona, Spain, 26-29 April 2009

[124] PERSON C., AHLONSOU, L.N. and GRANGEAT, C. New test bench for the characterization of SAR measurement probes used in tissue equivalent liquids, *Bioelectromagnetics Society 22nd Annual Meeting*, Munich Germany, June 11-16, 2000

[125] PERSON, C., TANNÉ, G., AHLONSOU, L.N., NGOUNOU, C. and GRANGEAT C. New reference antennas for SAR probe calibration in tissue equivalent liquid. *Millennium Conference on Antennas and Propagation, AP2000*, Davos, Switzerland: April 9-14, 2000

[126] PEYMAN, A. and GABRIEL, C. Tissue equivalent liquids for SAR measurement at microwave frequencies. *Bioelectromagnetics Society 24th Annual Meeting*, Quebec, Canada, June 2002, poster P-53

[127] POKOVIC, K. *Advanced Electromagnetic Probes for Near Field Evaluation*. Doc. Tech. Sci. Diss. ETH Nr. 13334. Switzerland, Zurich: Swiss Federal Institute of Technology, 1999

[128] POKOVIC, K., SCHMID, T. and KUSTER, N. Robust setup for precise calibration of E-field probes in tissue simulating liquids at mobile communication frequencies. In *Proceedings ICECOM'97*. Dubrovnik, Croatia, Oct. 12-17, 1997, pp. 120-124

[129] POKOVIC, K., SCHMID, T., CHRIST, A. and KUSTER, N. Design and characterization of E-field probes for lossy media. Submitted to *IEEE Trans. Microwave Theory Tech.*, 1999

[130] POURNAROPOULOS, C.L. and MISRA, D.K. The co-axial aperture electromagnetic sensor and its application in material characterization. *Meas. Sci. Tech.*, 1997, vol. 8, pp. 1191-1202

[131] PRESS, W.H., FLANNERY, B.P., TEUKOLSKY, S.A. and VETTERLING, W.T. *Numerical Recipes in FORTRAN 77: The Art of Scientific Computing*. New York: Cambridge University Press, 1992

[132] RAMO, S., WHINNERY, J.R. and VAN DUZER, T. *Fields and Waves in Communication Electronics*. New York, Wiley, 1993

[133] Rocher, F., Julien, T., Derat, B., "Impact of a Hand Phantom on the Measured Average SAR," presentation to ICES TC-34 committee, December 11, 2008

[134] Schiavoni A, Francavilla M, Forigo D, Deplano M, “A Procedure to Reduce the Qualification Time in SAR Compliance Tests”, BEMS 2005, June 2005

[135] Schelkunoff, S. A. (1936), Some Equivalence Theorems of Electromagnetics and Their Application to Radiation Problems. Bell System Technical Journal, 15: 92–112. doi:10.1002/j.1538-7305.1936.tb00720

[136] SCHMID, T., EGGER O. and KUSTER, N. Automated E-field scanning system for dosimetric assessments. *IEEE Trans. Microwave Theory Tech.*, Jan. 1996, vol. 44, no. 1, pp. 105-113

[137] SCHÖNBORN, F., BURKHARDT, M. and KUSTER, N. The difference of EM energy absorption between adults and children. *Health Phys.*, Feb. 1998, vol. 74, no. 2, pp. 160-168

[138] Serafin D. et al., Spherical near-field facility for microwave coupling assessments in the 100 MHz-6 GHz frequency range, IEEE Transactions on Electromagnetic Compatibility, vol. 40, no. 3, pp. 225–233, Aug. 1998

[139] TAYLOR, J.R. An Introduction to Error Analysis: The Study of Uncertainties In Physical Measurements. 2nd ed. Sausalito, CA: University Science Books, 1997

[140] Tilley, A.R. and Henry Dreyfuss Associates, The Measure of Man and Woman: Human Factors in Design,; Wiley, Dec. 31, 2001

[141] TOROPAINEN, A., VAINIKAINEN, P., and DROSSOS, A. Method for accurate measurement of complex permittivity of tissue equivalent liquids. *Electron. Lett.*, 2000, vol. 36, no. 1, pp. 32-34

[142] Tricoles G. and Farhat N.H., Microwave holography – Applications and techniques, IEEE Proceedings, vol. 65, pp. 108-121, January 1977

[143] UKAS LAB34, *The Expression of Uncertainty in EMC Testing*. Feltham, Middlesex, England: United Kingdom Accreditation Service, 2002

[144] UKAS M3003, *The Expression of Uncertainty and Confidence in Measurement.* Feltham, Middlesex, England: United Kingdom Accreditation Service, 1997

[145] USTUNER, K.F. and FERRAI, L.A. Discrete splines and spline filters. *IEEE Trans. Circuits Sys.*, July 1991, vol. 39, no. 7, pp 417-422

[146] VIGNERAS, V. Elaboration and characterization of biological tissues equivalent liquids in the frequency range 0.9-3 GHz, final report. France: PIOM Laboratory, University of Bordeaux, Nov. 2001

[147] VON HIPPEL, A. Dielectric Materials and Applications. Cambridge: MA: MIT Press, 1954

[148] Watanabe, S., Taki, M., Nojima, T., and Fujiwara, O., “Characteristics of the SAR distribution in a head exposed to electromagnetic fields radiated by a hand-held portable radio,” *IEEE Transactions on Microwave Theory and Techniques,* Vol. 44, No. 10, pp. 1874–1883, Oct. 1996

[149] Wu, T., Lin, X., Yang, J., Zhao, C., Zhang, C. and Shao, Q., "TD-SCDMA Mobile Phone’s SAR Measurement about OTA Hand Phantom," Progress in Electromagnetics Research Symposium, Xi’an, China, March 22-26, 2010

[150] Wu Z., Cann H. MC, Davis L.E., Hu J., Fontes A. and Xie C.G., Microwave tomographic system for oil- and gas-multiphase-flow imaging, Measurement Science and Technology, vol. 20, n° 10, 2009

[151] ISO/IEC Guide 98-1, *Uncertainty of measurement – Part 1: Introduction to the expression of uncertainty in measurement*

[152] ISO/IEC Guide 98-3-SP1:2008, *Uncertainty of measurement – Part 3: Guide to the expression of uncertainty in measurement (GUM:1995) – Supplement 1: Propagation of distributions using a Monte Carlo method*

[153] Álvarez, Yuri, Fernando Las-Heras, and Marcos Rodríguez Pino. "Reconstruction of equivalent currents distribution over arbitrary three-dimensional surfaces based on integral equation algorithms." IEEE Transactions on Antennas and Propagation 55.12 (2007): 3460-3468

[154] J. L. A. Quijano and G. Vecchi, "Improved-accuracy source reconstruction on arbitrary 3-D surfaces," IEEE Antennas and Wireless Propagation Letters, Vol. 8, 1046-1049, 2009

[155] J. L. A. Quijano and G. Vecchi, "Field and source equivalence in source reconstruction on 3D surfaces," Progress In Electromagnetics Research, Vol. 103, 67-100, 2010

[156] 1720-2012 – IEEE Recommended Practice for Near-Field Antenna Measurements

[157] R. Mitharwal and F. P. Andriulli A Regularized Boundary Element Formulation for Contactless SAR Evaluations within Homogeneous and Inhomogeneous Head Phantoms , (invited), Comptes Rendus Physique , Vol. 16, n.9, 2015, pp. 776-788

[158] O. Bottauscio, M. Chiampi, L. Zilberti, A boundary element approach to relate surface fields with the specific absorption rate (SAR) induced in 3-D human phantoms, Eng. Anal. Bound. Elem. 35(4) (2011) 657–666

INTERNATIONAL
ELECTROTECHNICAL
COMMISSION

3, rue de Varembé
PO Box 131
CH-1211 Geneva 20
Switzerland

Tel: + 41 22 919 02 11
Fax: + 41 22 919 03 00
info@iec.ch
www.iec.ch